DEFENSE RESEARCH LABORATORY
THE UNIVERSITY OF TEXAS
AUSTIN 12, TEXAS

Operating under Contract NOrd-16496
with the Bureau of Naval Weapons
Department of the Navy

GEOPHYSICAL INTERPRETATIONS OF POWER SPECTRAL ANALYSIS OF LOW FREQUENCY FLUCTUATIONS IN THE MAGNETOTELLURIC FIELD

by
Alexander A. J. Hoffman

Bumblebee Series
Report No. 310
Copy No. 12

January 1962

Bumblebee Report No. 310
January 1962

GEOPHYSICAL INTERPRETATIONS OF POWER SPECTRAL ANALYSIS OF LOW FREQUENCY FLUCTUATIONS IN THE MAGNETOTELLURIC FIELD

by Alexander A. J. Hoffman

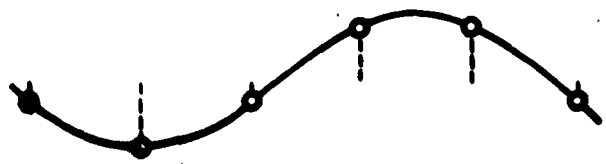

Based on a DISSERTATION presented to
THE FACULTY OF THE GRADUATE SCHOOL
THE UNIVERSITY OF TEXAS
in partial fulfillment of the requirements
for the degree of
DOCTOR OF PHILOSOPHY

Defense Research Laboratory
The University of Texas
Austin, Texas

ABSTRACT

A description of the recording equipment and geological configuration at the location of three Soviet geomagnetic observatories which participated in the IGY is followed by a discussion of the sample data processing procedures for power spectral analysis. Theory and applications of time-domain numerical filter operators are presented. A discussion of the application of the Tukey-Blackman method of power spectral analysis to single time series is followed by its extension to cross-power spectra, coherency and phase analysis of two time series. Power spectra of the horizontal components of the magnetic field and telluric field are computed for ten-hour periods recorded on 1 and 2 September 1957 at the Soviet Geomagnetic Observatory in Tbilisi. Spectral analyses of the East-West telluric field component were carried out for simultaneous recordings of several hours duration made on 20 September 1957 at three Soviet stations: Tbilisi, Lvov, and Ashkhabad. All analyses are based on microfilm copies furnished by the IGY World Data Center A. Each power spectrum shows a frequency dependence over a frequency range of 0.03 to 7 cpks of the form $P_0 f^{-n}$ where n varies from 1.1 to 2.5. The coherency between orthogonal components of the telluric and magnetic fields is computed for the data from Tbilisi. Magnetic power spectra from USSR, Canada, Texas, and Massachusetts are plotted on a common graph to show the frequency dependence over the range 0.03 to 400 cpks. The power spectra for Tbilisi are used to compute apparent resistivity in accordance with a formula developed by Cagniard. It is found that both components of the telluric field yield a value of 6 ohm meters for the electrical resistivity of the earth. It is suggested that this value applies to depths from 70 to 700 kilometers. There is no evidence of horizontal anisotropy of the earth's resistivity. Assuming that the earth behaves as a linear filter with the variation of a horizontal component of the earth's magnetic field as the random input or driving force and the corresponding component of the telluric field as the output or resulting function, the frequency response of the earth is computed using the results of cross-spectral analysis. Resultant computation shows the earth to behave as a uniform conductor. A comparison is made between frequencies at which peaks occur in the power spectra of the magnetotelluric field and the observed modes of free oscillation of the earth.

ACKNOWLEDGEMENTS

It is indeed a pleasure to acknowledge the help of those people and organizations who have contributed to this dissertation. The author wishes to express his appreciation to Dr. C. W. Horton, the dissertation supervisor, for suggesting the problem and for subsequent discussions which provided a stimulus for the work and a sounding board for ideas. The numerical calculations were carried out at The University of Texas Computation Center and paid for by The University Research Institute. Primary support for the work was received from the Department of the Navy through Contract NOrd-16498, Task UTX-2 with Defense Research Laboratory, The University of Texas. The author wishes to express his thanks to the staff of Defense Research Laboratory for the many personal courtesies in connection with preparation of the dissertation. The author wishes to thank Sir Charles Wright (Pacific Naval Laboratory, Canada), Drs. A. W. Straiton and H. W. Smith (Electrical Engineering Research Laboratory, The University of Texas) and Dr. Thomas Cantwell (Department of Geology and Geophysics, Massachusetts Institute of Technology) for permission to use their data and/or reproduce their work. The base maps in Figures 1 and 33 are used by permission of Goode Base Map Series, Department of Geography, University of Chicago. The author wishes to thank Drs. Guy, Hughes, and Kinsey for reading the dissertation and for their helpful suggestions. Finally the author wishes to express his thanks to his wife for her patience and endurance.

TABLE OF CONTENTS

TABLE OF FIGURES

TABLE OF TABLES

INTRODUCTION

This dissertation is an investigation of the power spectra of the magnetotelluric field of the earth and some geophysical interpretations of this power distribution. The frequency range considered is 0.03 to 10 cycles per kilosecond, a frequency range not previously investigated by power spectral analysis.

Between any two points on the surface of the earth there exists a time dependent difference of potential. The earth, a conductor, provides a path of current flow. The earth current or telluric current as it is sometimes called, ranges in magnitude from zero to several millivolts per kilometer and is easily measured. Many stations called earth current observatories, have been set up to make continuous recordings of telluric currents to provide a basis for systematic study. Historical accounts are plentiful and complete and will not be considered here [1, 2, 3].* It is sufficient to say that earth currents exist and are measurable.

Measurements of the magnetic field of the earth, near the surface of the earth, show this field is time dependent. It has been noted that the time variations in the earth currents and in the magnetic field at the surface of the earth are at times very similar in appearance at the same station. Certain characteristics such as world wide appearance, relations to sunspots, 27-day recurrence and tendency, simultaneous occurrence of disturbances, and so forth, are common to the two fields at many stations. It is generally believed that this similarity is more than chance and that the two are in some way related.

Since electrical measuring and recording instruments are all frequency sensitive, the present investigation is limited by the characteristics of the recordings at hand for investigation and analysis. The recording instruments used at the Soviet observatories respond to dc and the only frequency limitation in the response occurs at frequencies higher than those considered in the present investigation.

---

*Numbers in brackets refer to references in the bibliography.

The analysis here is different from the traditional approach in that, instead of concentrating on discrete events such as storms and sudden commencements, the analysis is limited to carefully selected records which most nearly approximate stationary time series. This selection is important since the data are subjected to spectral analysis. Time-domain numerical filters are used to implement the spectral analysis.

The data, recording equipment and recording stations are discussed in Chapter I. The various theoretical aspects of spectral analysis and filtering are considered in Chapters II through V. The power spectra are presented in Chapter VI. The geophysical interpretations are found in Chapter VII.

CHAPTER I

THE DATA AND DATA PROCESSING

Source of Data

A planned effort by the scientists of the USSR for recording of the variations in the earth's electromagnetic field has resulted in a series of zonal and meridional chains of recording stations extending across the USSR and from the Arctic to the Antarctic. A discussion of this effort including description of the equipment is available as part of the Soviet contribution to the International Geophysical Year [4].

The data on which this dissertation is based were obtained from the IGY World Data Center, Washington, D. C. Several rolls of microfilm copies of normal-run and rapid-run tellurograms and magnetograms selected from records deposited at the data center by the USSR were obtained through the Library of The University of Texas. Records were obtained for the following stations:

USSR	A020	Cape Chelyushin
USSR	B145	Lvov
USSR	C126	Ashkhabad
USSR	C364	Tbilisi
USSR	A976	Oasis

The records made at Cape Chelyushin and Oasis were unsuitable for the purpose at hand. The remaining stations, Lvov, Ashkhabad, and Tbilisi are three of the six stations referred to as the "third zonal chain" by V. Troitskaya [5]. They are located within a geographic band extending from 38°N to 49°N latitude (see Figure 1).

Description of Observatories and Equipment

The information presented here is obtained from reports to the Committee on Observatories of the International Association of Geomagnetism and Aeronomy [4].

Tbilisi

Tbilisi Observatory is located near the town of Dusheti, 57 kilometers northwest of Tbilisi in the Georgian Soviet Republic, USSR. The geographic

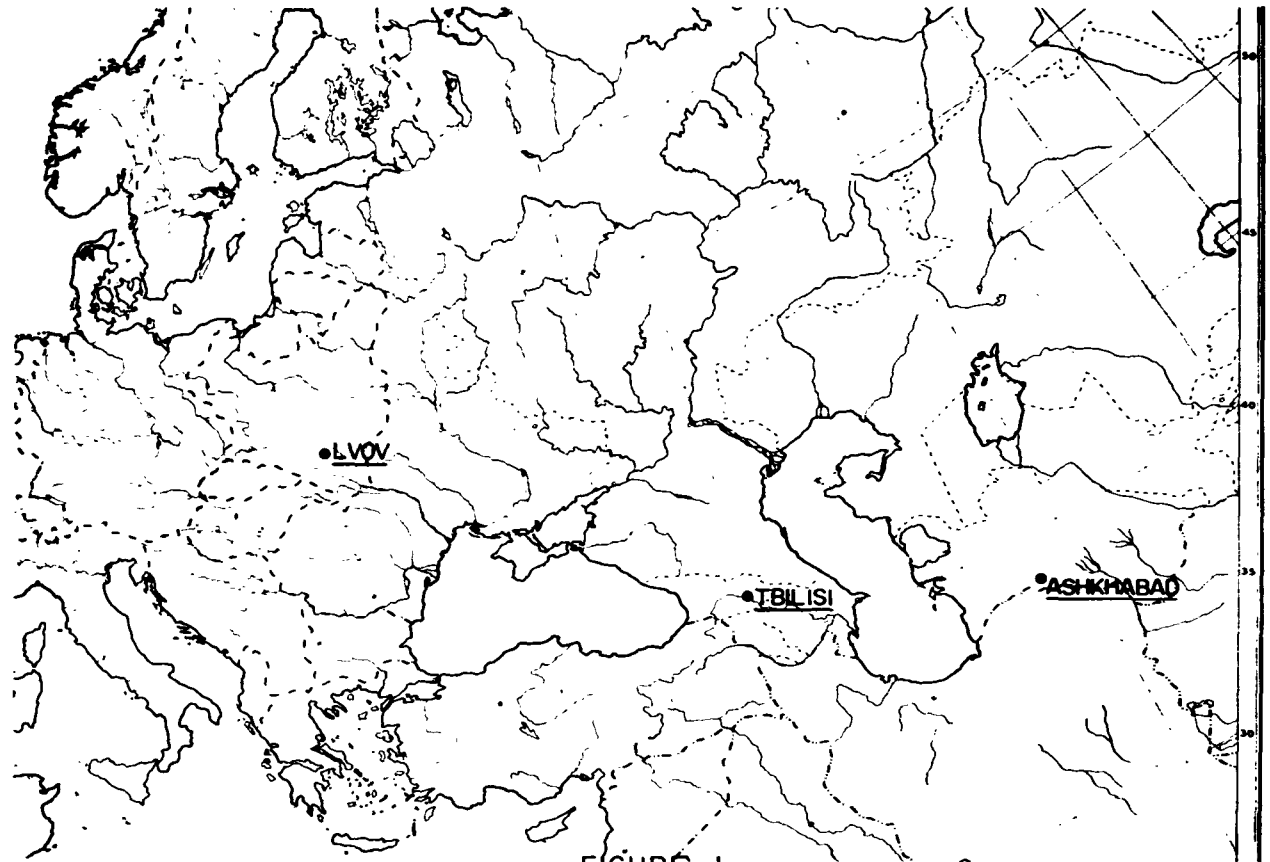

FIGURE 1

THE LOCATION OF THREE SOVIET IGY STATIONS LVOV, ASHKHABAD, AND TBILISI

Prepared by Henry M. Leppard
Published by the University of Chicago Press, Chicago, Illinois

location is 45°5'28"N, 44°42'16"E, the geomagnetic location is 36°7'N, 122°1'E, and the altitude is 981.8 meters above sea level. The recordings are marked with Greenwich Mean Time (GMT), which differs from local time by two hours, 58 minutes, 49 seconds. The observatory is located in the eastern suburb of the town on a small shrub-covered hill. An electric railway operates approximately 26 kilometers from the observatory, but as far as can be determined, it has no measurable local effect. It is believed that no artificial disturbances are present which affect the recordings.

The following quotation [4] gives the geological configuration of the recording area:

> The northern rim of the Gori-Mukhransk depression, on which the Dusheti Geophysical Observatory is located, is composed of Tertiary and Quaternary deposits of great thickness: sandstones, carbonate block conglomerates of this upper Cretaceous, clayey shales, clays, solidly cemented conglomerates of the middle Jurassic, etc. The Tertiary rocks are covered with a mantle of valley alluvium up to 150 m in thickness. Electric prospecting carried out in the environs of the station shows that the surface deposits have specific resistances that do not exceed 30 ohms/m; low values of the specific resistance up to 10 ohms/m are characteristic of clayey deposits of the northwestern part of the station site. Studies conducted in the area of the station by the method of telluric currents and vertical electric soundings have established the absence of anomalous fields near the station and a sufficiently homogeneous geoelectric structure of low resistance (conglomerates and sandstones of the Dusheti formation). The geomagnetic field of the environs of the Dusheti Observatory is well studied. Magnetic anomalies are absent over a considerable area adjoining the station.

The magnetographs at Tbilisi consist of two sets of the medium model Eshenhagen [6] type (imported from Germany in 1930). One of these is used as the recorder and the other for control purposes. Absolute measurements of D, H, and Z are made on the average of six times per month at the observatory. The time marks for the recording set are made by use of a Gaslu contact clock with an average accuracy of ±5 seconds.

The variations in the telluric field are recorded by automatic photo-galvanographs. The mirror galvanometers installed in the photo-galvanographs have a current sensitivity of the order 10^{-8} to 10^{-9} amperes. Lead electrodes are grounded in clayey deposits (at a depth of two meters) at the ends

of two mutually perpendicular one kilometer lines. The lines are oriented latitudinally and longitudinally to measure the East-West and North-South components of the telluric fields, respectively.

Ashkhabad

Ashkhabad Observatory is located near the village of Vannovsky, 21 kilometers west of Ashkhabad in the Turkman Soviet Republic, USSR. The geographic location is 37°57.0'N, 58°06.5'E, the geomagnetic location is 30.3°N, 133.1°E, and the altitude is 570 meters above sea level. The recordings are marked with Greenwich Mean Time (GMT) which differs from local time by 3 hours, 52 minutes, 20 seconds. The following quotation [4] gives the geological configuration on the recording area:

> The station is located on the front range of the Kopet-Dag, in the Firyuzinka River valley. The valley is composed of a sedimentary Cretaceous deposits (sandstones, argillites, aleurilites), and is covered with several meters of proluvium. The rocks have a preferential SSE dip and NNW strike. The magnetic pavilions are situated at the northern foot of the mountain 100 m from the geophysical station. The earth-current station is about 500 meters above sea level with maximum relative rises of 100-200 meters/km.

There are no artificial disturbances near the observatory.

Earth current recording equipment is on hand for 22mm/hour, 90 mm/hour, and 30 mm/min. The 22 mm/hour recording is used here. Short lines in the form of a cross of 370 m length connect lead ribbon electrodes (13 m long and 3.5 m wide) laid at a depth of 2 to 2.5 meters near the outcroppings of basement rocks. The lines are placed 50-60 cm underground. The electrodes are spread out in a zigzag fashion. The interelectrode resistances reach 150 ohms on the North-South line and 130 ohms on the East-West line.

Lvov

Lvov station is located in the Trans-Carpathian region of the Ukraine SSR, 10 km southeast of the town of Uzhgorod. The geographic location is 48°33.2'N, 22°23.8'E, the geomagnetic location is 47.0°N, 104.2°E, and the altitude is 150 meters above sea level.

The following description of the geological configuration is quoted from the International Association of Geomagnetism and Aeronomy [4]:

The locality is mountainous with relative eminences up to 100 m. The region is composed, basically, of volcanogenic and sedimentary rocks of neogen age. Under an upper layer of sandy loam and loess of thickness 5-10 m and specific resistance 3-5 ohm/m, is a volcanogenic thickness of effusive rocks with underlying tuffs, tuff breccia and tuffites with an aggregate thickness of about 500 meters and a specific resistance up to 200 ohm/m. The volcanogenic layer is distinguished by pronounced anisotropy. The lower lying strata of coal-bearing lagoon-continental deposits of thickness about 700 m has an elevated electrical conductivity. At a depth of 1500 m is a layer of high resistance that is used as the reference standard in electrical mapping.

Equipment is available for 90 mm/hour, 30 mm/min, and 22 mm/hour earth current recordings. The 90 mm/hour records are used here.

Selection of Data for Processing

Microfilm copies of the data were obtained for September, 1957, but no attempt was made to process all of the data. The time and expense of power spectral analysis makes it desirable to plan the work carefully to insure that the goals of the study can be achieved with a minimum of data processing. In addition to these considerations are the questions of quality in the records. Records with sudden commencements, storms, frequent off-paper sections, and very quiet records were rejected. Care was taken to select records which were moderately active but appeared stationary. Figures 2 to 7 are reproductions of typical records used in the study.

Pre-Machine Processing of Data

The most suitable records were photographically enlarged from the 35 mm microfilm to approximately 17 x 22 inches. Portions of the records near the edges of the enlargement were not used since lens distortion during the enlargement process was evident. The records were then digitized by hand. The accuracy of digitized data is ±1 gamma on the magnetic field records, ±1 minute on the declination records, and ±0.01 mv/km on the telluric records. The accuracy here is considerably greater than necessary since the statistical accuracy of the computed spectral estimates is the controlling factor [7].

The selection of the sampling interval was based on the appearance of the record. Approximate spectral estimates were made by visual inspection

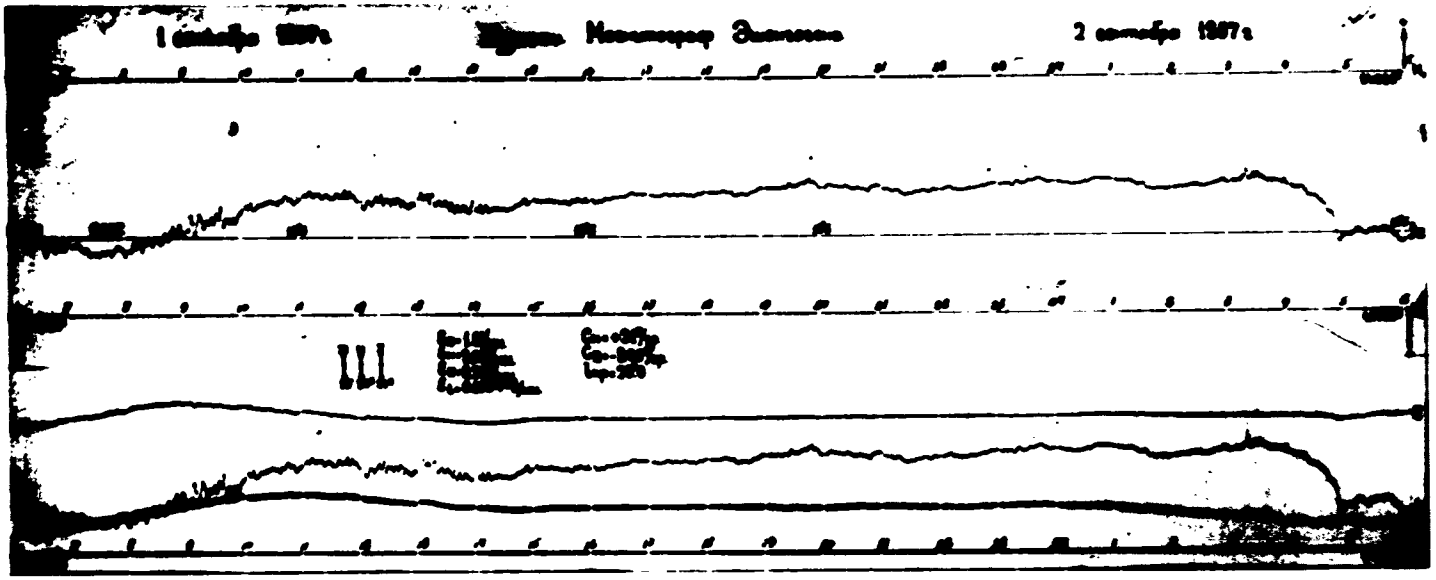

FIGURE 2
MAGNETOGRAM FOR TBILISI 1-2 SEPTEMBER 1957

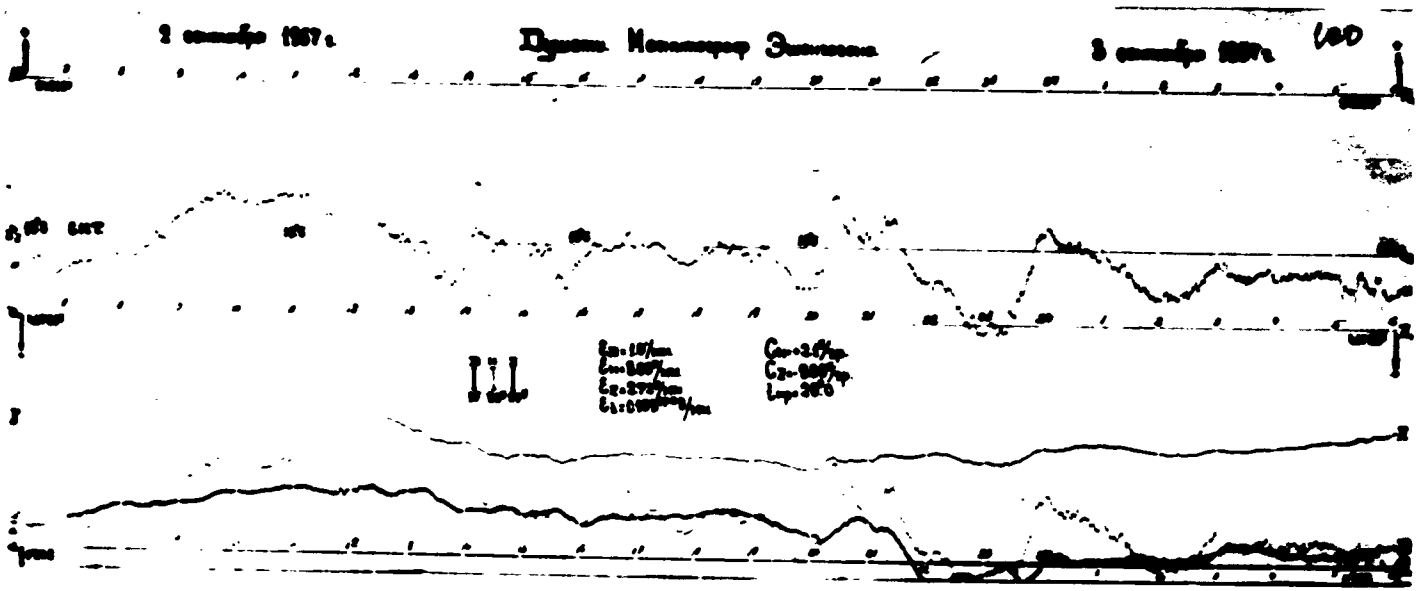

FIGURE 3
MAGNETOGRAM FOR TBILISI 2-3 SEPTEMBER 1957

FIGURE 4
TELLUROGRAM FOR TBILISI 20 SEPTEMBER 1957

FIGURE 5
TELLUROGRAM FOR TBILISI 20 SEPTEMBER 1957
(CONTINUATION OF FIGURE 4)

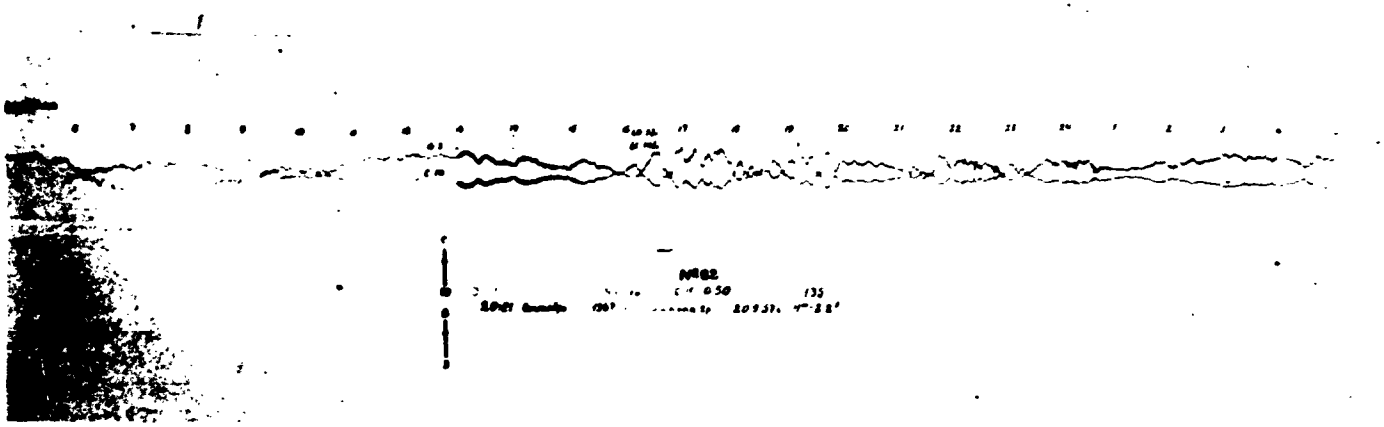

FIGURE 6
TELLUROGRAM FOR ASHKHABAD 20 SEPTEMBER 1957

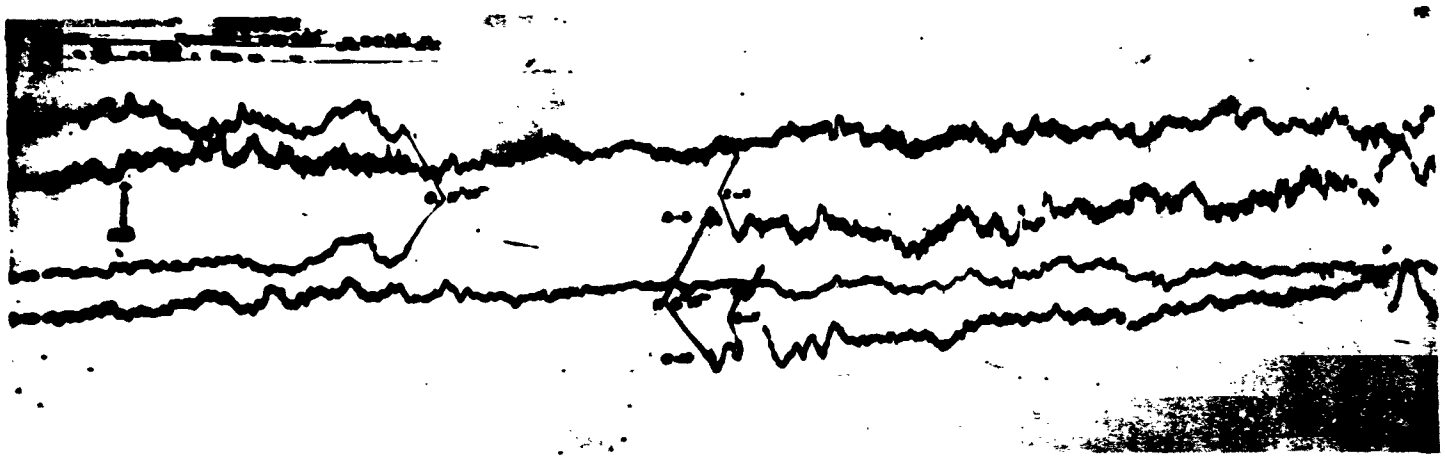

FIGURE 7
TELLUROGRAM FOR LVOV 20 SEPTEMBER 1957

of the record to assure selection of a sampling interval fine enough to prevent distortion of the spectrum through aliasing (see Chapter II).

The magnetograms contained records of the horizontal component of the magnetic field (H), the vertical component of the magnetic field (Z), and the declination (D). The H and D records were used to compute the North-South and East-West components of the horizontal magnetic field through the relations

N-S Magnetic = H cos D, and

E-W Magnetic = H sin D.

Machine Processing

Figure 8 is a flow chart showing the steps in the machine computation of the power spectrum of a single time series. In cases where simultaneous magnetic and telluric data are processed, the program is considerably more complicated since various combinations of cross-correlation, cross-power, coherency and phase angles along with apparent resistivity, apparent conductivity, and the frequency response of the earth are computed.

In the early stages of the work, computation was performed on the IBM 650 at the Computation Center of The University of Texas. Subsequently, the IBM 650 was replaced by a CDC 1604 machine. The bulk of the computation was performed on the new machine.

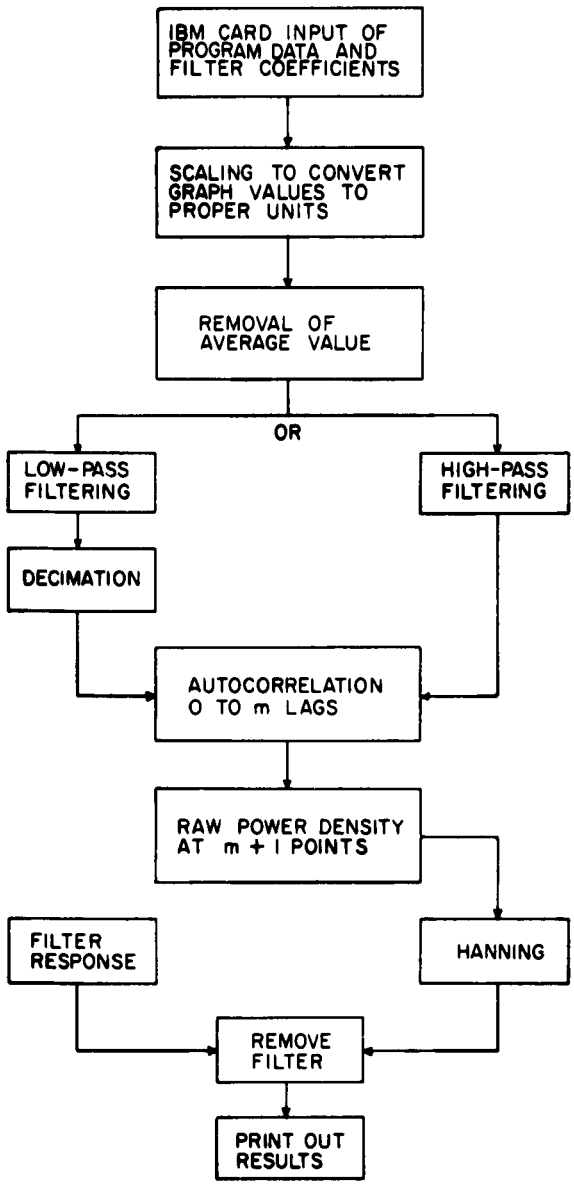

FIGURE 8
MACHINE COMPUTATION FLOW CHART FOR A SINGLE TIME SERIES

CHAPTER II

SAMPLE DATA CONSIDERATIONS

A continuous function of time is completely determined by its values at equally spaced intervals provided that the continuous function contains no frequencies higher than, say, W cycles per second, and the ordinates are given at points spaced 1/2W seconds apart, the series of values extending for all time [8]. Here the analysis is to be based on sampled values obtained from continuous records that are not infinite in extent and are not band limited. Analysis based on finite amounts of data is common to statistical work and will be considered in due course. The fact that the original functions are not band limited will be discussed in connection with the problem of aliasing.

Aliasing

An important consideration in the computation of power spectra from equi-spaced sample data is the problem of aliasing. Figure 9 shows portions of two sine waves of different frequencies. Attention is focused on the equally spaced sample data values which are the same for each sine wave even though the waves differ in frequency. Thus, given only the sample values, a sine wave of a given frequency may be confused with a sine wave of higher frequency. Specifically, if a harmonic time function $x(t)$ is sampled at equally spaced time intervals Δt, then a frequency

$$f_N = \frac{1}{2\Delta t} \quad ,$$

called the Nyquist or folding frequency [9], exists such that the functions with frequencies

$$f + n\, f_N \quad , \quad \text{for } n = 0,2,4,\cdots \ ,$$

are not distinguishable. For example, consider the function

$$x(f,t) = \sin 2\pi f t \quad ,$$

sampled at $k\Delta t$ ($k = 0, 1, 2,\cdots$) so that the sampled values of x are

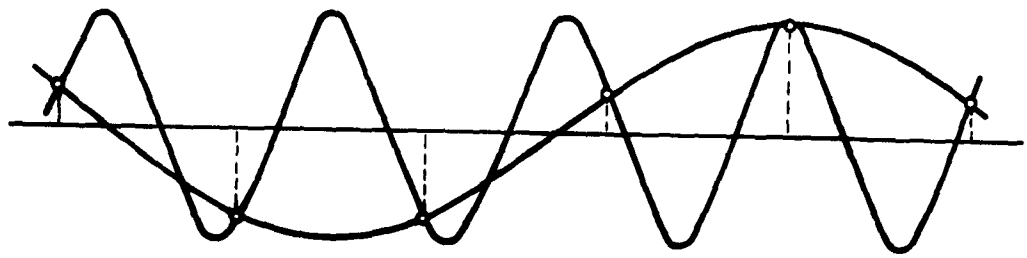

FIGURE 9
SINE WAVES OF DIFFERENT FREQUENCIES WITH THE SAME SET OF EQUALLY SPACED SAMPLE VALUES

$$x(f,k\Delta t) = \sin 2\pi fk\,\Delta t \quad .$$

Now consider the function

$$x(f \pm n\, f_N, t) = \sin 2\pi(f + n\, f_N)t \quad ,$$

where

$$f_N = \frac{1}{2\Delta t} \quad , \text{ and}$$

$$n = 0, 2, 4, 6, \cdots,$$

sampled at equi-spaced intervals Δt so that the sampled values are

$$x(f \pm n\, f_N, k\Delta t) = \sin 2\pi(f \pm n\, f_N)k\Delta t \quad .$$

Use of simple trigonometric identities reveals that

$$x(f, k\Delta t) = x(f \pm n\, f_N, k\Delta t) \quad .$$

Obviously, then, power contributed to a power spectrum at a given frequency f cannot be distinguished from powers contributed by frequencies $f \pm n\, f_N$. This translation of frequencies is known as aliasing [7]. If the data actually contain power at frequencies greater than f_N, this power will be "folded back" into the principal band which extends from 0 to f_N. Power that is folded back results in a distortion of the true power spectrum in the principal band.

To make the effect of aliasing negligible it is necessary to select a sampling interval "small enough" to place the Nyquist frequency beyond all significant power contributions.

Frequency Resolution

Questions of frequency resolution have to do with the number of power spectral estimates per unit frequency and to what extent a particular estimate has been affected by power at other frequencies.

Leaving aside for the moment the possibility of filtering, the selection of the length of the sampling interval, Δt, is determined by the relative

amount of power occurring at frequencies higher than the Nyquist frequency associated with Δt. The sampling interval must be selected small enough to bring the aliased power, if any, to a tolerable minimum. That is, the contribution due to aliased power should be less than the statistical accuracy of an estimate in the principal band. Once the length of sampling interval has been established and the autocorrelation is computed for m lags (see equation 31), the power spectrum is computed at m + 1 equally spaced frequency values in a band extending from zero to the Nyquist frequency [9]. For a fixed record length a compromise must be reached between frequency resolution and the stability of power spectral estimation. Attempts to increase the frequency resolution by increasing the number of lags are met by a decrease in the stability, since the stability is a function of the number of lags [7]. However, an increase in the frequency resolution can be effected without a corresponding decrease in stability by increasing the record length. This procedure may lead to a prohibitive amount of additional labor.

The refined power spectral estimate at a particular frequency is computed using a weighted average of the raw estimate at that frequency and the raw estimates immediately adjacent to that particular frequency (see equations 34, 35, and 36).

Purpose of Filtering

In the spectral computations considered here, a high-pass filter is used to prewhiten (specifically, flatten) the spectrum, and a low-pass filter is used to reshape the spectrum prior to decimation (see next page).

A common feature of the power spectra computed and plotted here is the rapid decrease of power with increasing frequency. Tukey points out how the computation of estimates on a spectrum with large slope leads to errors. The purpose of high-pass filtering is to make the spectrum flat before the power spectral computation. The filter is removed after computation to restore the spectrum to its true shape.

When it is of interest to examine the low frequency portion of the Nyquist band in greater detail, that is, compute spectral estimates at closer

frequency intervals, two ways of accomplishing this are available. As has already been mentioned, the number of lags could be increased. This requires a large amount of additional labor and for a fixed length leads to increased instability in the estimates. The other approach is to apply a low-pass filter to the original data, with sampling interval Δt, and then compute the power spectrum with respect to a new Nyquist frequency f'_N. The process of converting the sampling interval to a new sampling interval which is an integer multiple of the original interval is known as decimation.

If it is possible to compute an undistorted spectrum after decimation, then the original Δt was smaller than necessary. In general, decimation must be preceded by low-pass filtering. Figure 10 shows an example of a power spectrum before and after low-pass filtering.

Confidence Limits

The values of power spectral density are computed from finite amounts of data and therefore are statistical estimates of the true values. The Tukey method [7] provides confidence intervals by which the variability of the estimates may be computed. Confidence intervals are a familiar feature of statistical analysis [10] and will not be discussed here. However, it is important to note that the basis for the Tukey values is the assumption that the process is Gaussian and the distribution of the spectral estimates follows the so-called "chi-square" distribution.

All of the power spectra computed here have eighty percent confidence limits indicated on the graphs.

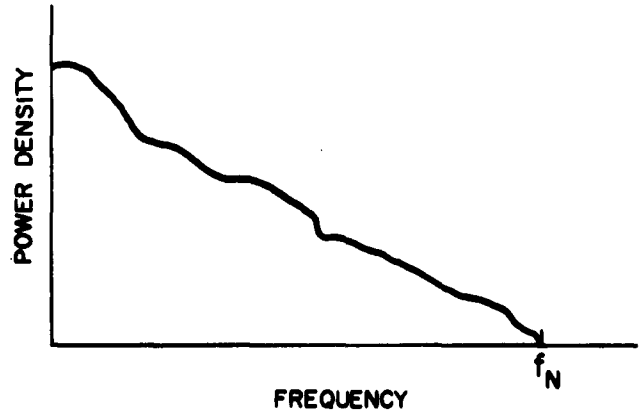

POWER SPECTRUM BEFORE LOW-PASS FILTERING

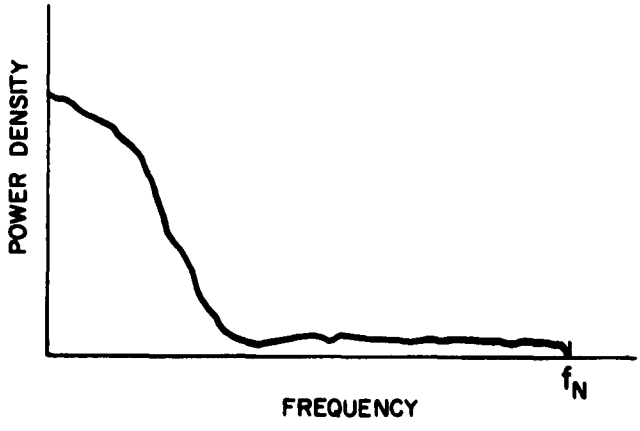

POWER SPECTRUM AFTER LOW-PASS FILTERING

FIGURE 10

EXAMPLE OF A POWER SPECTRUM BEFORE AND AFTER LOW-PASS FILTERING

CHAPTER III

TIME-DOMAIN FILTERS

Figure 11 shows a block diagram of a stationary linear passive electric wave filter. A four terminal electrical network is said to be a stationary linear passive filter if (1) the properties of the network do not change with time, (2) the output voltage remains at zero until a zero input voltage changes to a non-zero value, (3) a linear combination of input voltages results in an output voltage that is the sum of the effects due to each input voltage separately, and (4) there are no energy sources within the circuit. For a stationary linear passive filter, the output voltage, expressed as a function of time, may be obtained from the input through some relating operator. Here the interest is in linear operators which mathematically perform the same operation as an electrical filter, but are more general in that they are not limited by the realizability conditions imposed on physical filters. Both the impulse response and the frequency response are characteristic of the filter for particular inputs. That is, the impulse response is the output for a unit impulse (Dirac delta at t = 0) input, whereas the frequency response is the relation between the output and input for a sinusoidal input. In particular the impulse response relates the output, H(t), to the input, G(t), through the relation [11]

$$H(t) = \int_{0^-}^{\infty} G(t - \tau)\, W(\tau) d\tau \quad , \tag{1}$$

where G(t) is the input at time t

H(t) is the output at time t, and

W(t) is the impulse response.

The 0^- extends the lower limit to negative values since the Dirac delta input at t = 0 extends "across zero." The impulse response shows the "memory" property of the filter in that it determines how the past of the input effects the output at time t.

If the input is a unit amplitude sinusoidal function, say,

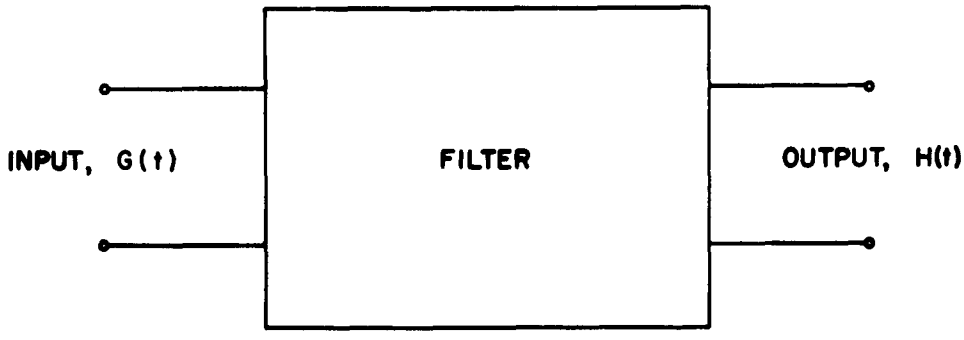

FIGURE 11
FOUR TERMINAL ELECTRICAL FILTER

$$G(t) = e^{j2\pi ft} \tag{2}$$

and then one uses equation (1) to find the output, one has

$$H(t) = \int_{0^-}^{\infty} W(\tau)\, e^{j2\pi f(t-\tau)} d\tau \quad , \tag{3}$$

or

$$H(t) = e^{j2\pi ft} \int_{0^-}^{\infty} W(\tau)\, e^{-j2\pi f\tau} d\tau. \tag{4}$$

Letting

$$Y(f) = \int_{0^-}^{\infty} W(\tau)\, e^{-j2\pi f\tau} d\tau \quad , \tag{5}$$

one has

$$H(t) = Y(f)\, G(t) \quad . \tag{6}$$

$Y(f)$, as defined in equation (5) is what is usually referred to as the frequency response of the filter.

In this paper filtering will be accomplished by a linear operation referred to as time-domain filtering [12]. The filter input consists of a set of numbers which represent the amplitude of the record to be analyzed at equally spaced points separated by the time interval Δt. The filtering operation is carried out by using the relation

$$v(t) = \sum_{k=0}^{K} a_k\, u(t - k\,\Delta t) \quad , \tag{7}$$

where $v(t)$ is the filter output at t,

$u(t)$ is the filter input at t, and

a_k are a set of $K + 1$ numerical coefficients which will be referred to as the filter coefficients of the linear operator.

Equation (7) may be considered as an approximation to equation (1) [13]. This is accomplished by replacing the infinite limit by the finite number K,

applying Simpson's rule to the integrand (using Δt as the spacing interval), and choosing the values of W to be

$$W(k\Delta t) = a_k \tag{8}$$

where $k = 0, 1, 2, \cdots, K$.

In his paper [13], Dr. Horton discusses the mean square error in this approximation and a method for calculating the numerical coefficients to be used to obtain a desired frequency response. The fact that this is an approximation will be suppressed here since the exact values of the frequency response for a corresponding physical filter need not be considered. The viewpoint is taken here that, given a function u(t) defined at discrete equally spaced values and given a set of K + 1 numbers, a_k, a new function v(t) may be computed according to the relation (7).

If the input function happens to be a unit sinusoidal function $\exp(j2\pi ft)$, then the computed (filtered or output) function becomes

$$v(t) = \sum_{k=0}^{K} a_k \, e^{j2\pi f(t - k\Delta t)} \quad , \tag{9}$$

or

$$v(t) = \left\{ \sum_{k=0}^{K} a_k \, e^{-j2\pi fk\Delta t} \right\} e^{j2\pi ft} \quad . \tag{10}$$

Letting

$$Y(f) = \sum_{k=0}^{K} a_k \, e^{-j2\pi fk\Delta t} \quad , \tag{11}$$

one has

$$v(t) = Y(f)\, u(t) \quad . \tag{12}$$

Y(f), as expressed by equation (11), will be referred to as the frequency response function. Since Y(f) is periodic of period $1/\Delta t$, a selection of

$$-\frac{1}{2\Delta t} \leq f \leq +\frac{1}{2\Delta t}$$

for the fundamental range of definition relates the cut-off frequency of the filter to the Nyquist frequency for a sampling interval Δt.

The two filters used in this paper are an 18-term high-pass filter [12] and a 9-term low-pass filter [13]. The numerical coefficients for these filters are given in Table 1.

The frequency response is computed (at N + 1 points) from the filter coefficients by letting

$$Y(f) = \sum_{n=0}^{N} a_n\, e^{-j2\pi nf\Delta t} \quad , \tag{14}$$

$$= A(f) - j\, B(f) \quad ,$$

so that

$$A(f) = \sum_{n=0}^{N} a_n \cos(2\pi nf\Delta t) \quad , \tag{15}$$

and

$$B(f) = \sum_{n=0}^{N} a_n \sin(2\pi nf\Delta t) \quad . \tag{16}$$

TABLE I

LINEAR OPERATORS USED TO FILTER RAW SAMPLED DATA

Case A: High-pass Filter (18 coefficients)

Case B: Low-pass Filter (9 coefficients)

i	Case A	Case B
0	49.2	0.0078
1	-100.0	0.0508
2	31.5	0.1266
3	72.8	0.1977
4	-13.4	0.2302
5	-33.2	0.1977
6	-17.9	0.1266
7	3.3	0.0508
8	9.9	0.0078
9	3.8	
10	-2.7	
11	-3.8	
12	-1.0	
13	1.2	
14	1.2	
15	0.1	
16	-0.6	
17	-0.4	

Recalling that the fundamental period is defined for the frequency range $0 \leq |f| \leq 1/2\Delta t$ it is convenient to set

$$f_N = \frac{1}{2\Delta t} \quad , \tag{17}$$

and

$$f_q = \frac{q}{m} f_N \quad , \tag{18}$$

where f_N is the Nyquist frequency. Equation (18) is substituted into equations (15) and (16) to give

$$A(f_q) = \sum_{n=0}^{N} a_n \cos\left(\pi \frac{nq}{m}\right) \quad , \tag{19}$$

and

$$B(f_q) = \sum_{n=0}^{N} a_n \sin\left(\pi \frac{nq}{m}\right) \quad , \tag{20}$$

where $q = 0, 1, 2, 3, \cdots, m$.

The frequency response is then computed from

$$|Y(f)| = \left| \sqrt{A(f)^2 + B(f)^2} \right| \tag{21}$$

and the phase delay is given by

$$\varphi(f) = \arctan\left[\frac{B(f)}{A(f)}\right] \quad . \tag{22}$$

Figure 12 shows a plot of the filter coefficients versus time for the high-pass filter, Case A of Table 1. Figure 13 shows a plot of the filter coefficients versus time for the low-pass filter, Case B of Table 1.

Figure 14 shows the frequency response of the high-pass and low-pass filters.

Figure 15 shows the phase delay for the high-pass filter. The phase delay for the low-pass filter is a straight line since the filter is symmetric and is not plotted here.

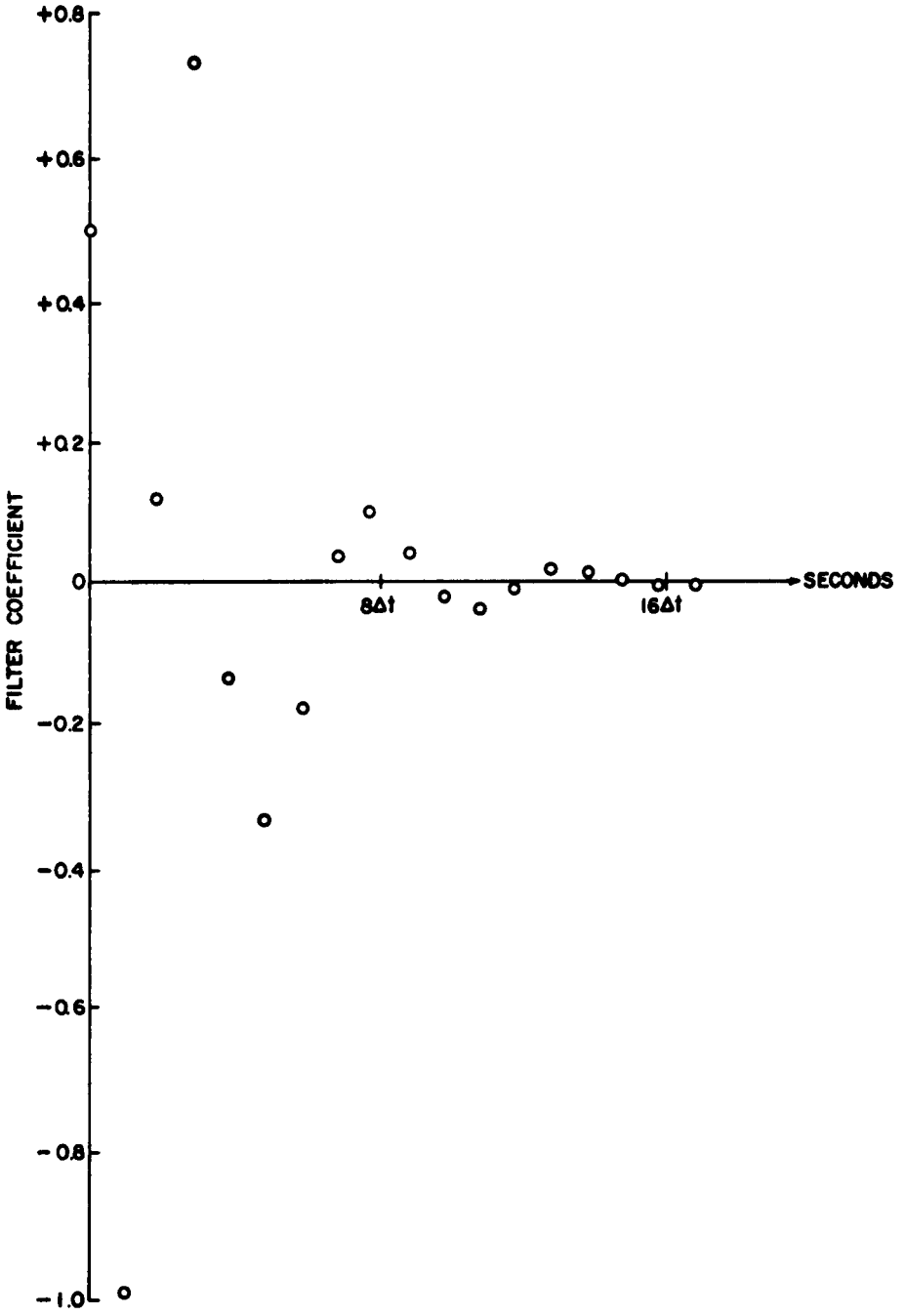

FIGURE 12
THE FILTER COEFFICIENTS OF THE HIGH-PASS FILTER, CASE A OF TABLE I

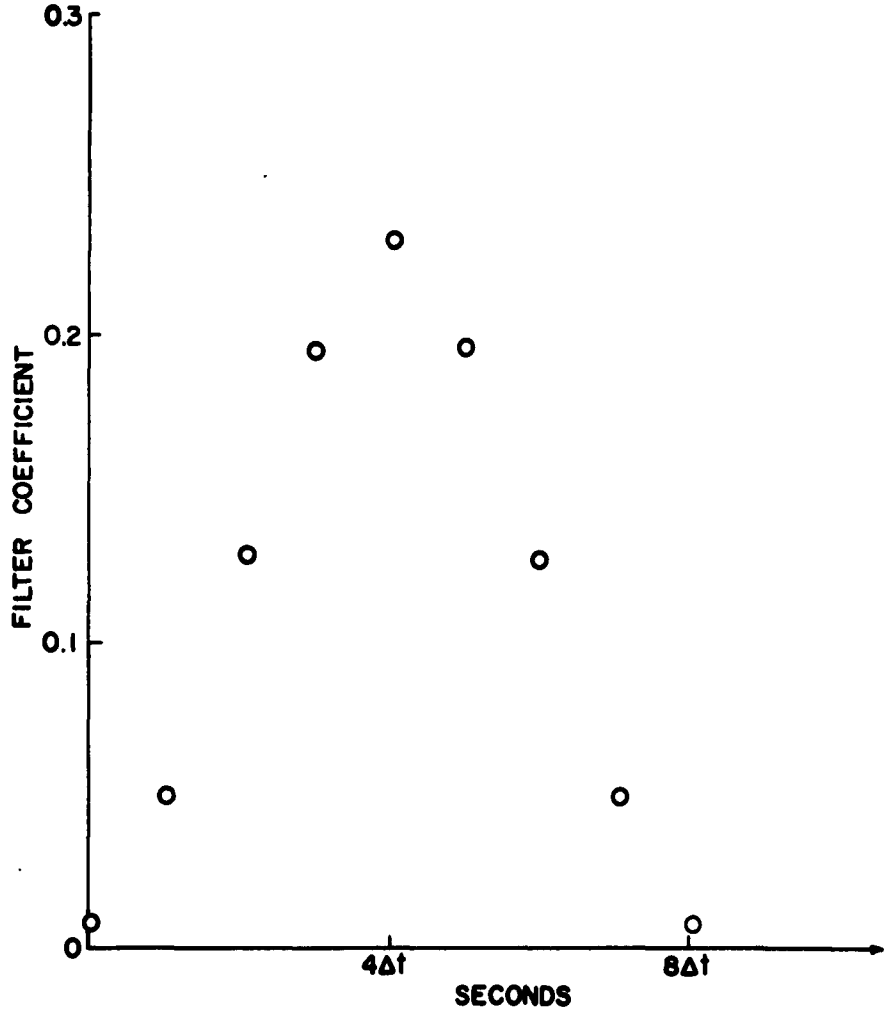

FIGURE 13
THE FILTER COEFFICIENTS OF THE LOW-PASS FILTER, CASE B OF TABLE I

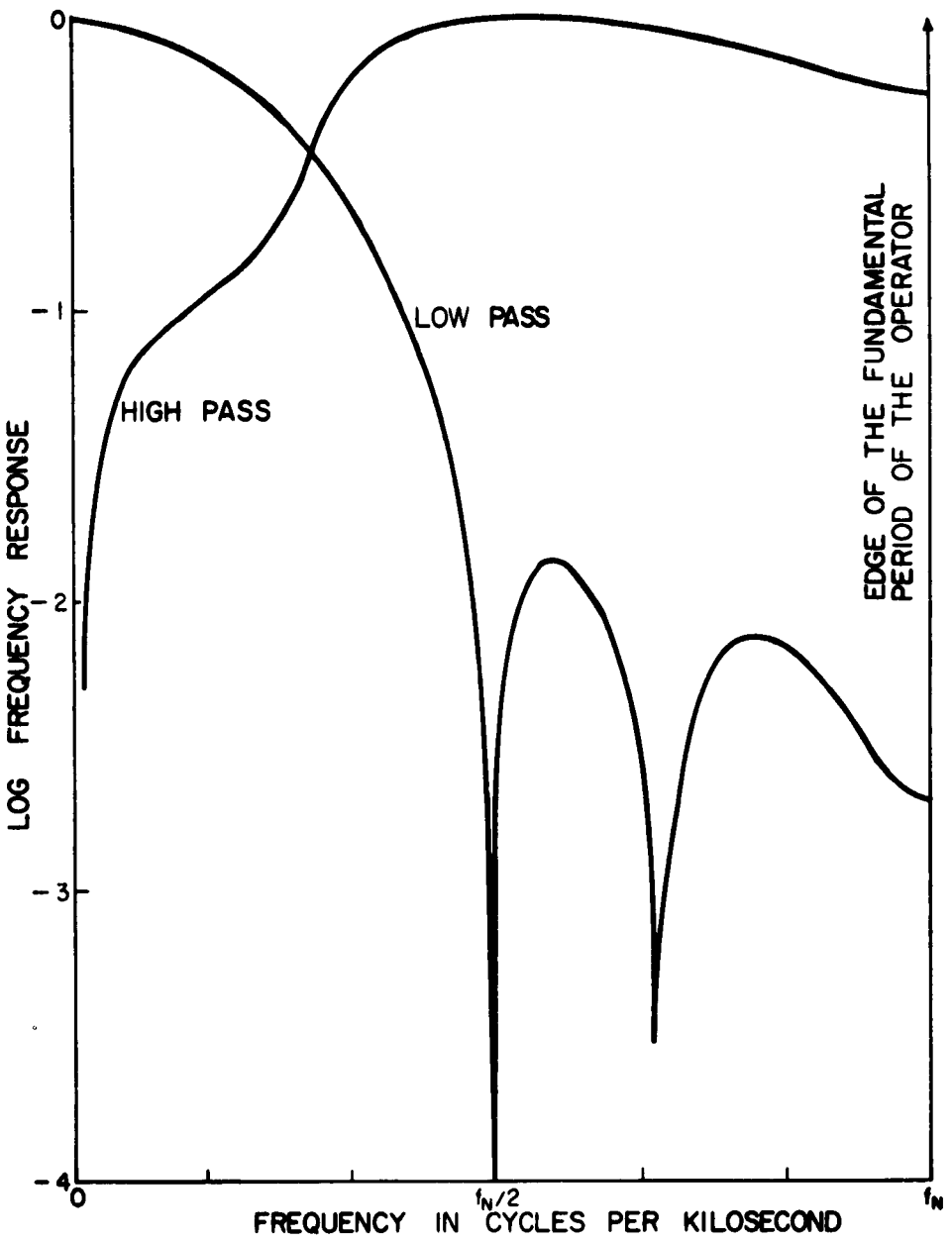

FIGURE 14
THE FREQUENCY RESPONSE OF LOW-PASS AND HIGH-PASS FILTERS, TABLE I.

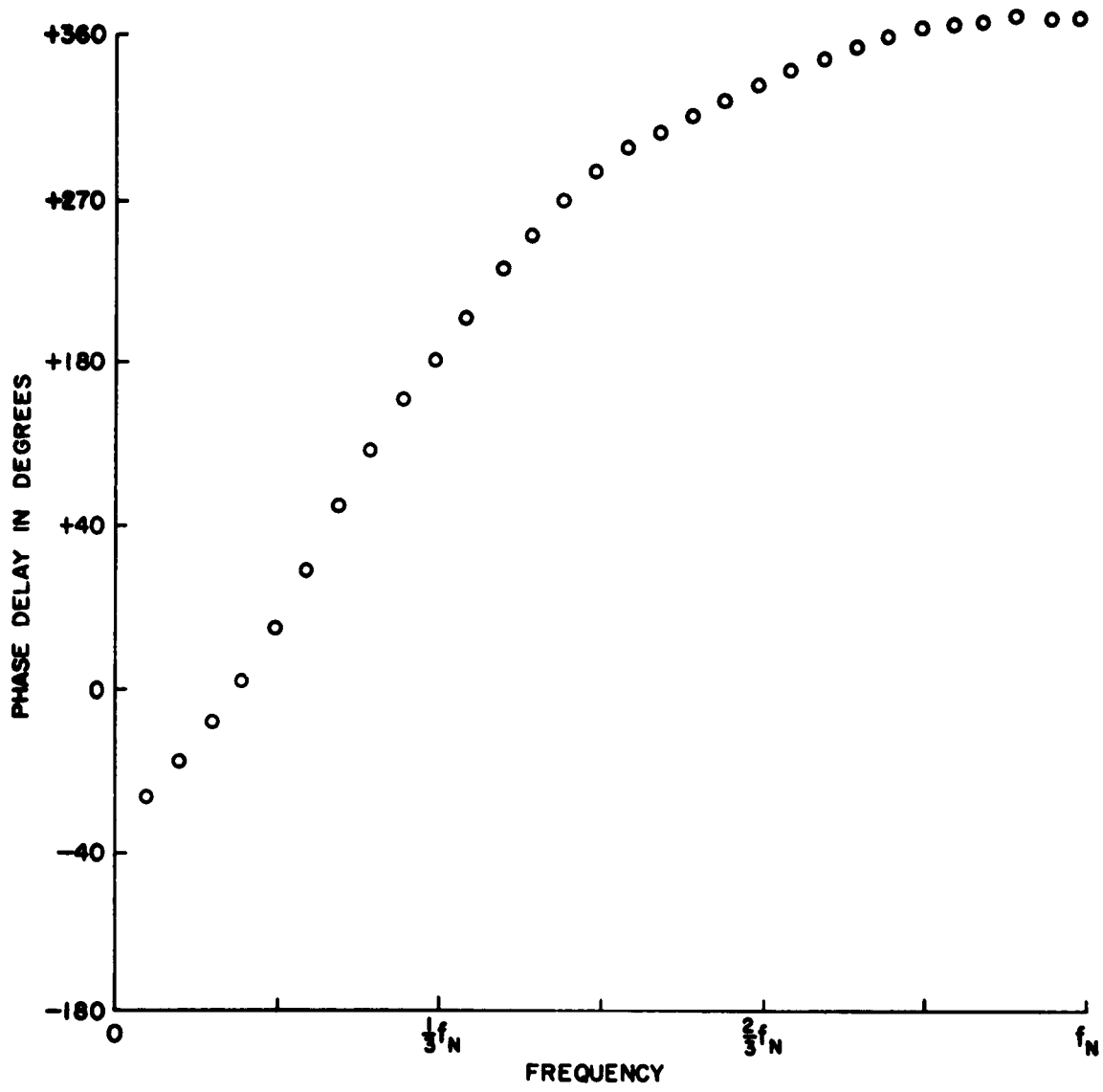

FIGURE 15
THE PHASE DELAY FOR HIGH-PASS FILTER,
CASE A OF TABLE I

CHAPTER IV

STATISTICAL ANALYSIS FOR A SINGLE TIME SERIES

The results presented in this dissertation are obtained by the application of the technique of power spectral analysis to the study of the low frequency magnetotelluric field of the earth. Computational procedures are used that yield the statistical variance spectrum of a time series. Other names for the resultant computation are power density spectrum, second-degree spectrum and quadratic spectrum. All of these names refer to the distribution of variance as a function of frequency. It is beyond the scope of this paper to present a formal derivation of the formulas used in power spectral computation; many complete discussions of this type are available [7, 15, 16, 17]. However, an outline of the results will be presented to acquaint the reader with the basis for the formulas used. The excuse for the use of the engineering term "power" in connection with statistical variance is that the variance for a time series with zero mean is equal to the ac power dissipated in a one ohm pure resistance [9].

For deterministic functions such as periodic and aperiodic functions a harmonic analysis is usually carried out by Fourier series analysis and by Fourier integral analysis, respectively. The discrete line spectrum for a periodic function and the continuous spectrum for the aperiodic function may be determined analytically because these deterministic functions are by definition "known for all values of time."

Random series [17] are a class of functions which are not deterministic and do not lend themselves to the harmonic analysis techniques discussed above. In this paper attention will be restricted to those random time series which very closely approximate a stationary random ergodic process. Functions which represent stationary random ergodic processes are characterized by probability distributions that do not change with time and the time average over a sample function of an ensemble of functions is equivalent to an average over the ensemble of functions. These functions are referred to as stationary time series. Records of the earth's magnetic and electric fields are selected

which are assumed to approximate closely the above conditions. It should be noted that proof of the ergodic hypothesis in a practical case appears to be impossible [15].

Wiener [18] has shown that the autocorrelation function, $\varphi_{xx}(\tau)$, defined by

$$\varphi_{xx}(\tau) = \lim_{T\to\infty} \frac{1}{T} \int_{-T/2}^{T/2} x(t)\, x(t+\tau)\, dt \quad , \tag{23}$$

for $-\infty < \tau < +\infty$,

where $x(t)$ is a stationary time series, has a Fourier transform, $\Phi_{xx}(f)$, given by

$$\Phi_{xx}(f) = \int_{-\infty}^{\infty} \varphi_{xx}(\tau)\, e^{-j2\pi f\tau}\, d\tau \quad , \tag{24}$$

which turns out to be the power density spectrum of $x(t)$. Stated another way, the Wiener theorem [19] shows that the power density spectrum of $x(t)$, defined by

$$\varphi_{xx}(f) = \lim_{T\to\infty} \frac{1}{T} \left| \int_{-T/2}^{T/2} x(t)\, e^{-j2\pi ft}\, dt \right|^2 \quad , \tag{25}$$

has a Fourier transform

$$\varphi_{xx}(\tau) = \int_{-\infty}^{\infty} \Phi_{xx}(f)\, e^{j2\pi ft}\, df \quad , \tag{26}$$

which turns out to be the autocorrelation function for $x(t)$.

The power spectral analysis is based on computational methods recommended by Blackman and Tukey [7]. The method consists of estimating the spectrum of a discrete time series by computing numerical approximations to equations (23) and (24). Since equation (23) is an even function of τ, equation (24) may be simplified to

$$\Phi_{xx}(f) = 2 \int_{0}^{\infty} \varphi_{xx}(\tau) \cos 2\pi ft\, dt \quad . \tag{27}$$

An important feature of the Tukey method is that it provides a means of estimating the power spectral density from finite sets of sampled data with a knowledge of the accuracy of the estimate. A brief outline of the procedure will be given, but no attempt will be made to reproduce this work [7] here.

An experimental data record of finite length is sampled at equally spaced intervals (Δt) yielding a discrete time series

$$X_1, X_2, X_3, \cdots, X_N,$$

which will be referred to as the raw data. As has already been shown (Chapter II) the selection of the length of the sampling interval for a particular record has important implications. To avoid trouble from aliasing a minimal requirement on the choice of Δt would be such that no more than one relative maxima or minima occur in any interval Δt.

The average value for the series,

$$< X(t) > = \frac{1}{N} \sum_{n=1}^{N} X_n \tag{28}$$

where $X_n = X(n\Delta t)$

for $n = 1, 2, \cdots, N,$

is subtracted from each X_n using the relation

$$\bar{X}_n = X_n - < X(t) > \tag{29}$$

to remove the dc or mean value from the series.

The $\bar{X}_n$ are then filtered (see equation 7). Each filtered value is computed by

$$x_n = \sum_{k=0}^{K} a_k \bar{X}_{n - k\Delta t} \quad , \tag{30}$$

where x_n are the filtered values,

a_k are the operator coefficients,

Δt is the sampling interval,

$\bar{X}$ are the raw data from which the average value has been subtracted, and,

$k+1$ is the number of filter coefficients.

It should be noted that this method of filtering reduced slightly the number of values available for the autocorrelation computation. Fortunately, suitable filters with relatively few coefficients were available.

The estimates of the unnormalized autocorrelation at lag $\tau(= n\Delta t)$ are computed from the filtered values by

$$C_{xx}(\tau) = \frac{1}{N-K-n} \sum_{p=1}^{N-K-n} x_p \cdot x_{p+\tau} \quad , \tag{31}$$

for $n = 0, 1, 2, \cdots, m$,

where $C_{xx}(\tau)$ is the computed autocorrelation at lag $\tau(= n\Delta t)$,

N is the number of raw data values,

$K+1$ is the number of filter coefficients,

m is the number of lags, and

x_p are the filtered values.

The $C_{xx}(\tau)$ are often referred to as the sample serial products, mean lagged products, or autocorrelation coefficients. Figures 16 and 17 are autocorrelations computed from high-pass filtered values and from low-pass filtered values. Comparison of Figures 16 and 17 shows the obvious effects of filtering and decimating.

The raw spectral density estimates are computed by applying a discrete finite cosine series transform to the mean lagged products according to the formula

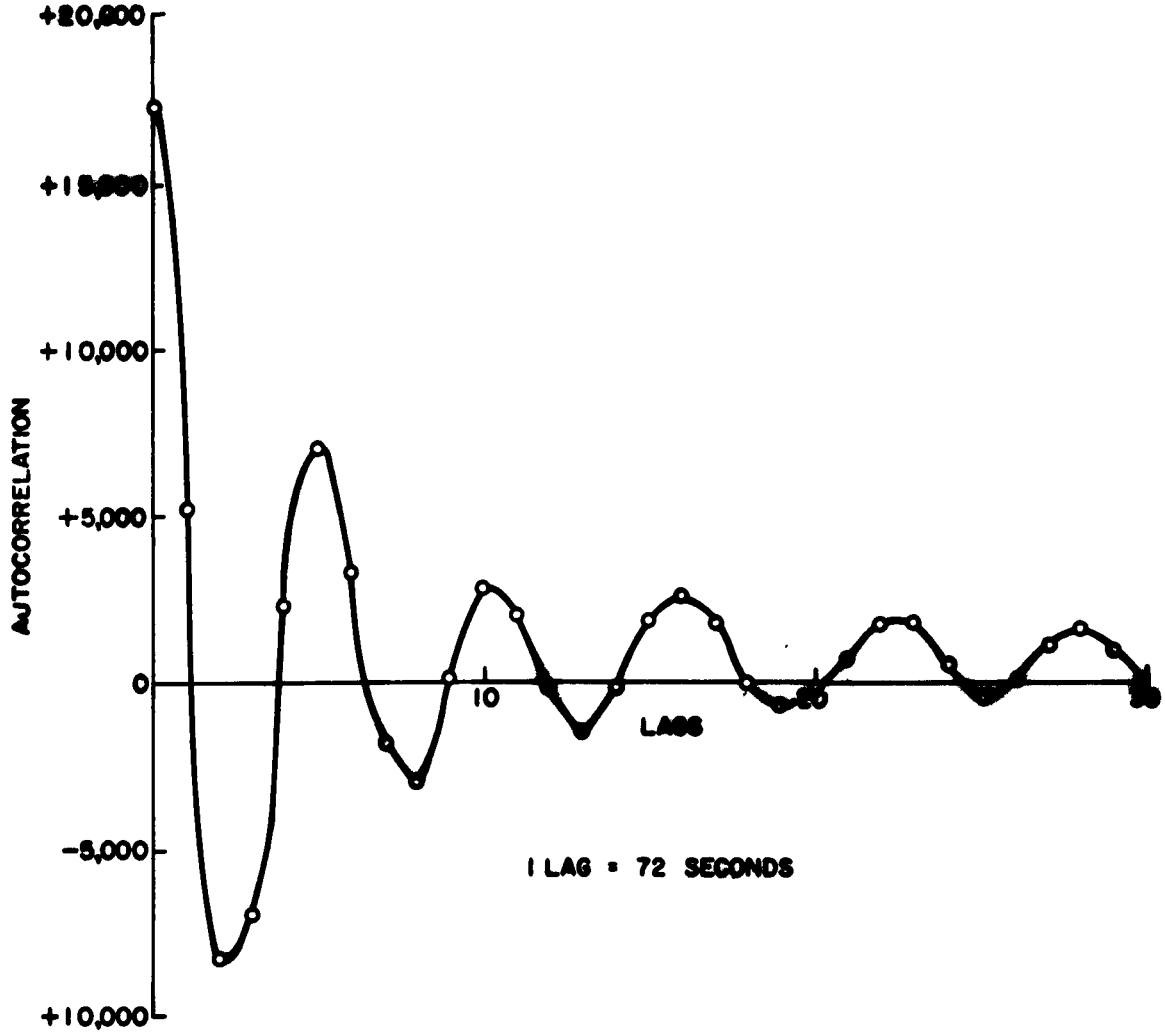

FIGURE 16

THE AUTOCORRELATION FOR HIGH-PASS FILTERED DATA FROM EAST-WEST MAGNETIC FIELD AT TBILISI 1 SEPTEMBER 1957

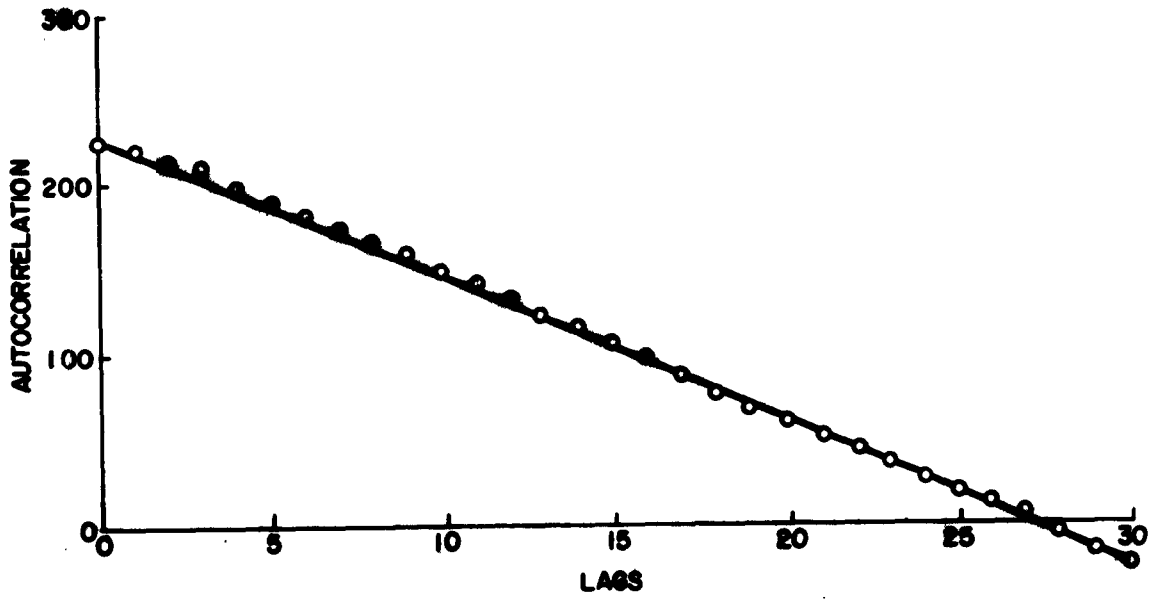

1 LAG = 288 SECONDS

FIGURE 17
THE AUTOCORRELATION FOR LOW-PASS FILTERED DATA FROM EAST-WEST MAGNETIC FIELD AT TBILISI 1 SEPTEMBER 1957

$$Q_{xx}(r) = \left[C_{xx}(0) + 2 \sum_{q=1}^{m-1} C_{xx}(q) \cos\left(\frac{qr\pi}{m}\right) + C_{xx}(m) \cos(\pi r) \right] \Delta t, \quad (32)$$

for r = 0, 1, 2,···, m.

It is necessary to compute $Q_{xx}(r)$ only for r in the above range since $Q_{xx}(r)$ is symmetric in r. The frequency corresponding to r is

$$f = \frac{r}{2m\Delta t} \quad . \quad (33)$$

The systematic statistical errors resulting from use of a finite length of data appear in the values of Q_{xx}. The Tukey technique to obtain improved spectral estimates involves a smoothing or refining operation performed on the raw estimates. The specific smoothing operation used here is referred to as hanning [7]. The refined spectral estimates, P'_{xx}, are computed using the relations

$$P'_{xx}(0) = 0.5 \, [Q_{xx}(0) + Q_{xx}(1)] \quad , \quad (34)$$

$$P'_{xx}(r) = 0.5 \, Q_{xx}(r) + 0.25 \, [Q_{xx}(r-1) + Q_{xx}(r+1)], \quad (35)$$

and

$$P'_{xx}(m) = 0.5 \, [Q_{xx}(m) + Q_{xx}(m-1)], \quad (36)$$

where r = 1, 2,···, m-1.

Finally the filter is removed by dividing each refined power spectral estimate by the square of the frequency response of the filter at that frequency (see equation 21). That is,

$$P_{xx}(f) = \frac{P'_{xx}(f)}{|Y(f)|^2} \quad (37)$$

where $P_{xx}(f)$ is the refined spectral estimate at f after filter removal,

$P'_{xx}(f)$ is the refined spectral estimate at f, and

$Y(f)$ is the filter response at f.

It is important to note that the spectral estimate as expressed in equation (37) is a function of frequency only and no information about phase is contained therein.

CHAPTER V

STATISTICAL ANALYSIS FOR TWO TIME SERIES

The statistical analysis for a single time series is extended to the case of two time series by defining the cross-correlation functions [18]

$$\varphi_{xy}(\tau) = \lim_{T\to\infty} \frac{1}{T} \int_{-T/2}^{T/2} x(t)\, y(t+\tau)\, dt \quad , \tag{38}$$

and

$$\varphi_{yx}(\tau) = \lim_{T\to\infty} \frac{1}{T} \int_{-T/2}^{T/2} y(t)\, x(t+\tau)\, d\tau \quad , \tag{39}$$

where $-\infty < \tau < +\infty$,

for the stationary time series X(t) and Y(t). The corresponding cross-spectral densities are given by

$$\Phi_{xy}(f) = \int_{-\infty}^{\infty} \varphi_{xy}(\tau)\, e^{-j2\pi f\tau}\, d\tau \quad , \tag{40}$$

and

$$\Phi_{yx}(f) = \int_{-\infty}^{\infty} \varphi_{yx}(\tau)\, e^{-j2\pi f\tau}\, d\tau \quad , \tag{41}$$

which are the Fourier transforms of equations (38) and (39), respectively. Again the method consists of computing estimates of equation (40) which are numerical approximations.

Two experimental records of finite length are sampled at equally spaced intervals (Δt) yielding the discrete time series

$$X_1, X_2, X_3, \cdots, X_N \quad , \text{ and}$$

$$Y_1, Y_2, Y_3, \cdots, Y_N \quad .$$

The average value is removed from each series and then each series is subjected to the filtering operation (see equations 29 and 30).

The cross-correlation functions, equations (38) and (39), are not symmetric functions of τ and changing the order of x and y changes the value. However, φ_{xy} and φ_{yx} are related by

$$\varphi_{xy}(\tau) = \varphi_{yx}(-\tau) \quad . \tag{42}$$

Furthermore, unlike the autocorrelation functions, the cross-correlation functions are not "even" functions of τ. This means that the Fourier transform will have both real and imaginary parts. The estimates of the unnormalized cross-correlation at lag $\pm\tau(\tau = \pm n\Delta t)$ are computed from the filter values by

$$C_{xy}(\tau) = \frac{1}{N-K-n} \sum_{p=1}^{N-K-n} x_p \, y_{p+\tau} \quad , \tag{43}$$

and

$$C_{xy}(-\tau) = \frac{1}{N-K-n} \sum_{p=1}^{N-K-n} x_p \, y_{p-\tau} \quad , \tag{44}$$

for n = 0, 1, 2,$\cdots$, m,

where $C_{xy}(\tau)$ is the positive shift computed autocorrelation at lag τ,

$C_{xy}(-\tau)$ is the negative shift computed autocorrelation at lag τ,

N is the number of raw data values,

K+1 is the number of filter coefficients,

m is the number of lags, and, x_p and y_p are the filtered values.

By separating the odd and even contributions to the cross-correlations, the Fourier transformation can be carried out by taking the sine and cosine transformations separately. That is, defining

$$R_{xy}^{even}(\tau) = \frac{1}{2}\left[C_{xy}(\tau) + C_{xy}(-\tau)\right] \quad , \tag{45}$$

and

$$R_{xy}^{odd}(\tau) = \frac{1}{2}\left[C_{xy}(\tau) - C_{xy}(-\tau)\right] \quad , \tag{46}$$

the cross-spectral density is computed by

$$Q_{xy}(r) = Re\left[Q_{xy}(r)\right] + j\ I_m\left[Q_{xy}(r)\right] \quad , \tag{47}$$

in which

$$Re\left[Q_{xy}(r)\right] = \left[R_{xy}^{even}(1) + 2\sum_{q=1}^{m-1} R_{xy}^{even}(q)\cos\left(\frac{qr\pi}{m}\right) + R_{xy}^{even}(m)\cos(r\pi)\right]\Delta t \quad , \tag{48}$$

and

$$I_m\left[Q_{xy}(r)\right] = \left[2\sum_{q=1}^{m-1} R_{xy}^{odd}(q)\sin\left(\frac{qr\pi}{m}\right) + R_{xy}^{odd}(m)\sin(r\pi)\right]\Delta t \quad , \tag{49}$$

for $r = 0, 1, 2, \cdots, m$,

where the frequency corresponding to r is

$$f = \frac{r}{2m\Delta t} \quad . \tag{50}$$

The real and imaginary parts of Q_{xy} are each refined by hanning (see equations 34, 35, and 36) and the filter is removed from each (see equation 37). The resultant cross-spectral density is written as

$$P_{xy}(f) = Re\left[P_{xy}(f)\right] + j\ I_m\left[P_{xy}(f)\right] \quad , \tag{51}$$

or

$$P_{xy}(f) = |P_{xy}(f)|\, e^{j\theta_{xy}(f)} \quad , \tag{52}$$

where

$$|P_{xy}(f)| = + \sqrt{\left\{ \mathrm{Re}\left[P_{xy}(f) \right] \right\}^2 + \left\{ I_m \left[P_{xy}(f) \right] \right\}^2}$$

and

$$\theta_{xy}(f) = \arctan \left[\frac{I_m \left[P_{xy}(f) \right]}{\mathrm{Re}\left[P_{xy}(f) \right]} \right] \tag{54}$$

The argument of the cross-spectral density $\theta_{xy}(f)$, represents the phase difference between the power spectral density of the X and Y record at frequency f. Specifically,

$$\theta_{xy}(f) = \theta_x(f) - \theta_y(f) \quad , \tag{55}$$

where

$\theta_{xy}(f)$ is the phase difference at f,

$\theta_x(f)$ is the phase of the f component of x record, and

$\theta_y(f)$ is the phase of the f component of y record.

The ratio of the magnitude of the cross-power density to the square root of the product of the (auto-) power densities of the x and y records is a measure of the coherency between the records [19]. That is, the coherency coefficient is defined by

$$\mathrm{Coh}_{xy}(f) = \frac{|P_{xy}(f)|}{\sqrt{P_{xx}(f) \cdot P_{yy}(f)}} \tag{56}$$

From the relation [12]

$$\left| P_{xy}(f) \right| \leq \sqrt{P_{xx}(f) \cdot P_{yy}(f)} \quad , \tag{57}$$

it is clear that $P_{xy}(f)$ is different from zero only when common frequencies exist in the X and Y records. For perfectly coherent records the equality prevails and the coherency is equal to unity. In practice, when finite amounts of data are used, the computed values of the coherency may range to values greater than one.

CHAPTER VI

POWER SPECTRA OF THE MAGNETOTELLURIC FIELD

The previous chapters present the methods of data selection, data processing, and the practical formulas of power spectral analysis. This chapter contains the computational results. Table 2 shows a summary of the data analyzed that are computed and the computational parameters associated with each sample. Geophysical interpretations of these computed results are found in Chapter VII.

East-West Telluric Current at Three Russian Stations

Figures 18, 19, and 20 are graphs of the power spectra of the East-West component of the telluric current computed from several hours of rapid-run tellurograms recorded simultaneously at Ashkhabad, Lvov, and Tbilisi on 20 September 1957. The 80% confidence intervals for the decimated (x) and undecimated (o) spectra are indicated in each graph. The values from which the graphs are plotted are given in Tables 3 through 8. All three graphs show a characteristic linear trend superposed by a series of small spectral peaks. In each graph a small amount of aliasing is evident near the Nyquist frequency of the spectra computed from low-pass filtered data. If each graph is approximated by a straight line, it is found that a line of slope -1.6 very nearly fits all three. Within the limits of this approximation an analytical relation of the form

$$P(f) = P_0 f^{-n} \tag{58}$$

where $n = -1.6$,

exists between the power density and frequency for the frequency range covered by these graphs. The question of an empirical formula and the meaning of the spectral peaks will be considered in due course.

It is of interest to compare the power density at these three stations at a particular frequency. At 1 cpks, using Lvov as a reference, the power

TABLE 2

A SUMMARY OF DATA ANALYZED

Figure Number	18	19	20	21, 23	22, 24	25, 27	26, 28	29
Date	20 Sept	20 Sept	20 Sept	1 Sept	2 Sept	1 Sept	2 Sept	1-2 Sept
Telluric Field	E-W	E-W	E-W	E-W	E-W	N-S	N-S	E-W
Magnetic Field	xx	xx	xx	N-S	N-S	E-W	E-W	xx
Paper Speed	22 mm/hr	90 mm/hr	78 mm/hr	22 mm/hr	22 mm/hr	22 mm/hr	22 mm/hr	22 mm/hr
Sample Length, hrs	24	5.5	7.8	10	10	10	10	20
Δt, sec	150	31.6	47.3	72	72	72	72	72
No. of Samples	579	624	590	501	501	501	501	1001
Decimation	4	4	4	4	4	4	4	4
New Δt, sec	600	126.4	189.2	288	288	288	288	288
No. of Decimated Samples	144	156	147	125	125	125	125	250

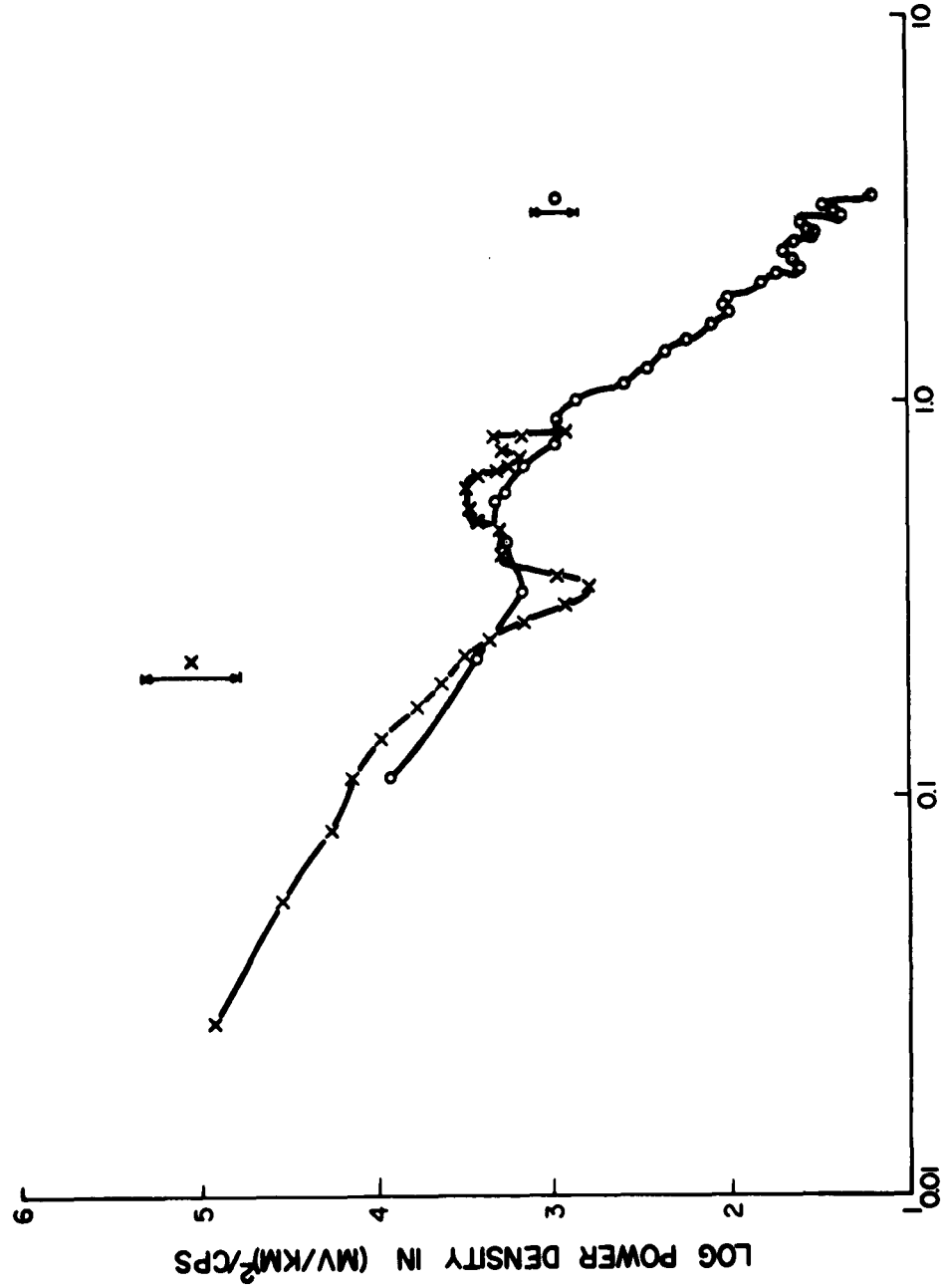

FIGURE 18

THE POWER SPECTRUM OF EAST-WEST TELLURIC FIELD AT ASHKHABAD 20 SEPTEMBER 1957

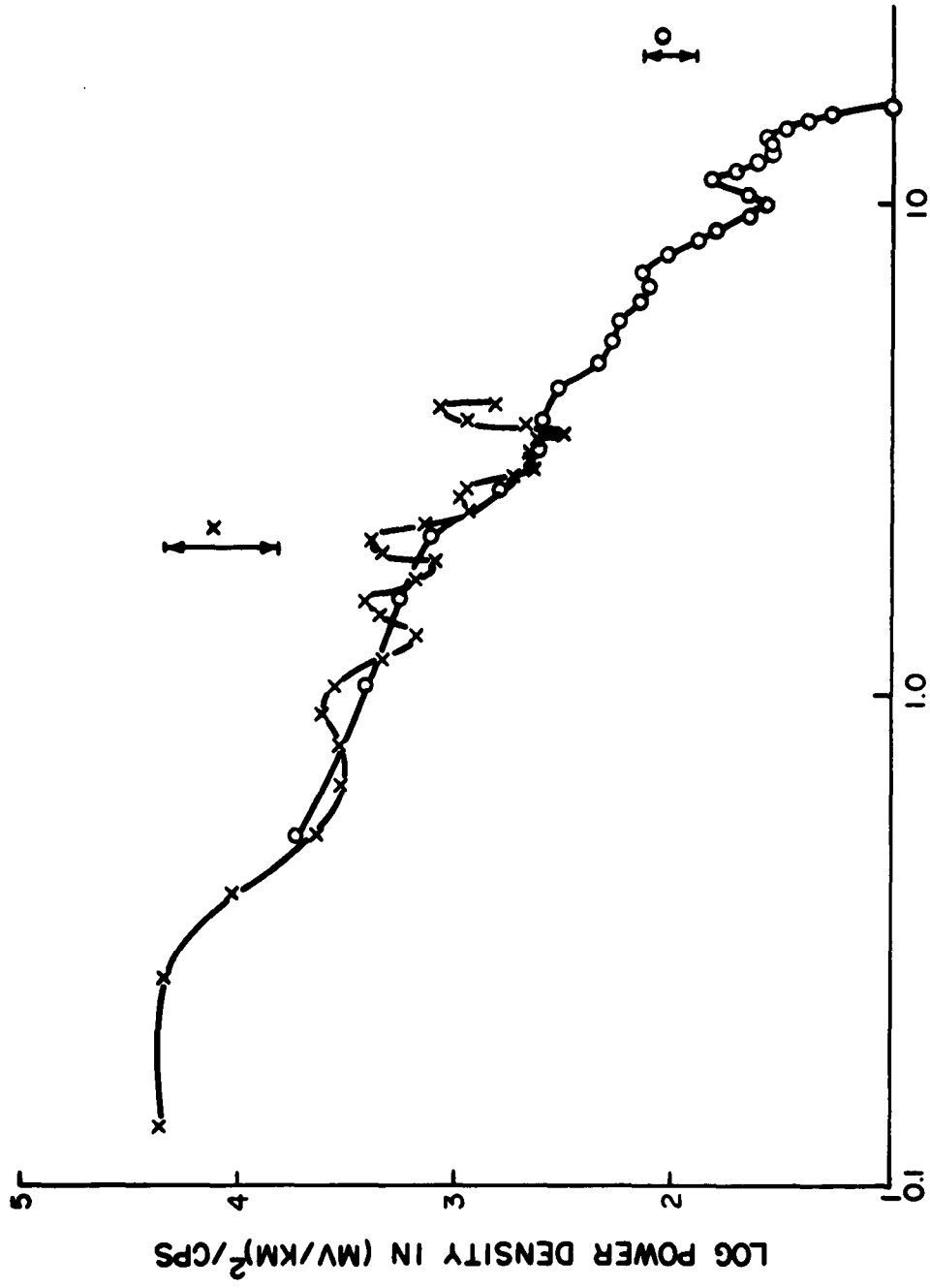

FIGURE 19

THE POWER SPECTRUM OF EAST-WEST TELLURIC FIELD AT LVOV 20 SEPTEMBER 1957

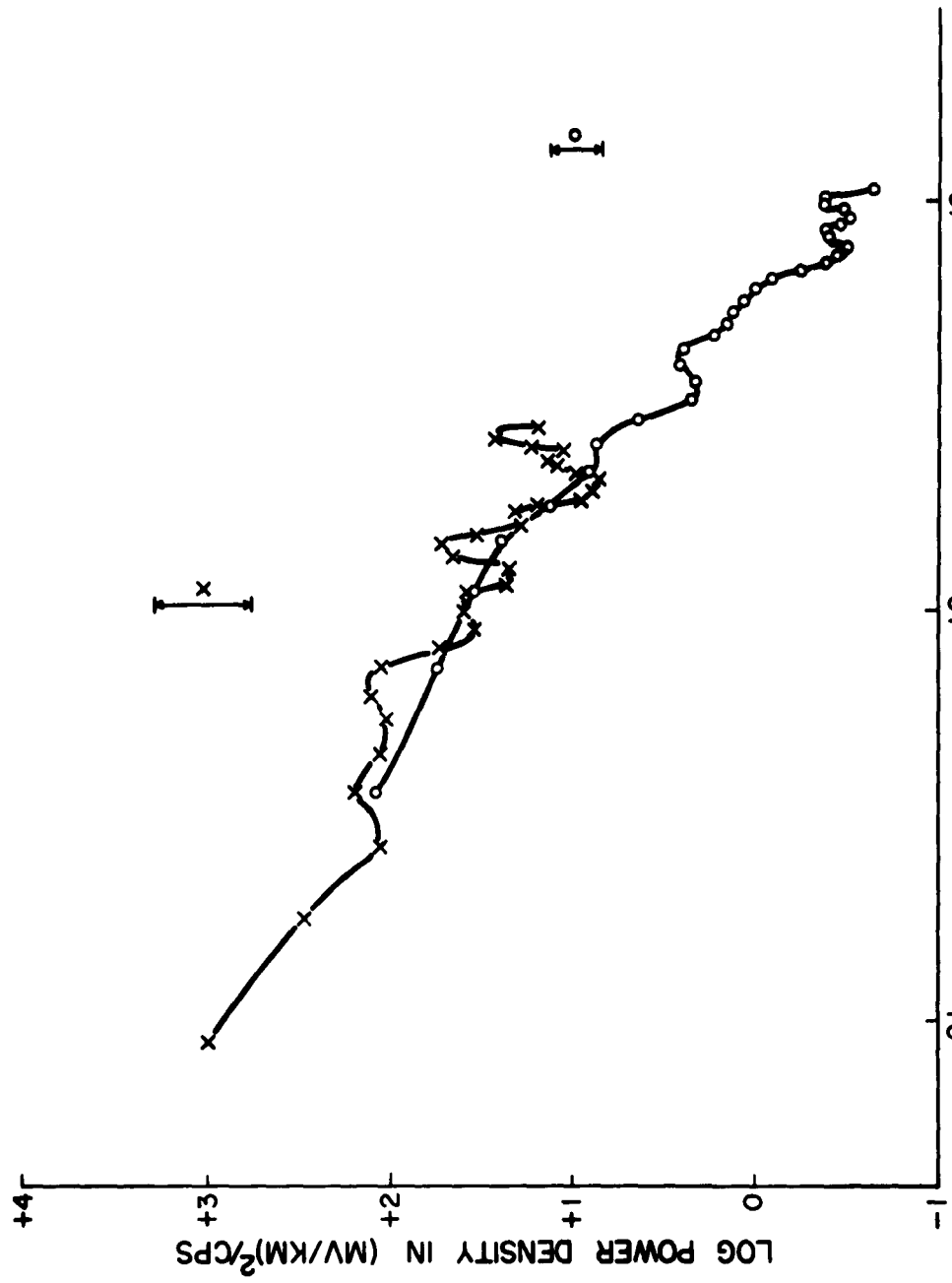

FIGURE 20

THE POWER SPECTRUM OF EAST-WEST TELLURIC FIELD AT TBILISI 20 SEPTEMBER 1957

	AUTOCORRELATION	FREQUENCY	PERIOD	POWER DENSITY
1	.141837E+02	.000E+00	.000	.000000E+00
2	.123920E+02	.278E-04	600.000	.866770E+05
3	.111016E+02	.556E-04	300.000	.343512E+05
4	.102550E+02	.833E-04	200.000	.177925E+05
5	.871901E+01	.111E-03	150.000	.140715E+05
6	.759887E+01	.139E-03	120.000	.990420E+04
7	.695464E+01	.167E-03	100.000	.606458E+04
8	.653183E+01	.194E-03	85.714	.448033E+04
9	.612126E+01	.222E-03	75.000	.337211E+04
10	.568163E+01	.250E-03	66.667	.233831E+04
11	.535285E+01	.278E-03	60.000	.153280E+04
12	.512184E+01	.306E-03	54.545	.898129E+03
13	.490455E+01	.333E-03	50.000	.633444E+03
14	.490734E+01	.361E-03	46.154	.964231E+03
15	.440409E+01	.389E-03	42.857	.168762E+04
16	.412987E+01	.417E-03	40.000	.207727E+04
17	.399599E+01	.444E-03	37.500	.199364E+04
18	.355403E+01	.472E-03	35.294	.211508E+04
19	.304744E+01	.500E-03	33.333	.281794E+04
20	.293748E+01	.528E-03	31.579	.313296E+04
21	.243778E+01	.556E-03	30.000	.218798E+04
22	.224384E+01	.583E-03	28.571	.198563E+04
23	.221846E+01	.611E-03	27.273	.309661E+04
24	.192461E+01	.639E-03	26.087	.280845E+04
25	.204194E+01	.667E-03	25.000	.206803E+04
26	.206849E+01	.694E-03	24.000	.186636E+04
27	.194847E+01	.722E-03	23.077	.151786E+04
28	.212907E+01	.750E-03	22.222	.193032E+04
29	.192044E+01	.778E-03	21.429	.237375E+04
30	.181704E+01	.806E-03	20.690	.157916E+04
31	.181628E+01	.833E-03	20.000	.891445E+03

TABLE 3

THE POWER SPECTRUM FOR THE EAST-WEST TELLURIC FIELD AT ASHKHABAD
20 SEPTEMBER 1957 (LOW-PASS FILTERED).

	AUTOCORRELATION	FREQUENCY	PERIOD	POWER DENSITY
1	.179439E+05	.000E+00	.000	.000000E+00
2	.292615E+04	.111E-03	150.000	.897712E+04
3	-.949157E+04	.222E-03	75.000	.295033E+04
4	-.533074E+04	.333E-03	50.000	.155729E+04
5	.101460E+04	.444E-03	37.500	.196698E+04
6	.317897E+04	.556E-03	30.000	.220064E+04
7	.171715E+04	.667E-03	25.000	.154380E+04
8	-.960888E+02	.778E-03	21.429	.100167E+04
9	-.144527E+04	.889E-03	18.750	.100586E+04
10	-.150309E+04	.100E-02	16.667	.742043E+03
11	.717671E+03	.111E-02	15.000	.426244E+03
12	.109009E+04	.122E-02	13.636	.319017E+03
13	-.522785E+03	.133E-02	12.500	.254073E+03
14	-.226249E+03	.144E-02	11.538	.179531E+03
15	.133347E+04	.156E-02	10.714	.131611E+03
16	.570191E+03	.167E-02	10.000	.106342E+03
17	-.628134E+03	.178E-02	9.375	.112996E+03
18	-.139616E+04	.189E-02	8.824	.106757E+03
19	-.106033E+04	.200E-02	8.333	.788724E+02
20	.194110E+03	.211E-02	7.895	.574017E+02
21	.457800E+03	.222E-02	7.500	.417640E+02
22	.113025E+04	.233E-02	7.143	.442818E+02
23	.826872E+03	.244E-02	6.818	.515664E+02
24	-.176093E+04	.256E-02	6.522	.438601E+02
25	-.216693E+04	.267E-02	6.250	.363167E+02
26	.537400E+03	.278E-02	6.000	.376139E+02
27	.245529E+04	.289E-02	5.769	.328361E+02
28	.676671E+03	.300E-02	5.556	.259808E+02
29	-.183471E+04	.311E-02	5.357	.257291E+02
30	-.513085E+03	.322E-02	5.172	.306650E+02
31	.377067E+02	.333E-02	5.000	.157647E+02

TABLE 4

THE POWER SPECTRUM FOR THE EAST-WEST TELLURIC FIELD AT ASHKABAD 20 SEPTEMBER 1957 (HIGH-PASS FILTERED).

	AUTOCORRELATION	FREQUENCY	PERIOD	POWER DENSITY
1	.249597E+02	.000E+00	.000	.000000E+00
2	.200757E+02	.132E-03	126.400	.223627E+05
3	.143485E+02	.264E-03	63.200	.217677E+05
4	.117722E+02	.396E-03	42.133	.104099E+05
5	.103865E+02	.527E-03	31.600	.428982E+04
6	.810345E+01	.659E-03	25.280	.327285E+04
7	.656234E+01	.791E-03	21.067	.339714E+04
8	.550026E+01	.923E-03	18.057	.400704E+04
9	.421846E+01	.105E-02	15.800	.356261E+04
10	.204951E+01	.119E-02	14.044	.211246E+04
11	.224725E+00	.132E-02	12.640	.145312E+04
12	-.155644E+01	.145E-02	11.491	.214154E+04
13	-.359934E+01	.158E-02	10.533	.243596E+04
14	-.543769E+01	.171E-02	9.723	.149564E+04
15	-.541180E+01	.185E-02	9.029	.120960E+04
16	-.403015E+01	.198E-02	8.427	.218324E+04
17	-.462940E+01	.211E-02	7.900	.233770E+04
18	-.632479E+01	.224E-02	7.435	.135818E+04
19	-.672586E+01	.237E-02	7.022	.825243E+03
20	-.599494E+01	.251E-02	6.653	.941175E+03
21	-.565225E+01	.264E-02	6.320	.876061E+03
22	-.549113E+01	.277E-02	6.019	.528636E+03
23	-.513436E+01	.290E-02	5.745	.429583E+03
24	-.435678E+01	.303E-02	5.496	.543620E+03
25	-.362216E+01	.316E-02	5.267	.548557E+03
26	-.315495E+01	.330E-02	5.056	.405881E+03
27	-.277284E+01	.343E-02	4.862	.307463E+03
28	-.218406E+01	.356E-02	4.681	.472505E+03
29	-.201542E+01	.369E-02	4.514	.878581E+03
30	-.224663E+01	.382E-02	4.359	.116149E+04
31	-.174977E+01	.396E-02	4.213	.655667E+03

TABLE 5

THE POWER SPECTRUM FOR THE EAST-WEST TELLURIC FIELD AT LVOV 20 SEPTEMBER 1957 (LOW-PASS FILTERED).

	AUTOCORRELATION	FREQUENCY	PERIOD	POWER DENSITY
1	.542315E+05	.000E+00	.000	.000000E+00
2	.222632E+04	.527E-03	31.600	.529469E+04
3	-.302254E+05	.105E-02	15.800	.252012E+04
4	-.831475E+04	.158E-02	10.533	.178999E+04
5	.968791E+04	.211E-02	7.900	.113665E+04
6	.124626E+05	.264E-02	6.320	.599837E+03
7	-.184197E+04	.316E-02	5.267	.405788E+03
8	-.768729E+04	.369E-02	4.514	.399254E+03
9	-.480041E+03	.422E-02	3.950	.316888E+03
10	.186293E+04	.475E-02	3.511	.207710E+03
11	-.202412E+04	.527E-02	3.160	.184046E+03
12	.456927E+03	.580E-02	2.873	.175130E+03
13	.286874E+03	.633E-02	2.633	.137327E+03
14	-.123826E+04	.686E-02	2.431	.128924E+03
15	-.162086E+03	.738E-02	2.257	.135249E+03
16	-.199699E+04	.791E-02	2.107	.102847E+03
17	.936901E+03	.844E-02	1.975	.750166E+02
18	.531504E+04	.897E-02	1.859	.627144E+02
19	.310242E+03	.949E-02	1.756	.452286E+02
20	-.638295E+04	.100E-01	1.663	.370239E+02
21	-.276170E+04	.105E-01	1.580	.458348E+02
22	.527089E+04	.111E-01	1.505	.561107E+02
23	.393865E+04	.116E-01	1.436	.501630E+02
24	-.122666E+04	.121E-01	1.374	.409907E+02
25	-.650960E+04	.127E-01	1.317	.349222E+02
26	.123383E+03	.132E-01	1.264	.346569E+02
27	.588585E+04	.137E-01	1.215	.371423E+02
28	-.887667E+03	.142E-01	1.170	.294143E+02
29	-.212820E+04	.148E-01	1.129	.235786E+02
30	-.221547E+04	.153E-01	1.090	.188827E+02
31	.129949E+04	.158E-01	1.053	.970753E+01

TABLE 6

THE POWER SPECTRUM FOR THE EAST-WEST TELLURIC FIELD AT LVOV
20 SEPTEMBER 1957 (HIGH-PASS FILTERED).

	AUTOCORRELATION	FREQUENCY	PERIOD	POWER DENSITY
1	.527668E+00	.000E+00	.000	.000000E+00
2	.452818E+00	.881E-04	189.200	.976567E+03
3	.360401E+00	.176E-03	94.600	.298734E+03
4	.308487E+00	.264E-03	63.067	.119504E+03
5	.279587E+00	.352E-03	47.300	.152760E+03
6	.249109E+00	.440E-03	37.840	.117310E+03
7	.249223E+00	.529E-03	31.533	.101320E+03
8	.266438E+00	.617E-03	27.029	.137529E+03
9	.266475E+00	.705E-03	23.650	.111521E+03
10	.246519E+00	.793E-03	21.022	.545452E+02
11	.231296E+00	.881E-03	18.920	.351943E+02
12	.218261E+00	.969E-03	17.200	.415971E+02
13	.199516E+00	.106E-02	15.767	.375442E+02
14	.177892E+00	.115E-02	14.554	.221671E+02
15	.187680E+00	.123E-02	13.514	.227775E+02
16	.207658E+00	.132E-02	12.613	.460398E+02
17	.197242E+00	.141E-02	11.825	.575541E+02
18	.158906E+00	.150E-02	11.129	.347276E+02
19	.127072E+00	.159E-02	10.511	.186129E+02
20	.100968E+00	.167E-02	9.958	.204121E+02
21	.632944E-01	.176E-02	9.460	.161251E+02
22	.423435E-01	.185E-02	9.010	.909478E+01
23	.394748E-01	.194E-02	8.600	.312655E+01
24	.386641E-01	.203E-02	8.226	.779160E+01
25	.384960E-01	.211E-02	7.883	.951384E+01
26	.481945E-01	.220E-02	7.568	.141426E+02
27	.614213E-01	.229E-02	7.277	.139312E+02
28	.626074E-01	.238E-02	7.007	.114823E+02
29	.436504E-01	.247E-02	6.757	.172622E+02
30	.146695E-01	.255E-02	6.524	.271249E+02
31	-.190410E-01	.264E-02	6.307	.153122E+02

TABLE 7

THE POWER SPECTRUM FOR THE EAST-WEST TELLURIC FIELD AT TBILISI
20 SEPTEMBER 1957 (LOW-PASS FILTERED).

	AUTOCORRELATION	FREQUENCY	PERIOD	POWER DENSITY
1	.521954E+03	.000E+00	.000	.000000E+00
2	.521579E+02	.352E-03	47.300	.126653E+03
3	-.289376E+03	.705E-03	23.650	.578031E+02
4	-.958594E+02	.106E-02	15.767	.359559E+02
5	.127578E+03	.141E-02	11.825	.259795E+02
6	.998306E+02	.176E-02	9.460	.140052E+02
7	-.195070E+02	.211E-02	7.883	.831244E+01
8	-.597786E+02	.247E-02	6.757	.775461E+01
9	-.494442E+02	.282E-02	5.913	.456011E+01
10	-.588006E+01	.317E-02	5.256	.234601E+01
11	.564351E+02	.352E-02	4.730	.222932E+01
12	.211993E+02	.388E-02	4.300	.277142E+01
13	-.492906E+02	.423E-02	3.942	.260917E+01
14	-.496180E+02	.458E-02	3.638	.188579E+01
15	-.968609E+01	.493E-02	3.379	.153600E+01
16	.475798E+02	.529E-02	3.153	.140298E+01
17	.364598E+02	.564E-02	2.956	.122181E+01
18	-.263554E+01	.599E-02	2.782	.109477E+01
19	-.428643E+02	.634E-02	2.628	.876305E+00
20	-.360134E+02	.669E-02	2.489	.606516E+00
21	.183575E+02	.705E-02	2.365	.443000E+00
22	.281596E+02	.740E-02	2.252	.366511E+00
23	-.302384E+02	.775E-02	2.150	.334333E+00
24	-.320544E+02	.810E-02	2.057	.424907E+00
25	-.110150E+02	.846E-02	1.971	.437602E+00
26	.330273E+02	.881E-02	1.892	.347043E+00
27	.306792E+02	.916E-02	1.819	.315703E+00
28	-.466457E+02	.951E-02	1.752	.348084E+00
29	-.353344E+02	.987E-02	1.689	.450148E+00
30	.371368E+02	.102E-01	1.631	.437743E+00
31	.563057E+02	.106E-01	1.577	.225042E+00

TABLE 8

THE POWER SPECTRUM FOR THE EAST-WEST TELLURIC FIELD AT TBILISI 20 SEPTEMBER 1957 (HIGH-PASS FILTERED).

densities are -6.3 db at Ashkhabad and -18.8 db at Tbilisi. These relative power levels reflect the differences in local topography at each position.

Magnetotelluric Field at Tbilisi

The records made at Tbilisi on 1 and 2 September 1957 were subjected to detailed analysis. The results are presented in Tables 9 through 18 and Figures 21 through 29. In particular, the power spectra of the North-South and East-West components of the magnetic and telluric fields at Tbilisi are computed for the two ten-hour periods; 0600 hours to 1600 hours (GMT) on 1 September 1957 and 0500 hours to 1500 hours (GMT) on 2 September 1957. An additional computation was made for the East-West telluric component for the twenty-hour period 0600 hours (GMT) on 1 September 1957 to 0200 hours (GMT) on 2 September 1957. A comparison between the power spectra for the twenty-hour sample (shown in Figure 29) and the ten-hour samples (shown in Figures 23 and 24) does not reveal significant difference between the ten- and twenty-hour samples.

For all of the 1 and 2 September data, power spectra were computed using the original sampling interval (72 seconds) and then power spectra were computed after low-pass filtering and decimation to a new sampling interval of 288 seconds. For some reason that cannot be explained, when the East-West component of the magnetic field and the North-South component of the telluric field were analyzed with the aid of a low-pass filter, the power spectra were erratic and unreliable. This showed up both in numerous negative values for the power spectral densities and large values of coherency (see Tables 13 and 17). These data were rejected.

The spectra of the North-South magnetic and East-West telluric components do not show any striking departures in behavior from the curves for 20 September. The empirical formula in equation (58) can again be made to fit the magnetic spectra with n = 2 and the telluric spectra with a slope of n between 1.1 and 1.2.

A comparison of the power levels at 1 cpks shows that the variation in any component from 1 to 2 September is less than 1 db.

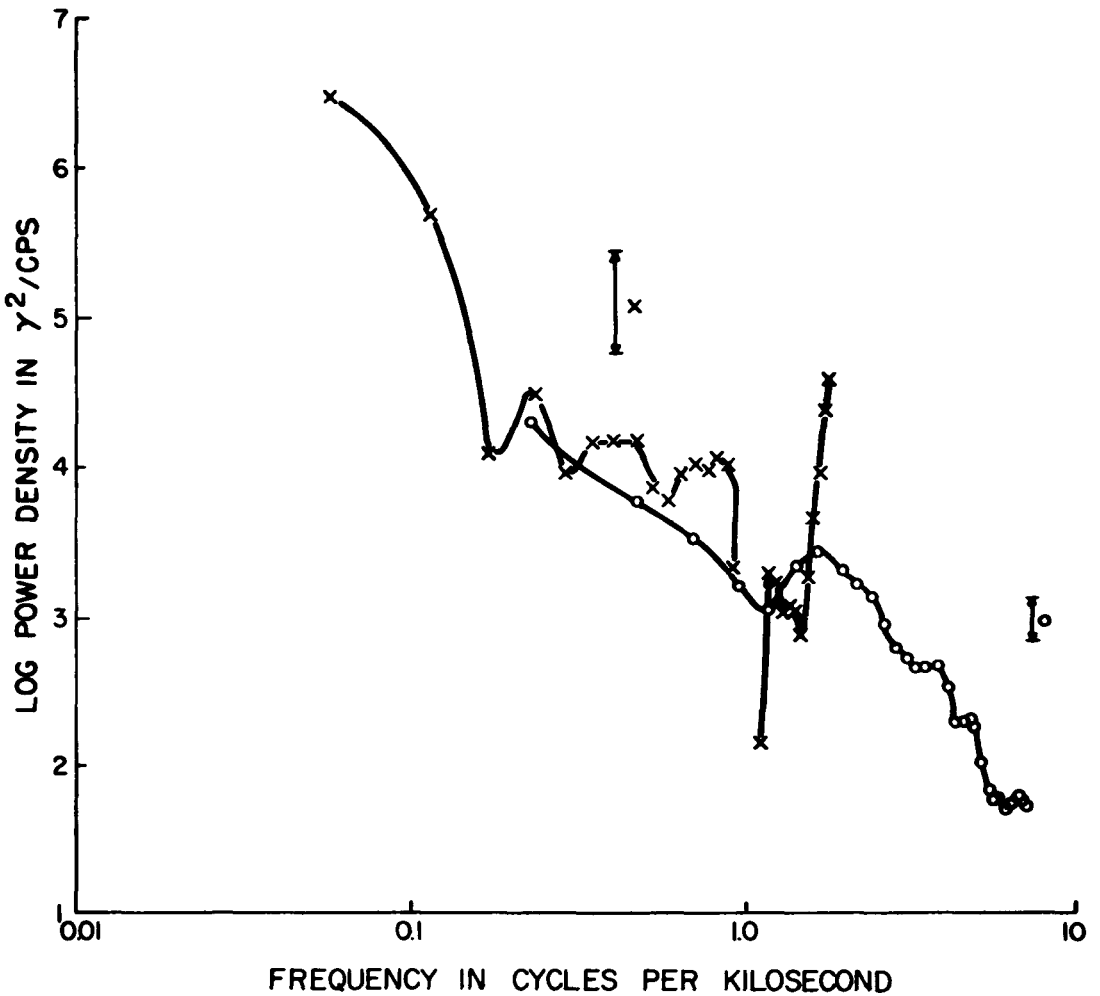

FIGURE 21

THE POWER SPECTRUM OF NORTH-SOUTH MAGNETIC FIELD AT TBILISI I SEPTEMBER 1957

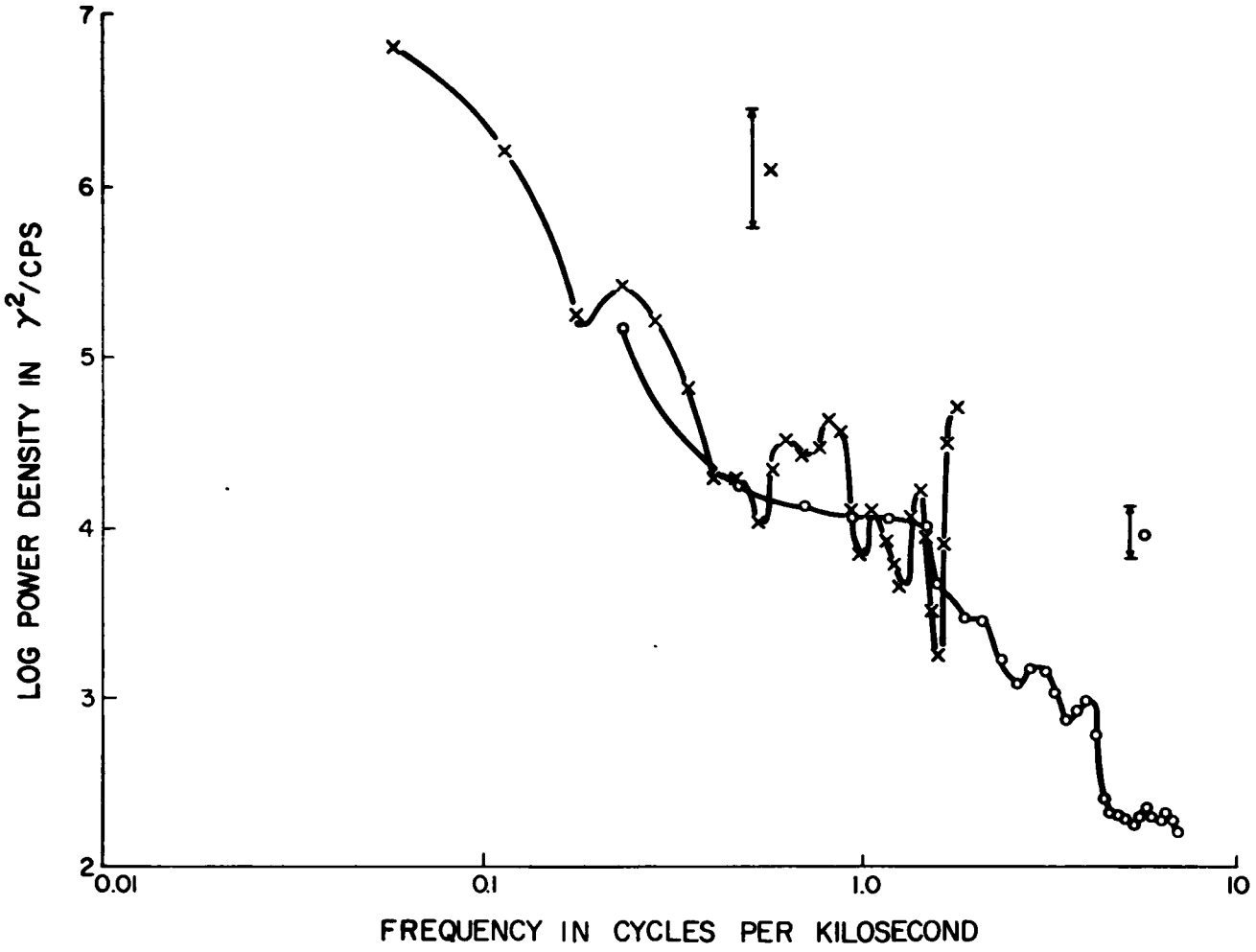

FIGURE 22

THE POWER SPECTRUM OF NORTH-SOUTH MAGNETIC FIELD AT TBILISI 2 SEPTEMBER 1957

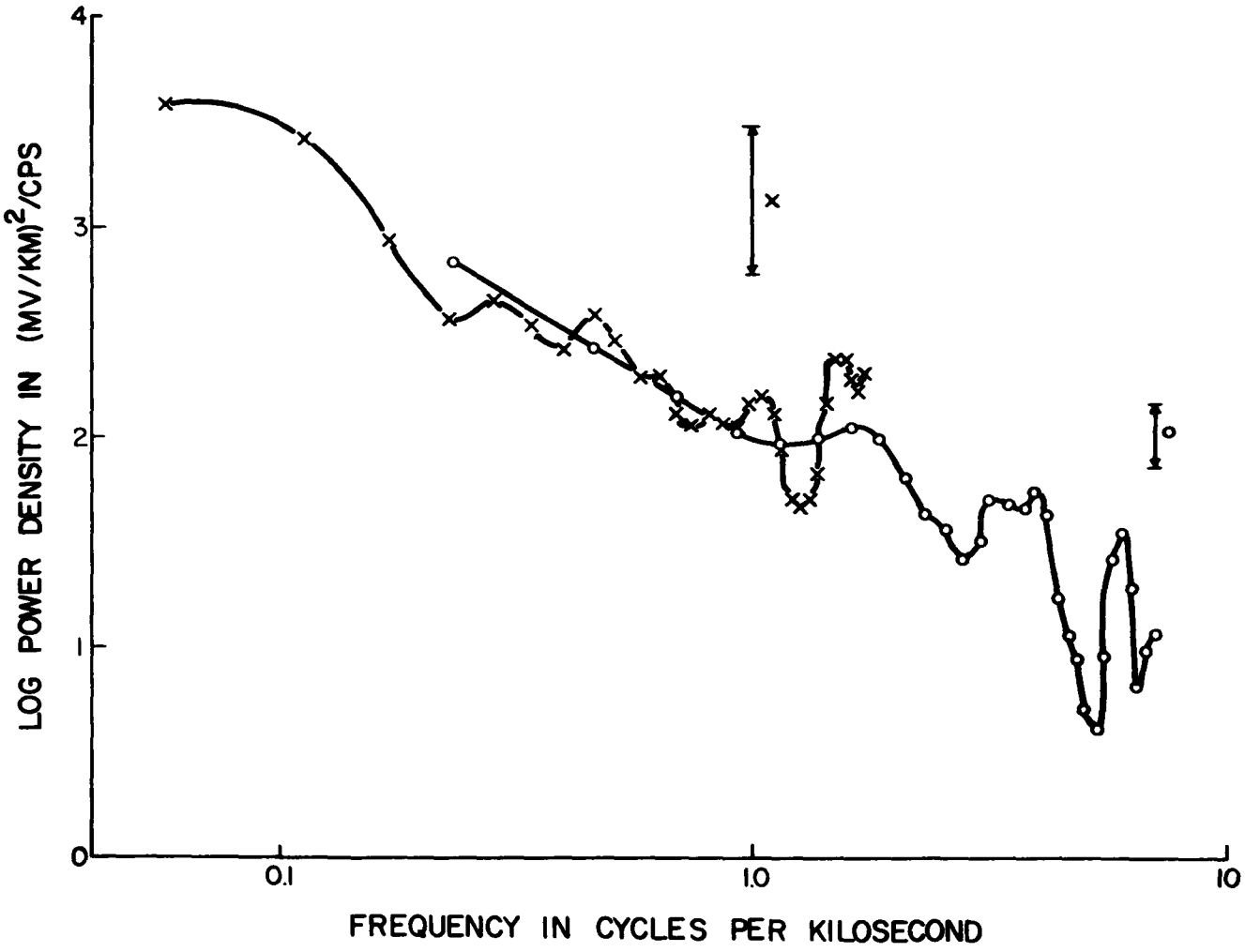

FIGURE 23

THE POWER SPECTRUM OF EAST-WEST TELLURIC FIELD AT TBILISI 1 SEPTEMBER 1957

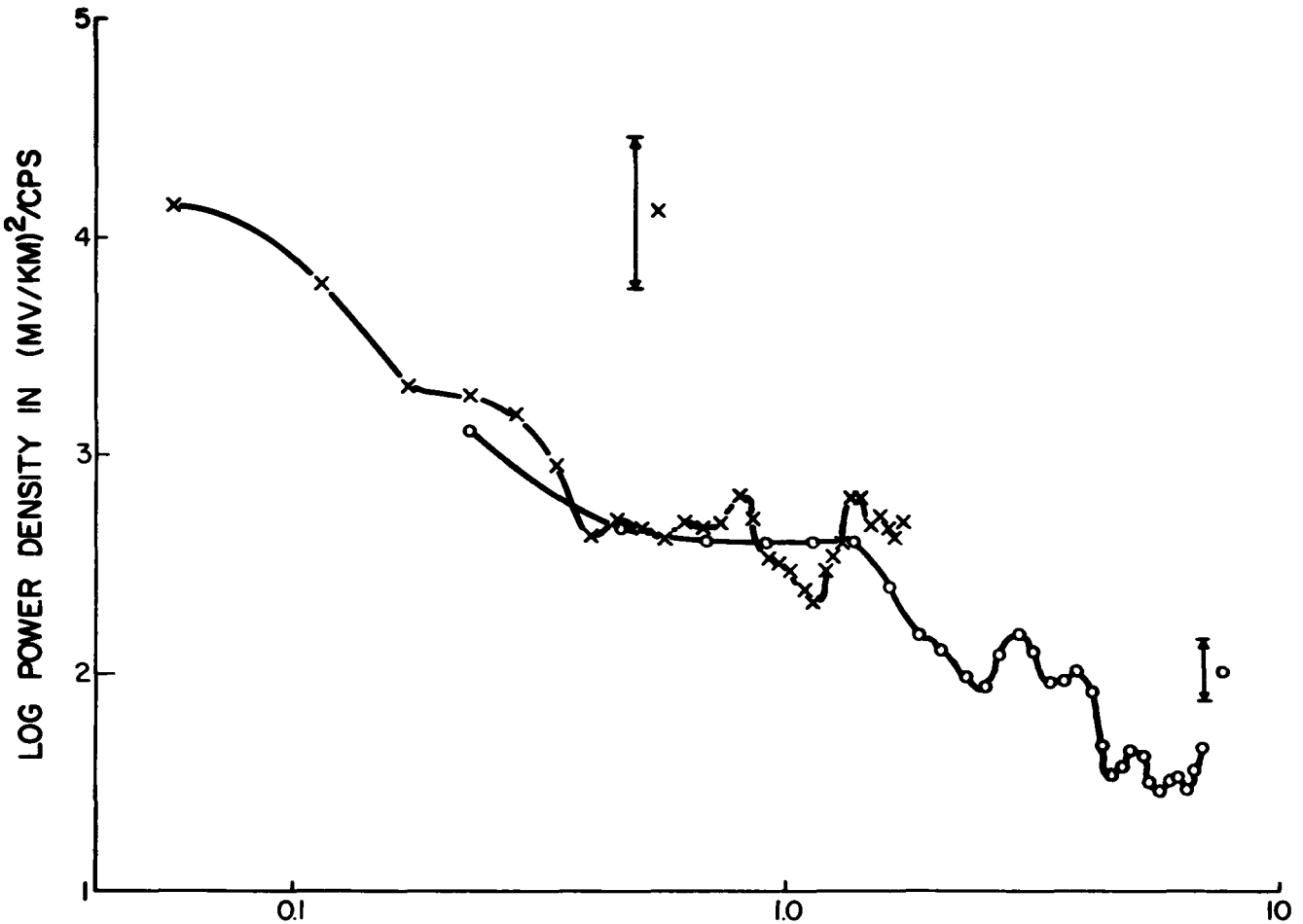

FIGURE 24

THE POWER SPECTRUM OF EAST-WEST TELLURIC FIELD
AT TBILISI 2 SEPTEMBER 1957

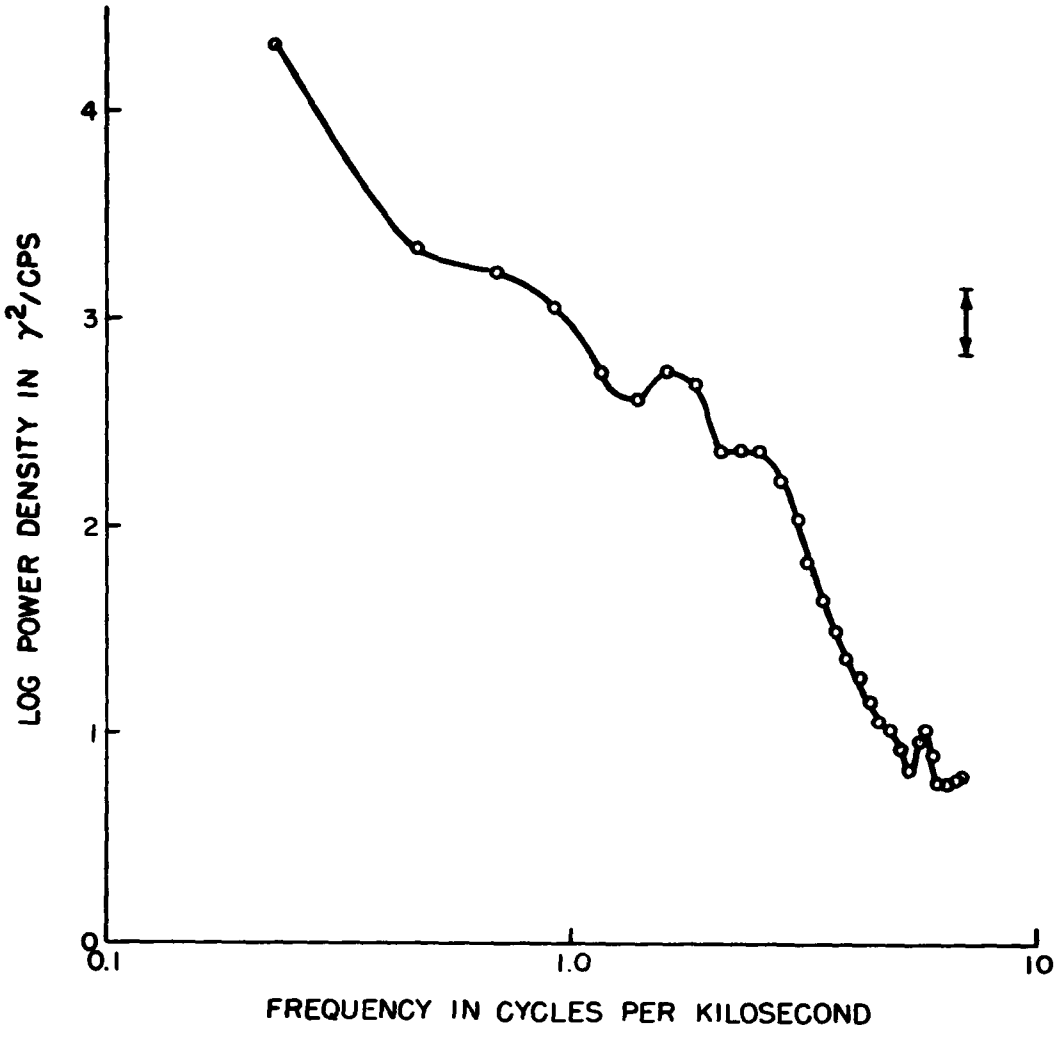

FIGURE 25

THE POWER SPECTRUM OF EAST-WEST MAGNETIC FIELD AT TBILISI I SEPTEMBER 1957

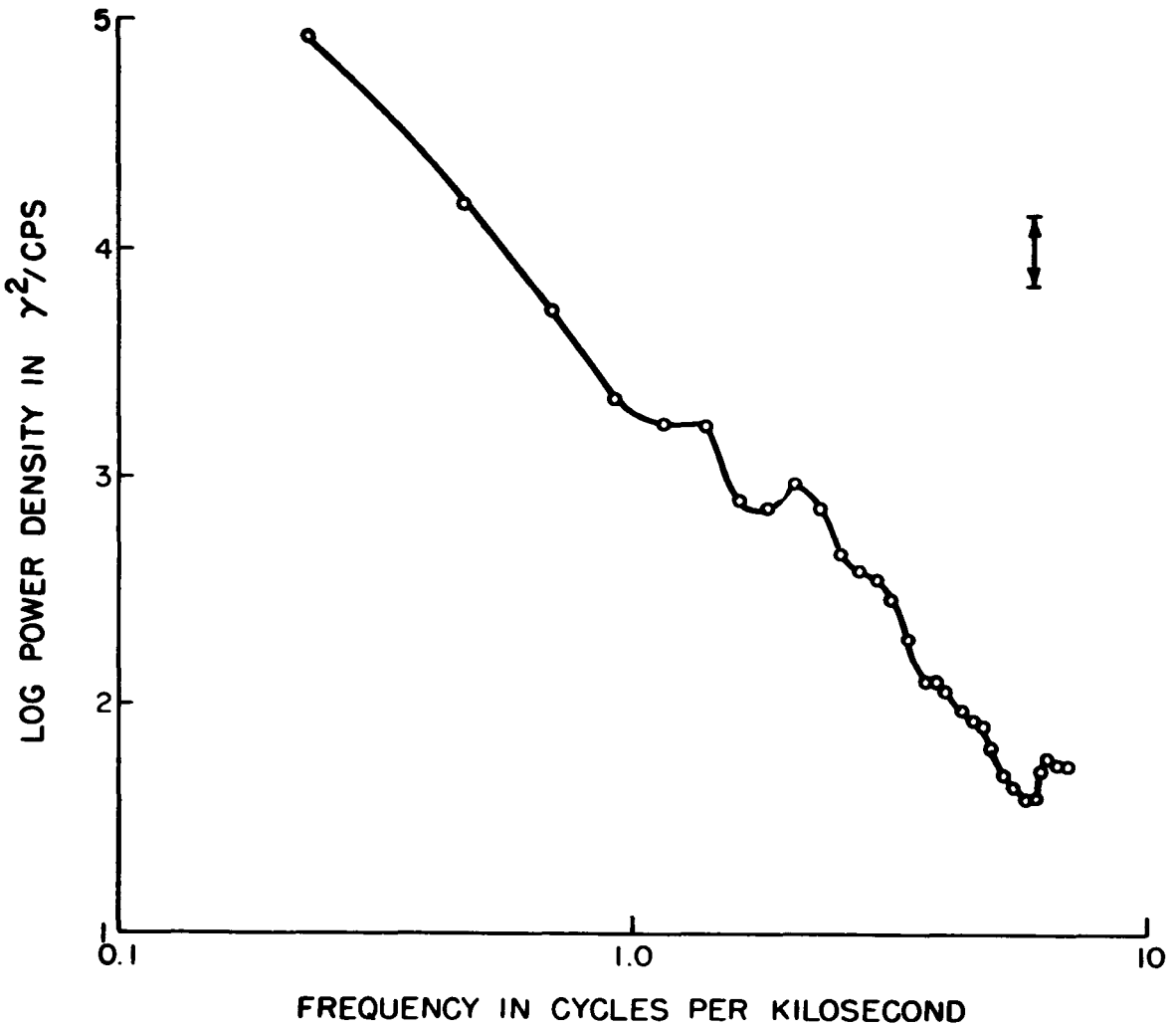

FIGURE 26
THE POWER SPECTRUM OF EAST-WEST MAGNETIC FIELD
AT TBILISI 2 SEPTEMBER 1957

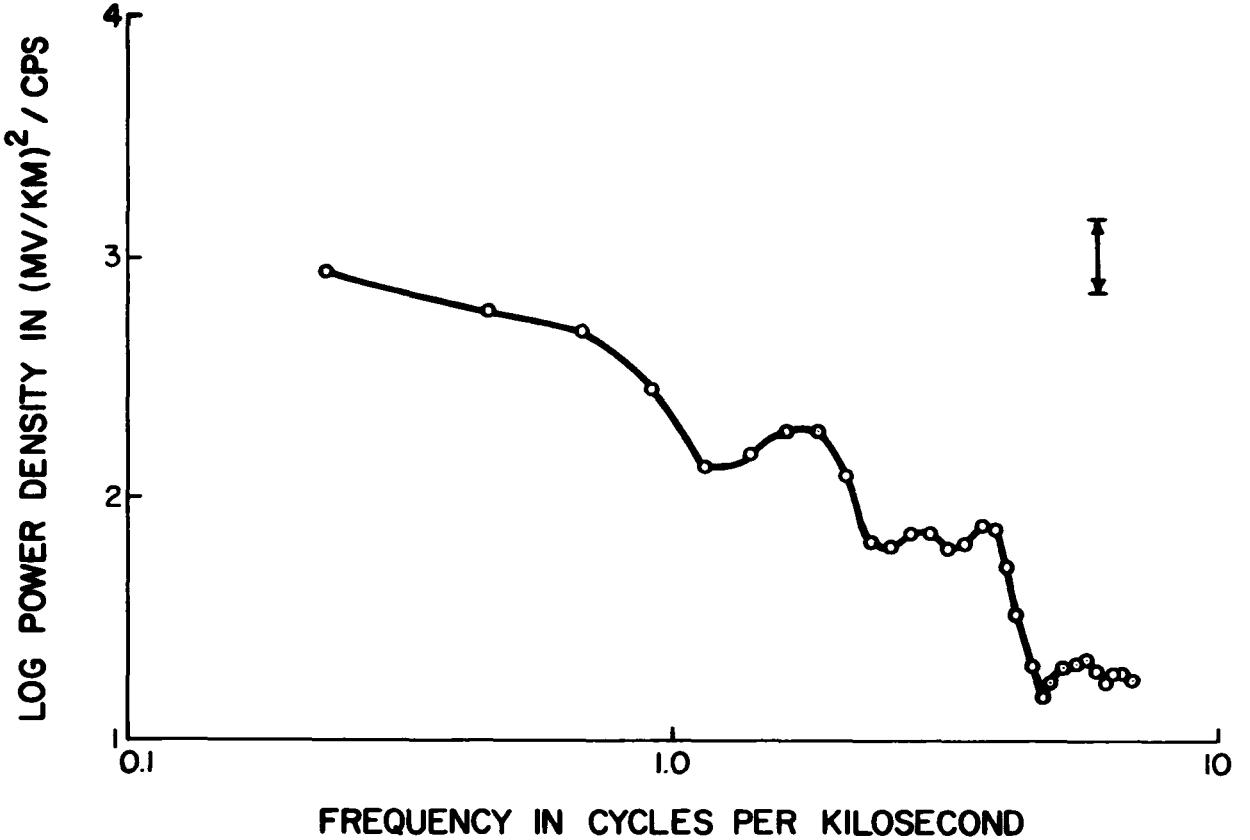

FIGURE 27

THE POWER SPECTRUM OF NORTH-SOUTH TELLURIC FIELD AT TBILISI I SEPTEMBER 1957

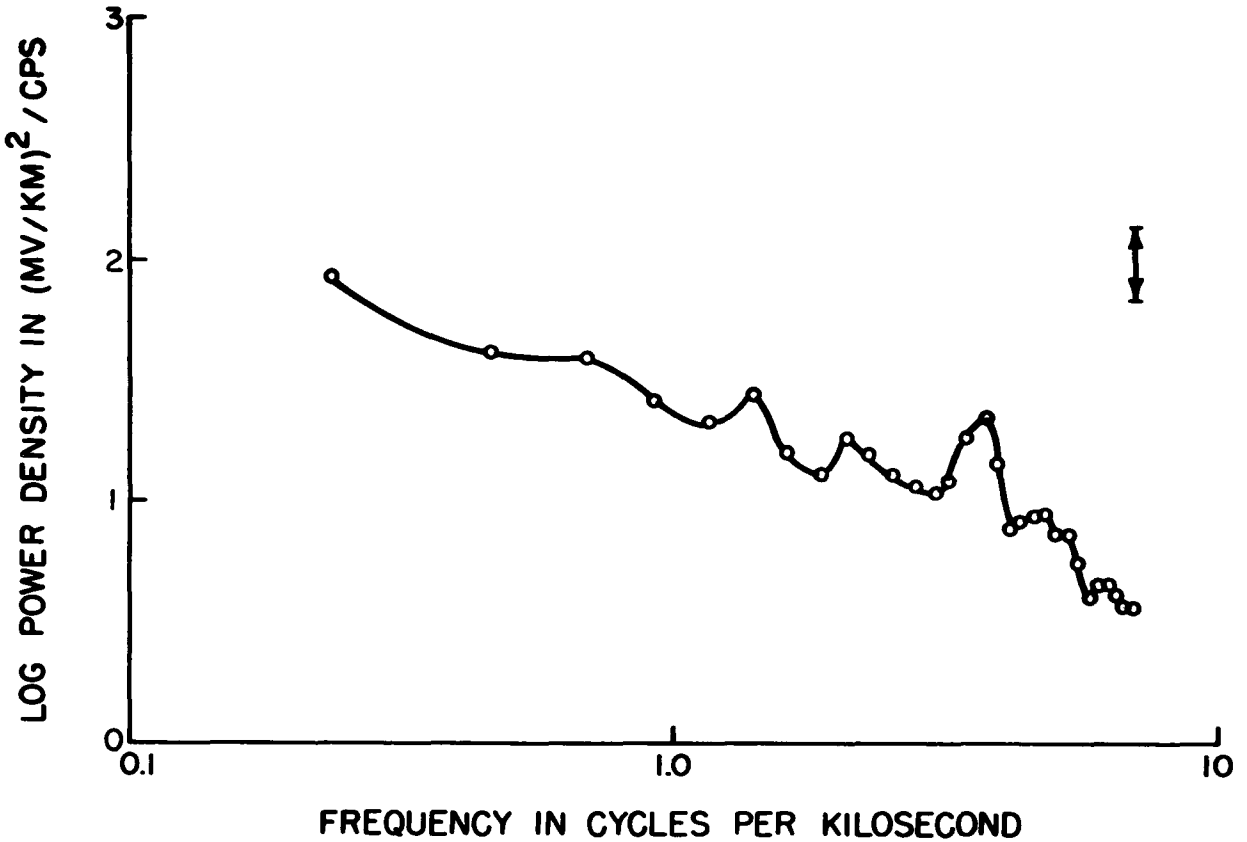

FIGURE 28

THE POWER SPECTRUM OF NORTH-SOUTH TELLURIC FIELD AT TBILISI 2 SEPTEMBER 1957

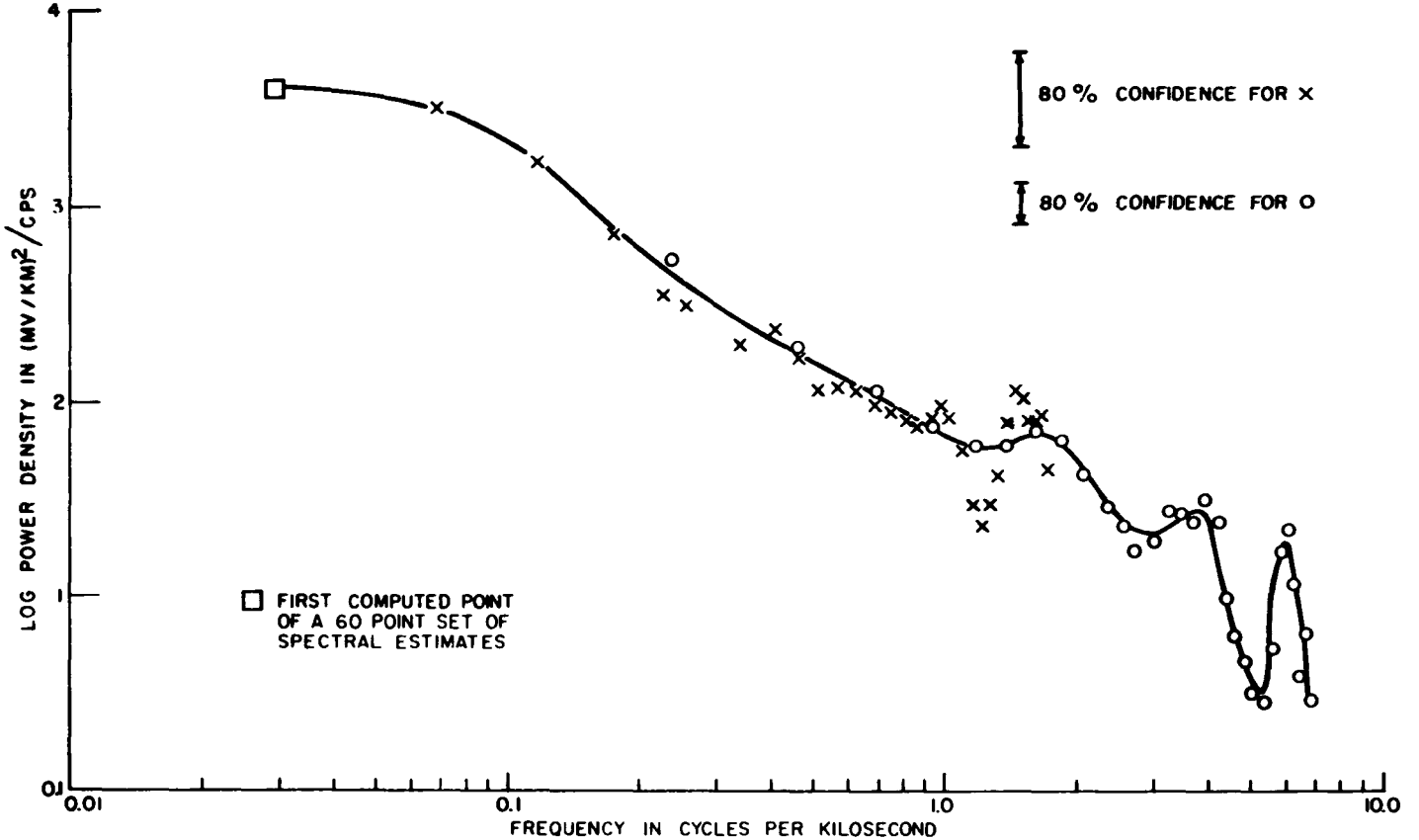

FIGURE 29

THE POWER SPECTRUM OF EAST-WEST TELLURIC FIELD AT TBILISI 1-2 SEPTEMBER 1957

	AUTOCORRELATION	FREQUENCY	PERIOD	POWER DENSITY
1	.111927E+01	.000E+00	.000	.000000E+00
2	.964989E+00	.579E-04	288.000	.306533E+04
3	.813778E+00	.116E-03	144.000	.173019E+04
4	.706746E+00	.174E-03	96.000	.739613E+03
5	.636353E+00	.231E-03	72.000	.414087E+03
6	.557655E+00	.289E-03	57.600	.353632E+03
7	.502514E+00	.347E-03	48.000	.257352E+03
8	.460640E+00	.405E-03	41.143	.195588E+03
9	.386045E+00	.463E-03	36.000	.230166E+03
10	.347015E+00	.521E-03	32.000	.171586E+03
11	.293465E+00	.579E-03	28.800	.115192E+03
12	.235451E+00	.637E-03	26.182	.121073E+03
13	.197398E+00	.694E-03	24.000	.114374E+03
14	.167107E+00	.752E-03	22.154	.101032E+03
15	.139452E+00	.810E-03	20.571	.887191E+02
16	.966622E-01	.868E-03	19.200	.815121E+02
17	.631499E-01	.926E-03	18.000	.767610E+02
18	.917138E-02	.984E-03	16.941	.869785E+02
19	-.221510E-01	.104E-02	16.000	.976911E+02
20	-.321277E-01	.110E-02	15.158	.874828E+02
21	-.184531E-01	.116E-02	14.400	.575089E+02
22	.648993E-02	.122E-02	13.714	.303470E+02
23	.158395E-01	.127E-02	13.091	.234011E+02
24	.123592E-01	.133E-02	12.522	.302503E+02
25	-.179451E-01	.139E-02	12.000	.435613E+02
26	-.608128E-01	.145E-02	11.520	.825516E+02
27	-.966493E-01	.150E-02	11.077	.122263E+03
28	-.110420E+00	.156E-02	10.667	.109925E+03
29	-.784250E-01	.162E-02	10.286	.328892E+02
30	-.721355E-01	.168E-02	9.931	.887128E+02
31	-.612256E-01	.174E-02	9.600	.500789E+02

TABLE 9

THE POWER SPECTRUM FOR THE EAST-WEST TELLURIC FIELD AT TBILISI
1-2 SEPTEMBER 1957 (LOW-PASS FILTERED).

	AUTOCORRELATION	FREQUENCY	PERIOD	POWER DENSITY
1	.498126E+04	.000E+00	.000	.000000E+00
2	-.372095E+03	.231E-03	72.000	.414487E+03
3	-.300428E+04	.463E-03	36.000	.171882E+03
4	-.145405E+03	.694E-03	24.000	.103381E+03
5	.165148E+04	.926E-03	18.000	.708166E+02
6	-.758578E+02	.116E-02	14.400	.565561E+02
7	-.100168E+04	.139E-02	12.000	.570442E+02
8	.938160E+03	.162E-02	10.286	.647195E+02
9	-.980898E+02	.185E-02	9.000	.574098E+02
10	-.297661E+03	.208E-02	8.000	.376909E+02
11	-.215272E+02	.231E-02	7.200	.270151E+02
12	.102245E+01	.255E-02	6.545	.219163E+02
13	.189779E+02	.278E-02	6.000	.165020E+02
14	-.853661E+02	.301E-02	5.538	.186011E+02
15	.609078E+03	.324E-02	5.143	.281894E+02
16	-.882691E+03	.347E-02	4.800	.266271E+02
17	-.443019E+02	.370E-02	4.500	.236774E+02
18	.930281E+03	.394E-02	4.235	.310236E+02
19	-.286435E+02	.417E-02	4.000	.242912E+02
20	-.104106E+04	.440E-02	3.789	.988067E+01
21	-.129441E+03	.463E-02	3.600	.627292E+01
22	.141566E+04	.486E-02	3.429	.488245E+01
23	-.510356E+03	.509E-02	3.273	.319039E+01
24	-.706014E+03	.532E-02	3.130	.287962E+01
25	.363506E+03	.556E-02	3.000	.562041E+01
26	.420156E+03	.579E-02	2.880	.166903E+02
27	-.379849E+03	.602E-02	2.769	.222770E+02
28	-.404489E+03	.625E-02	2.667	.110764E+02
29	.740547E+03	.648E-02	2.571	.389341E+01
30	-.229801E+03	.671E-02	2.483	.558628E+01
31	-.592975E+02	.694E-02	2.400	.287188E+01

TABLE 10

THE POWER SPECTRUM FOR THE EAST-WEST TELLURIC FIELD AT TBILISI
1-2 SEPTEMBER 1957 (HIGH-PASS FILTERED).

	FREQUENCY CPS	EAST MAGNETIC POWER DENSITY	NORTH TELLURIC POWER DENSITY	COHERENCY	PHASE ANGLE RADIANS	QUADRANT
1	.0000E+00	.000000E+00	.000000E+00	.000	.000	I
2	.2315E-03	.204371E+05	.873495E+02	.156	-.229	IV
3	.4630F-03	.223129E+04	.588589E+02	.304	-.500	II
4	.6944E-03	.168931E+04	.492909E+02	.392	-.717	II
5	.9259F-03	.114526E+04	.276742E+02	.194	-1.463	II
6	.1157E-02	.552310E+03	.139576E+02	.397	.183	I
7	.1389E-02	.411301E+03	.151778E+02	.180	-.431	IV
8	.1620E-02	.557486E+03	.193127E+02	.495	1.351	III
9	.1852E-02	.393651E+03	.189245E+02	.583	1.473	III
10	.2083E-02	.230070E+03	.125549E+02	.477	-1.257	IV
11	.2315E-02	.232791E+03	.679243E+01	.203	-1.248	IV
12	.2546E-02	.221001E+03	.619776E+01	.194	.168	III
13	.2778E-02	.160258E+03	.711137E+01	.285	.630	III
14	.3009E-02	.103771E+03	.700021E+01	.460	1.145	III
15	.3241E-02	.659260E+02	.614308E+01	.395	1.092	III
16	.3472E-02	.441234E+02	.635370E+01	.130	-1.296	II
17	.3704E-02	.317142E+02	.797664E+01	.374	1.182	I
18	.3935E-02	.231521E+02	.744702E+01	.404	.993	I
19	.4167E-02	.189792E+02	.513301E+01	.358	1.009	I
20	.4398E-02	.144836E+02	.344126E+01	.207	.882	I
21	.4630E-02	.112530E+02	.216063E+01	.261	.666	I
22	.4861E-02	.105010E+02	.155319E+01	.400	1.103	I
23	.5093E-02	.827891E+01	.175900E+01	.386	1.240	I
24	.5324E-02	.685980E+01	.201641E+01	.321	1.213	I
25	.5556E-02	.927685E+01	.206877E+01	.147	1.214	I
26	.5787E-02	.105721E+02	.219511E+01	.147	-.563	IV
27	.6019E-02	.798375E+01	.195015E+01	.288	-.930	IV
28	.6250E-02	.588684E+01	.170615E+01	.225	-.975	IV
29	.6481E-02	.587671E+01	.193754E+01	.221	-.344	IV
30	.6713E-02	.599560E+01	.193564E+01	.194	.623	I
31	.6944E-02	.621162E+01	.177208E+01	.237	1.387	I

TABLE 11

THE POWER SPECTRUM, COHERENCY, AND PHASE RELATIONS FOR THE EAST-WEST MAGNETIC AND NORTH-SOUTH TELLURIC FIELDS AT TBILISI 1 SEPTEMBER 1957 (HIGH-PASS FILTERED).

	FREQUENCY CPS	NORTH MAGNETIC POWER DENSITY	EAST TELLURIC POWER DENSITY	COHERENCY	PHASE ANGLE RADIANS	QUADRANT
1	.0000E+00	.000000E+00	.000000E+00	.000	.000	I
2	.2315E-03	.204343E+05	.665264E+03	.473	1.488	III
3	.4630E-03	.606577E+04	.272754E+03	.705	1.112	III
4	.6944E-03	.352230E+04	.158631E+03	.580	.781	III
5	.9259E-03	.162063E+04	.108684E+03	.402	.103	III
6	.1157E-02	.120722E+04	.907645E+02	.513	-.751	II
7	.1389E-02	.239660E+04	.999797E+02	.595	1.566	I
8	.1620E-02	.296456E+04	.111352E+03	.378	1.415	I
9	.1852E-02	.224849E+04	.968500E+02	.058	-.992	II
10	.2083E-02	.178971E+04	.640632E+02	.086	-1.192	IV
11	.2315E-02	.144717E+04	.444434E+02	.137	-.664	IV
12	.2546E-02	.975921E+03	.353092E+02	.019	-.235	IV
13	.2778E-02	.650580E+03	.269368E+02	.121	-.296	II
14	.3009E-02	.549157E+03	.323601E+02	.135	.151	III
15	.3241E-02	.489699E+03	.502170E+02	.201	-.589	II
16	.3472E-02	.496454E+03	.473100E+02	.296	-.899	II
17	.3704E-02	.500879E+03	.428525E+02	.199	-.527	II
18	.3935E-02	.346991E+03	.559853E+02	.224	.469	III
19	.4167E-02	.217195E+03	.429230E+02	.311	.939	III
20	.4398E-02	.205799E+03	.175287E+02	.172	-.933	IV
21	.4630E-02	.211551E+03	.118651E+02	.441	.339	I
22	.4861E-02	.170836E+03	.893002E+01	.270	.238	I
23	.5093E-02	.109101E+03	.529517E+01	.148	1.197	III
24	.5324E-02	.701586E+02	.509988E+01	.044	1.379	III
25	.5556E-02	.620401E+02	.918812E+01	.117	.212	I
26	.5787E-02	.625340E+02	.263535E+02	.160	-.164	IV
27	.6019E-02	.527108E+02	.361649E+02	.137	-.005	IV
28	.6250E-02	.579660E+02	.186685E+02	.092	.580	I
29	.6481E-02	.649137E+02	.666019E+01	.209	-.907	II
30	.6713E-02	.593841E+02	.985159E+01	.214	-.477	II
31	.6944E-02	.528363E+02	.114029E+02	.117	.209	III

TABLE 12

THE POWER SPECTRUM, COHERENCY, AND PHASE RELATIONS FOR THE NORTH-SOUTH MAGNETIC AND EAST-WEST TELLURIC FIELDS AT TBILISI 1 SEPTEMBER 1957 (HIGH-PASS FILTERED).

	FREQUENCY CPS	EAST MAGNETIC POWER DENSITY	NORTH TELLURIC POWER DENSITY	COHERENCY	PHASE ANGLE RADIANS	QUADRANT
1	.0000E+00	.000000E+00	.000000E+00	.000	.000	I
2	.5787E-04	.359567E+07	.520721E+03	5.085	1.274	I
3	.1157E-03	.962308E+06	-.690353E+04	1.731	-.199	II
4	.1736E-03	.147761E+06	-.419507E+04	3.123	1.428	III
5	.2315E-03	.106722E+06	-.229330E+04	1.939	.492	I
6	.2894E-03	.601551E+05	.391593E+04	2.167	-.246	II
7	.3472E-03	.479968E+05	.685332E+04	1.833	1.180	III
8	.4051E-03	.324870E+05	.389698E+04	2.288	-.987	IV
9	.4630E-03	.216391E+05	-.268251E+04	2.796	-.176	IV
10	.5208E-03	.131583E+05	-.278152E+04	2.613	.739	I
11	.5787E-03	.112626E+05	-.578838E+03	3.003	1.554	I
12	.6366E-03	.118089E+05	.486312E+03	1.403	1.494	I
13	.6944E-03	.163452E+05	-.219450E+04	.644	1.444	I
14	.7523E-03	.201043E+05	-.379425E+04	.445	-1.557	II
15	.8102E-03	.240799E+05	-.684648E+03	1.401	1.350	II
16	.8681E-03	.208365E+05	.285876E+04	1.160	-.654	II
17	.9259E-03	.957528E+04	.415481E+04	1.650	.314	III
18	.9838E-03	.236155E+04	.188872E+04	4.008	1.393	III
19	.1042E-02	.197478E+04	-.289050E+03	6.214	-.616	IV
20	.1100E-02	.237956E+04	-.770257E+03	.600	-1.479	II
21	.1157E-02	.432897E+04	.365006E+03	3.029	1.053	III
22	.1215E-02	.625786E+04	.905997E+03	2.204	-.907	IV
23	.1273E-02	.652423E+04	-.974677E+03	1.490	.219	I
24	.1331E-02	.626862E+04	-.274069E+04	.089	-.316	II
25	.1389E-02	.596013E+04	-.193125E+04	1.398	-1.208	IV
26	.1447E-02	.499956E+04	-.122009E+04	3.946	-.312	IV
27	.1505E-02	.562977E+04	-.246699E+04	4.077	.549	I
28	.1562E-02	.769661E+04	-.722945E+03	8.284	1.460	I
29	.1620E-02	.145387E+05	.311332E+04	2.959	-.735	II
30	.1678E-02	.339223E+05	.426359E+04	1.163	.101	III
31	.1736E-02	.517888E+05	.351051E+04	.599	.605	III

TABLE 13

THE POWER SPECTRUM, COHERENCY, AND PHASE RELATIONS FOR THE EAST-WEST MAGNETIC AND NORTH-SOUTH TELLURIC FIELDS AT TIBILISI 1 SEPTEMBER 1957 (LOW-PASS FILTERED).

	FREQUENCY CPS	NORTH MAGNETIC POWER DENSITY	EAST TELLURIC POWER DENSITY	COHERENCY	PHASE ANGLE RADIANS	QUADRANT
1	.0000E+00	.000000E+00	.000000E+00	.000	.000	I
2	.5787E-04	.297211E+07	.395607E+04	.547	-.938	IV
3	.1157E-03	.504008E+06	.266055E+04	.650	-1.036	IV
4	.1736E-03	.128806E+05	.889756E+03	.664	-.978	IV
5	.2315E-03	.323479E+05	.363445E+03	.672	-1.486	IV
6	.2894E-03	.967938E+04	.446169E+03	.531	-1.318	IV
7	.3472E-03	.149315E+05	.342810E+03	.594	1.518	III
8	.4051E-03	.151222E+05	.263154E+03	.723	1.348	III
9	.4630E-03	.153255E+05	.388039E+03	.850	-1.567	IV
10	.5208E-03	.798834E+04	.282348E+03	.712	-1.425	IV
11	.5787E-03	.640021E+04	.190949E+03	.547	1.061	III
12	.6366E-03	.932041E+04	.197420E+03	.561	.943	III
13	.6944E-03	.108529E+05	.129727E+03	.433	1.101	III
14	.7523E-03	.103431E+05	.114223E+03	.293	1.398	III
15	.8102E-03	.123136E+05	.130427E+03	.184	-1.316	IV
16	.8681E-03	.108381E+05	.113649E+03	.222	-1.466	IV
17	.9259E-03	.234856E+04	.115985E+03	.435	-1.569	IV
18	.9838E-03	-.275044E+04	.146136E+03	.128	1.036	I
19	.1042E-02	-.172795E+04	.151778E+03	.228	-1.262	II
20	.1100E-02	.141374E+05	.128095E+03	1.503	-.692	II
21	.1157E-02	.209059E+04	.859152E+02	.343	-.583	II
22	.1215E-02	.181129E+04	.519171E+02	.096	-.646	IV
23	.1273E-02	.112926E+04	.485369E+02	.833	.114	I
24	.1331E-02	.120558E+04	.521863E+02	.848	.654	I
25	.1389E-02	.116416E+04	.677890E+02	.247	-.574	II
26	.1447E-02	.816714E+03	.145108E+03	.426	.505	III
27	.1505E-02	.209445E+04	.235280E+03	.281	1.297	I
28	.1562E-02	.491107E+04	.233481E+03	.696	1.185	I
29	.1620E-02	.100840E+05	.182067E+03	.895	1.246	I
30	.1678E-02	.254788E+05	.173383E+03	.631	1.321	I
31	.1736E-02	.407136E+05	.212965E+03	.287	1.262	I

TABLE 14

THE POWER SPECTRUM, COHERENCY, AND PHASE RELATIONS FOR THE NORTH-SOUTH MAGNETIC AND EAST-WEST TELLURIC FIELDS AT TBILISI 1 SEPTEMBER 1957 (LOW-PASS FILTERED).

	FREQUENCY CPS	EAST MAGNETIC POWER DENSITY	NORTH TELLURIC POWER DENSITY	COHERENCY	PHASE ANGLE RADIANS	QUADRANT
1	.0000E+00	.000000E+00	.000000E+00	.000	.000	I
2	.2315E-03	.852460E+05	.837228E+02	.312	.831	III
3	.4630E-03	.156278E+05	.407809E+02	.178	.690	III
4	.6944E-03	.549728E+04	.398703E+02	.113	.909	III
5	.9259E-03	.221102E+04	.262174E+02	.143	-1.371	IV
6	.1157E-02	.166935E+04	.215277E+02	.227	-.562	IV
7	.1389E-02	.162524E+04	.271426E+02	.391	-.757	IV
8	.1620E-02	.799237E+03	.157699E+02	.453	-.698	IV
9	.1852E-02	.727425E+03	.135575E+02	.372	-1.552	IV
10	.2083E-02	.938735E+03	.182015E+02	.501	1.209	III
11	.2315E-02	.706632E+03	.164296E+02	.533	1.274	III
12	.2546E-02	.455599E+03	.129299E+02	.328	-1.384	IV
13	.2778E-02	.384812E+03	.117252E+02	.366	-.207	IV
14	.3009E-02	.356838E+03	.117939E+02	.292	-.381	IV
15	.3241E-02	.289201E+03	.121967E+02	.227	1.218	III
16	.3472E-02	.184111E+03	.185722E+02	.176	-1.511	IV
17	.3704E-02	.123154E+03	.227235E+02	.330	-.207	IV
18	.3935E-02	.124390E+03	.142868E+02	.311	-.106	IV
19	.4167E-02	.113519E+03	.793736E+01	.157	-.477	IV
20	.4398E-02	.922756E+02	.811669E+01	.055	-.346	IV
21	.4630E-02	.841471E+02	.864242E+01	.144	1.001	III
22	.4861E-02	.801736E+02	.870279E+01	.298	.988	III
23	.5093E-02	.648929E+02	.735236E+01	.067	.597	III
24	.5324E-02	.494705E+02	.711057E+01	.218	1.527	I
25	.5556E-02	.434712E+02	.576243E+01	.203	-1.258	II
26	.5787E-02	.396309E+02	.400302E+01	.248	-1.420	II
27	.6019E-02	.398325E+02	.448780E+01	.279	1.508	I
28	.6250E-02	.504730E+02	.461931E+01	.259	-1.246	II
29	.6481E-02	.591540E+02	.401933E+01	.246	-.572	II
30	.6713E-02	.561966E+02	.373536E+01	.222	.077	III
31	.6944E-02	.539688E+02	.379467E+01	.208	.282	III

TABLE 15

THE POWER SPECTRUM, COHERENCY, AND PHASE RELATIONS FOR THE EAST-WEST MAGNETIC AND NORTH-SOUTH TELLURIC FIELDS AT TBILISI 2 SEPTEMBER 1957 (HIGH-PASS FILTERED).

	FREQUENCY CPS	NORTH MAGNETIC POWER DENSITY	EAST TELLURIC POWER DENSITY	COHERENCY	PHASE ANGLE RADIANS	QUADRANT
1	.0000E+00	.000000E+00	.000000E+00	.000	.000	I
2	.2315E-03	.155193E+06	.126662E+04	.720	-1.390	IV
3	.4630E-03	.286707E+05	.478496E+03	.734	1.184	III
4	.6944E-03	.143359E+05	.400888E+03	.555	-.005	II
5	.9259E-03	.115131E+05	.383621E+03	.555	-.903	II
6	.1157E-02	.115208E+05	.397929E+03	.674	-1.377	II
7	.1389E-02	.105706E+05	.401189E+03	.622	-1.489	II
8	.1620E-02	.493192E+04	.245158E+03	.393	1.544	I
9	.1852E-02	.314496E+04	.148882E+03	.248	-.502	IV
10	.2083E-02	.292402E+04	.126227E+03	.472	-.969	IV
11	.2315E-02	.175567E+04	.956425E+02	.377	-1.474	IV
12	.2546E-02	.127257E+04	.865718E+02	.382	.486	III
13	.2778E-02	.150612E+04	.122596E+03	.519	-.164	II
14	.3009E-02	.150020E+04	.150103E+03	.545	-.575	II
15	.3241E-02	.110473E+04	.122687E+03	.395	-1.142	II
16	.3472E-02	.757736E+03	.891390E+02	.307	1.022	I
17	.3704E-02	.852063E+03	.926495E+02	.344	-.003	IV
18	.3935E-02	.100110E+04	.102476E+03	.508	-.521	IV
19	.4167E-02	.609316E+03	.813855E+02	.390	-.764	IV
20	.4398E-02	.240420E+03	.463921E+02	.202	.771	III
21	.4630E-02	.204814E+03	.335496E+02	.444	.932	III
22	.4861E-02	.200426E+03	.371517E+02	.328	.720	III
23	.5093E-02	.198319E+03	.435687E+02	.198	.360	III
24	.5324E-02	.178334E+03	.411861E+02	.328	1.112	III
25	.5556E-02	.196202E+03	.304448E+02	.293	-1.548	IV
26	.5787E-02	.224892E+03	.281660E+02	.242	-1.359	IV
27	.6019E-02	.193591E+03	.328383E+02	.394	1.198	III
28	.6250E-02	.181690E+03	.333263E+02	.416	.949	III
29	.6481E-02	.208333E+03	.292440E+02	.328	.597	III
30	.6713E-02	.188288E+03	.358971E+02	.274	-.001	II
31	.6944E-02	.157976E+03	.456319E+02	.263	-.292	II

TABLE 16

THE POWER SPECTRUM, COHERENCY, AND PHASE RELATIONS FOR THE NORTH-SOUTH MAGNETIC AND EAST-WEST TELLURIC FIELDS AT TBILISI 2 SEPTEMBER 1957 (HIGH-PASS FILTERED).

	FREQUENCY CPS	EAST MAGNETIC POWER DENSITY	NORTH TELLURIC POWER DENSITY	COHERENCY	PHASE ANGLE RADIANS	QUADRANT
1	.0000E+00	.000000E+00	.000000E+00	.000	.000	I
2	.5787E-04	.877893E+07	-.114342E+05	2.093	.461	I
3	.1157E-03	.158445E+07	.472632E+05	3.914	-.854	II
4	.1736E-03	.198570E+06	.187434E+05	17.808	.941	III
5	.2315E-03	.180091E+06	-.832733E+05	6.037	-.424	IV
6	.2894E-03	.797278E+05	-.164129E+05	7.259	1.261	I
7	.3472E-03	.500364E+05	.252255E+05	2.745	.142	I
8	.4051E-03	.241785E+05	.745034E+04	15.610	1.521	I
9	.4630E-03	.183935E+05	-.684656E+04	14.025	-.460	II
10	.5208E-03	.112965E+05	.340072E+02	211.065	.179	III
11	.5787E-03	.122776E+05	.214872E+05	8.501	1.110	III
12	.6366E-03	.124565E+05	.199503E+05	6.930	-1.004	IV
13	.6944E-03	.121304E+05	.390151E+03	32.855	-.146	IV
14	.7523E-03	.189461E+05	-.125492E+05	2.868	.276	I
15	.8102E-03	.336426E+05	-.214569E+05	2.257	.660	I
16	.8681E-03	.299479E+05	-.188727E+05	3.037	-1.406	II
17	.9259E-03	.654663E+04	-.166765E+04	17.250	-.314	II
18	.9838E-03	-.281981E+04	.131439E+05	7.499	.551	III
19	.1042E-02	-.105985E+04	.184896E+05	10.109	-1.447	IV
20	.1100E-02	-.144169E+04	.850596E+04	11.126	.038	I
21	.1157E-02	.193925E+04	.776436E+02	90.870	1.558	I
22	.1215E-02	.540804E+04	-.247408E+04	9.975	-.269	II
23	.1273E-02	.605840E+04	-.898226E+04	5.257	.818	III
24	.1331E-02	.416273E+04	-.133632E+05	5.905	-1.394	IV
25	.1389E-02	.441596E+04	-.455425E+04	11.057	-.408	IV
26	.1447E-02	.485367E+04	.132068E+05	5.500	.517	I
27	.1505E-02	.407095E+04	.159468E+05	5.404	1.160	I
28	.1562E-02	.658549E+04	-.304200E+04	12.179	-1.027	II
29	.1620E-02	.132363E+05	-.141262E+05	3.588	.256	III
30	.1678E-02	.485693E+05	-.110350E+04	3.790	-1.496	IV
31	.1736E-02	.895075E+05	.967475E+04	2.734	-1.369	IV

TABLE 17

THE POWER SPECTRUM, COHERENCY, AND PHASE RELATIONS FOR THE EAST-WEST MAGNETIC AND NORTH-SOUTH TELLURIC FIELDS AT TBILISI 2 SEPTEMBER 1957 (LOW-PASS FILTERED).

	FREQUENCY CPS	NORTH MAGNETIC POWER DENSITY	EAST TELLURIC POWER DENSITY	COHERENCY	PHASE ANGLE RADIANS	QUADRANT
1	.0000E+00	.000000E+00	.000000E+00	.000	.000	I
2	.5787E-04	.651997E+07	.142112E+05	.829	-.915	IV
3	.1157E-03	.167472E+07	.603369E+04	1.009	-1.151	IV
4	.1736E-03	.179239E+06	.208805E+04	.870	-1.270	IV
5	.2315E-03	.251227E+06	.183523E+04	.951	-1.443	IV
6	.2894E-03	.160884E+06	.159004E+04	.910	1.392	III
7	.3472E-03	.735048E+05	.889114E+03	.952	1.272	III
8	.4051E-03	.205235E+05	.426568E+03	.794	.849	III
9	.4630E-03	.199652E+05	.486099E+03	.668	1.392	III
10	.5208E-03	.112365E+05	.453524E+03	.552	-1.483	IV
11	.5787E-03	.221775E+05	.418923E+03	.713	.782	III
12	.6366E-03	.329472E+05	.499077E+03	.880	.238	III
13	.6944E-03	.282396E+05	.459245E+03	.726	.137	III
14	.7523E-03	.298767E+05	.474781E+03	.553	-.335	II
15	.8102E-03	.478488E+05	.617121E+03	.624	-.575	II
16	.8681E-03	.388776E+05	.506797E+03	.616	-.615	II
17	.9259E-03	.128422E+05	.338396E+03	.574	-.455	II
18	.9838E-03	.672932E+04	.314987E+03	1.057	-1.219	II
19	.1042E-02	.130190E+05	.291878E+03	1.016	1.380	I
20	.1100E-02	.107947E+05	.233741E+03	.832	.987	I
21	.1157E-02	.837001E+04	.213406E+03	.416	1.210	I
22	.1215E-02	.641882E+04	.285169E+03	.724	-1.166	II
23	.1273E-02	.378106E+04	.316342E+03	.988	-.882	II
24	.1331E-02	.113150E+05	.403797E+03	.841	-1.237	II
25	.1389E-02	.170318E+05	.626219E+03	.833	-1.567	II
26	.1447E-02	.891268E+04	.624057E+03	.859	1.436	I
27	.1505E-02	.327152E+04	.484938E+03	.823	1.345	I
28	.1562E-02	.172392E+04	.501196E+03	.578	1.209	I
29	.1620E-02	.888589E+04	.456640E+03	.159	.985	I
30	.1678E-02	.325676E+05	.410829E+03	.270	.603	I
31	.1736E-02	.517513E+05	.495431E+03	.365	-.615	IV

TABLE 18

THE POWER SPECTRUM, COHERENCY, AND PHASE RELATIONS FOR THE NORTH-SOUTH MAGNETIC AND EAST-WEST TELLURIC FIELDS AT TBILISI 2 SEPTEMBER 1957 (LOW-PASS FILTERED).

In addition to the power spectra, Tables 9 through 18 show the coherency (see equation 56) and phase angles between the orthogonal components of the telluric and magnetic fields. Figure 30 contains a few plots of the coherency between the components of the magnetotelluric fields. The phase angles have an erratic behavior and hence are not plotted.

Comparison with other Magnetotelluric Power Spectra

Although each of the spectra plotted for Lvov, Ashkhabad, and Tbilisi cover a frequency range of 2.4 decades of frequency, it is evident that this is a small portion of the total magnetotelluric power spectrum. In order to provide a more comprehensive viewpoint, composite spectra are plotted in Figures 31 and 32 with selections from data computed here combined with spectra obtained from other authors.

The magnetotelluric data for Ralston, Canada, were recorded on 31 July 1959 and were supplied by C. W. Horton. A description of these data may be found in papers by Horton and Hoffman [21, 22].

The magnetotelluric data for Littleton, Massachusetts, were recorded by Dr. Thomas Cantwell on 5 December 1959. These spectra are given in his dissertation [19] as Case 27-3.

The magnetotelluric data for Austin, Texas, were recorded on 27 March 1961, by Dr. H. W. Smith and Mr. F. X. Bostick of the Electrical Engineering Research Laboratories, The University of Texas. Descriptions of the recording equipment used by Smith and Bostick are found in the reports of the Electrical Engineering Research Laboratories [22, 23].

The locations of these various stations are shown in Figure 33. Despite the fact that the data were recorded over a period of 2 1/2 years and extend over a longitude range of 170°, the data appear to fit a uniform trend. It is suggested that the trends established in Figures 31 and 32 are a first approximation to the ambient magnetotelluric field at the earth's surface. Although fluctuations of the power density at one station may vary 10 db (Dr. H. W. Smith, personal communication) and the level between two stations may be as great as 20 db (Lvov and Tbilisi), these variations are small compared to the variation of 80 db in the telluric field plotted in Figure 32.

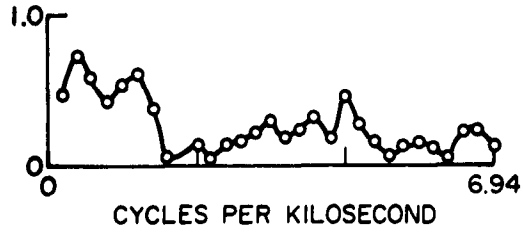

E-W TELLURIC AND N-S MAGNETIC
1 SEPT 1957

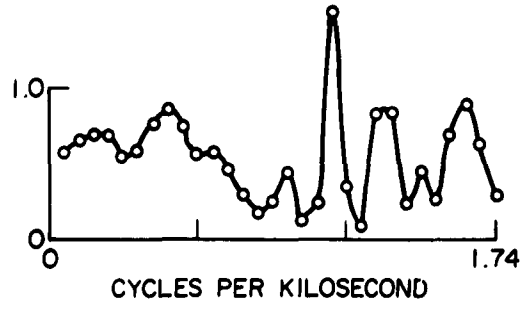

E-W TELLURIC AND N-S MAGNETIC
1 SEPT 1957

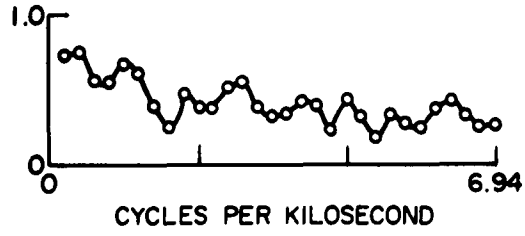

E-W TELLURIC AND N-S MAGNETIC
2 SEPT 1957

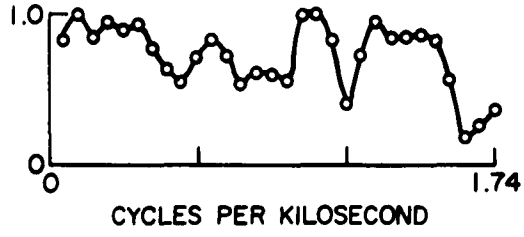

E-W TELLURIC AND N-S MAGNETIC
2 SEPT 1957

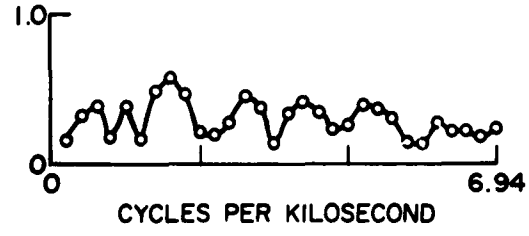

N-S TELLURIC AND E-W MAGNETIC
1 SEPT 1957

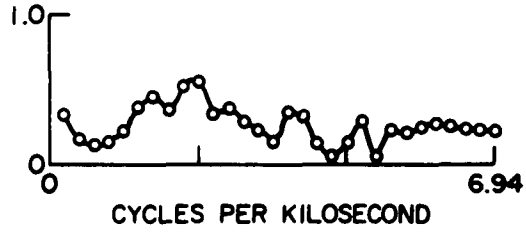

N-S TELLURIC AND E-W MAGNETIC
2 SEPT 1957

FIGURE 30

THE COHERENCY FUNCTION $Coh_{HE}(f)$ FOR THE MAGNETOTELLURIC FIELD AT TBILISI 1-2 SEPTEMBER 1957

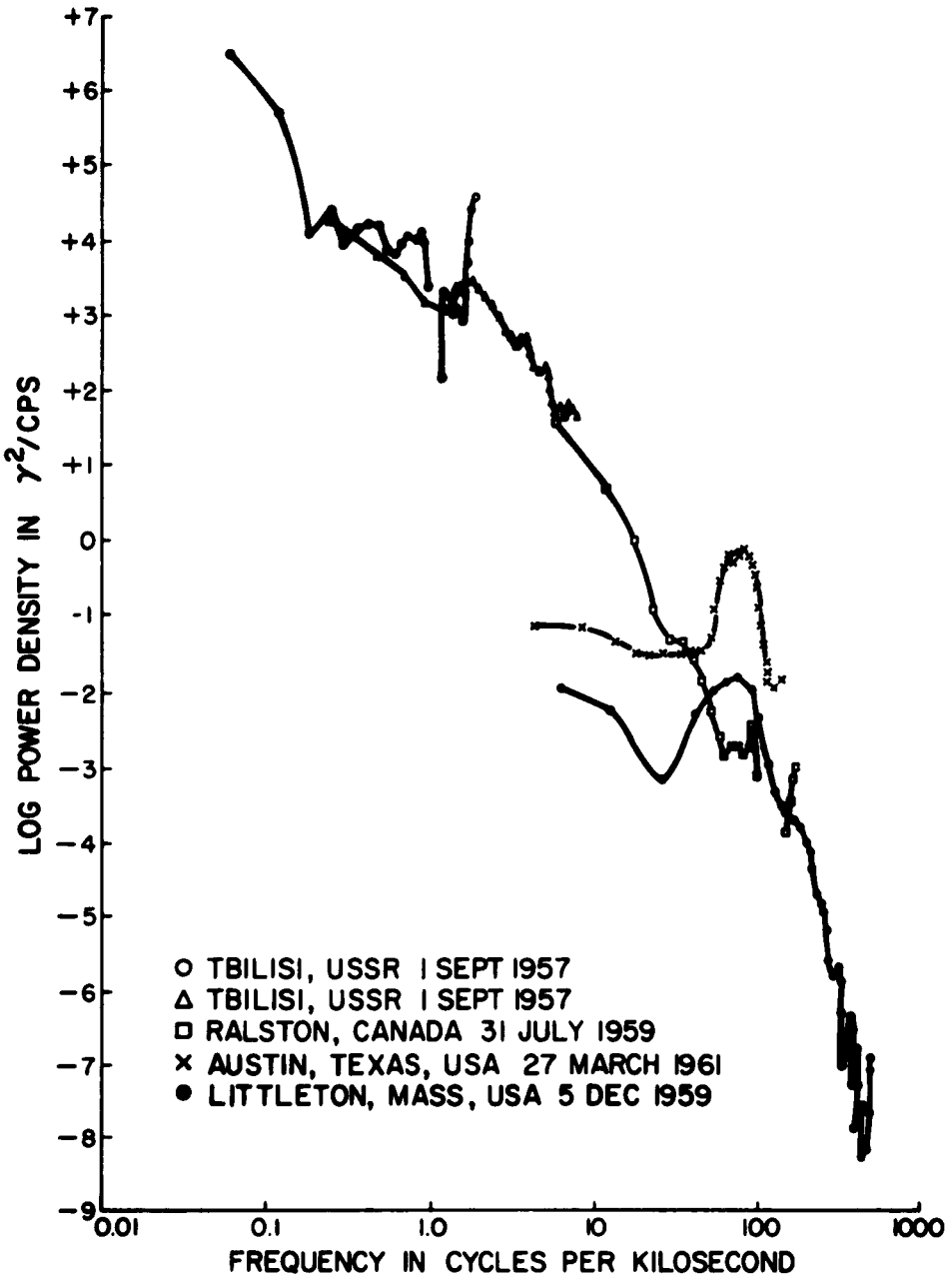

FIGURE 31
A COMPOSITE GRAPH OF THE POWER SPECTRA OF THE NORTH-SOUTH MAGNETIC FIELD FOR USSR, CANADA, MASSACHUSETTS, AND TEXAS

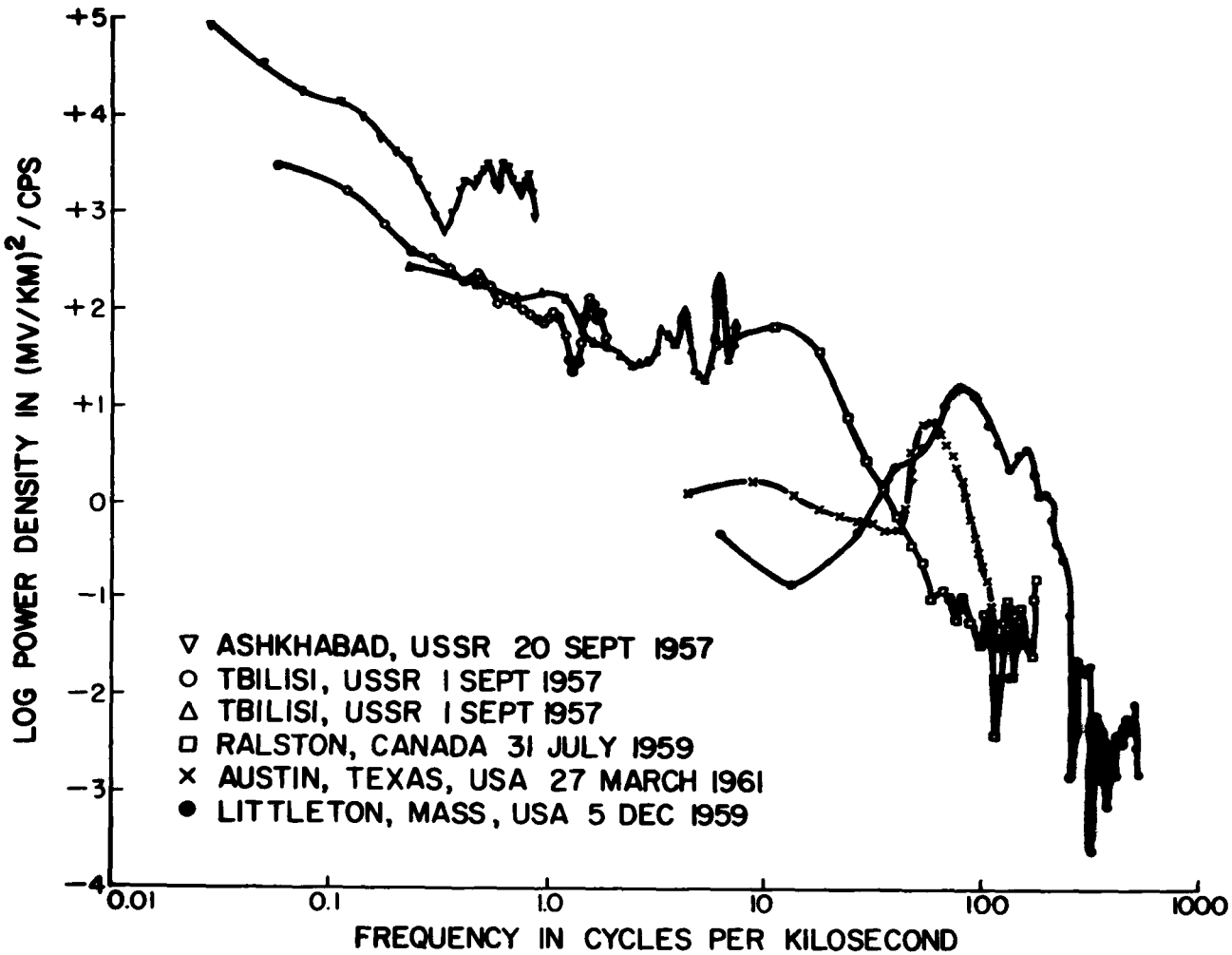

FIGURE 32

A COMPOSITE GRAPH OF THE POWER SPECTRA OF THE EAST-WEST TELLURIC FIELD FOR USSR, CANADA, MASSACHUSETTS, AND TEXAS

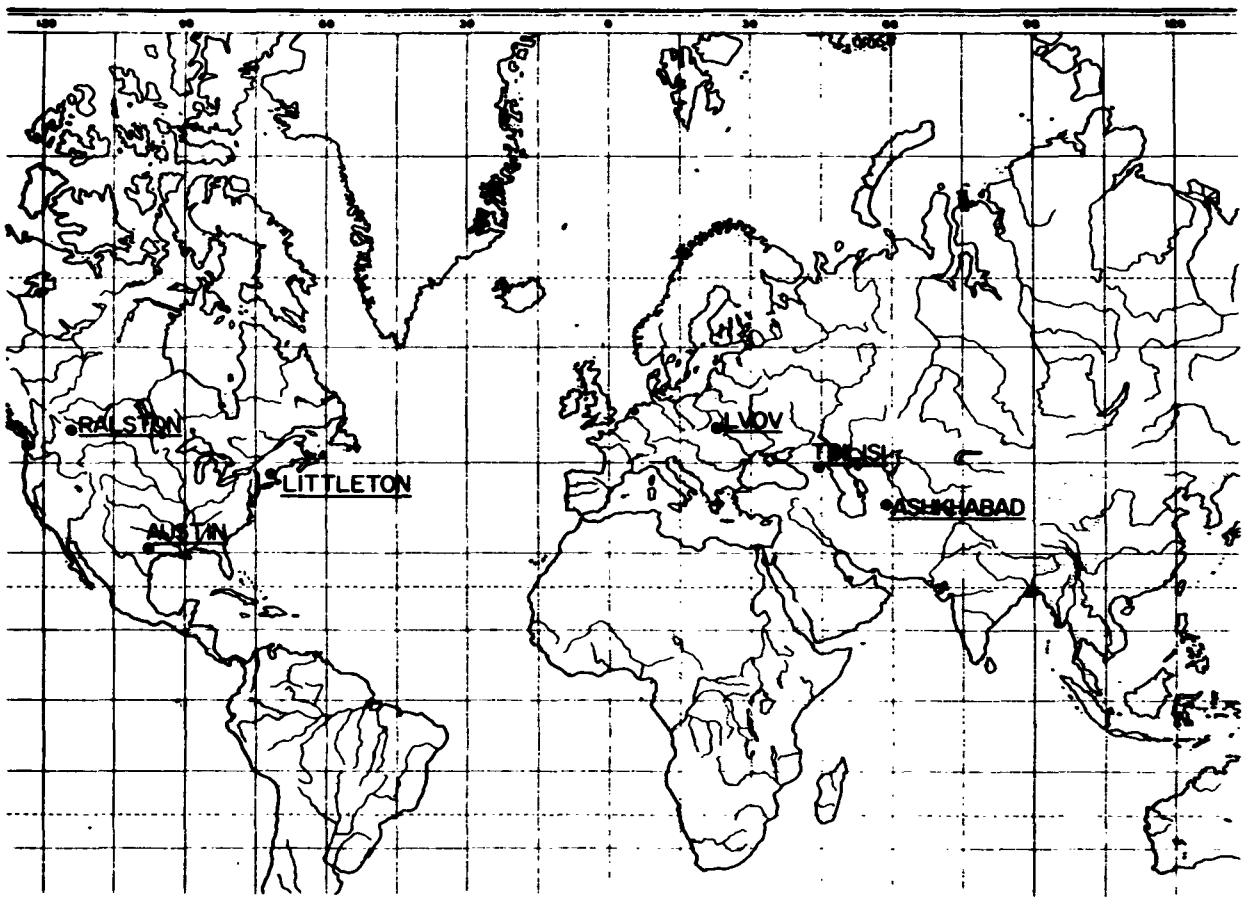

FIGURE 33
LOCATION OF STATIONS IN USSR, CANADA, MASSACHUSETTS, AND TEXAS

Prepared by Henry M. Leppard
Published by the University of Chicago Press, Chicago, Illinois

The corresponding variation in the power density of the magnetic field plotted in Figure 31 is 150 db.

The following empirical formulas represent useful approximations to the data presented in Figures 31 and 32. When f is expressed in cycles per kilosecond, the magnetic field can be expressed by

$$P_H(f) = 10^5\left[1 + 25f^2 + f^4 + 1.3 \times 10^{-4} f^6\right]^{-1} \text{ (gammas)}^2/\text{cps}, \quad (59)$$

for 0.1 cpks < f < 400 cpks.

Superimposed on this background spectrum is an intense band of power at 80 cpks in the Canadian data. The electric field can be expressed by (again f in cpks).

$$P_E(f) = 10^5\left[1 + 100f + 20f^2 + f^3\right]^{-1}\left(\frac{\text{mv}}{\text{km}}\right)^2/\text{cps} \quad , \quad (60)$$

for 0.03 cpks < f < 400 cpks.

The experimental data for $P_E(f)$ scatter more strongly than the data for $P_H(f)$. This is undoubtedly due to the influence of the earth's structure on the telluric field.

CHAPTER VII

GEOPHYSICAL INTERPRETATION OF THE POWER SPECTRA

Spectral analysis may be used as a basis for geophysical interpretation. Here the power spectra are used to compute an apparent resistivity of the earth to compute the frequency response of the earth as a linear filter, and to make an interesting comparison between peaks in the power spectra and modes of free oscillation of the earth.

The Apparent Resistivity of the Earth

If one considers the energy sources of the magnetotelluric field to be above the earth, and the power impinges on the earth as a plane electromagnetic wave, most of the power is reflected, because of the great contrast in the electrical properties of the air and the earth, but some is propagated into the earth. To a first approximation the tangential electric field at the earth's surface is zero and the tangential magnetic field is double that of the incident wave. The earth is not a perfect conductor, so that the tangential electric field is not zero, and thus is sensitive to the electrical properties of the earth. The reason for this sensitivity is that the incident wave and the waves reflected from the subsurface strata almost cancel at the surface [25]. The extent to which the wave incident on the earth penetrates the earth depends upon the contrasting electrical properties of a layered earth and the power spectrum of the incident wave. The depth of penetration is the depth at which the magnitude of the wave is equal to 1/e of its magnitude at the surface. This depth is called the skin depth and is a function of frequency [26].

Assume that the air and earth are each semi-infinite electrically homogeneous, isotropic media such that the air-earth interface is a plane located at $z = 0$ in the right-handed rectangular cartesian coordinate system shown in Figure 34.

The electric and magnetic fields at any point in a homogeneous, isotropic, and charge free medium satisfy Maxwell's equations in the form [26]

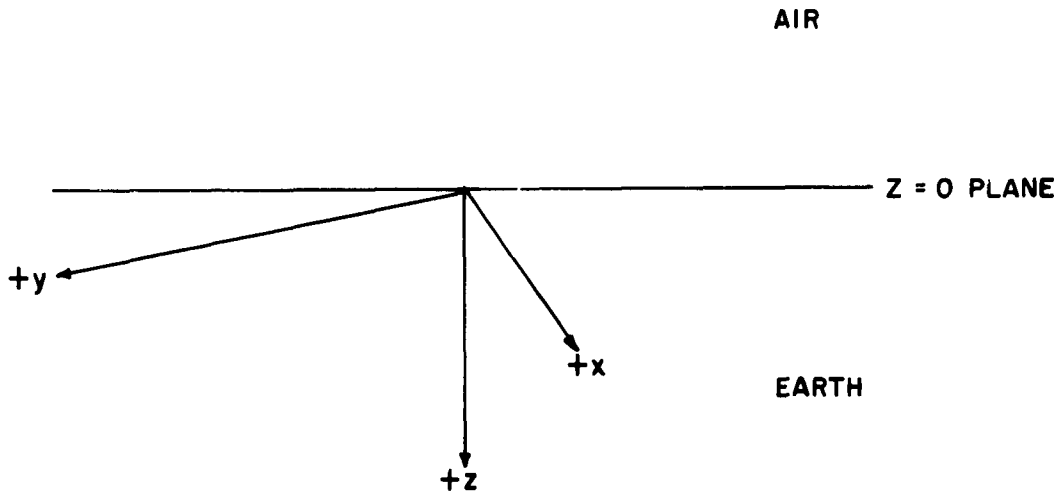

FIGURE 34
THE AIR-EARTH INTERFACE

$$\nabla \times \vec{E} = -\mu \frac{\partial \vec{H}}{\partial t} \quad , \tag{61a}$$

$$\nabla \times \vec{H} = \frac{1}{\rho} \vec{E} + \epsilon \frac{\partial \vec{E}}{\partial t} \quad , \tag{61b}$$

$$\nabla \cdot \vec{E} = 0 \quad , \tag{61c}$$

and

$$\nabla \cdot \vec{H} = 0 \quad , \tag{61d}$$

where $\vec{E}$ is the electric field strength in volts per meter,

$\vec{H}$ is the magnetic field strength in amperes per meter,

μ is the magnetic permeability in henry per meter,

ϵ is electric permittivity in farad per meter,

$\rho(=\frac{1}{\sigma})$ is the resistivity in ohm-meters, and

σ is the conductivity in mho per meter.

The usual conditions for neglecting the displacement current [26], i.e.,

$$\left(\frac{\sigma}{\epsilon\omega}\right)^2 \gg 1 \quad , \tag{62}$$

are amply met here so that equation (61b) may be approximated by

$$\nabla \times \vec{H} = \frac{1}{\rho} \vec{E} \quad . \tag{63}$$

If it be assumed that linearly polarized plane electromagnetic waves are propagated in the positive z direction such that the x-axis is in the direction of the electric field and the y-axis is in the direction of the magnetic field, then there is no variation of the fields in the x or y directions. For the above conditions, equations (61a) and (63) reduce to

$$\frac{\partial E_x}{\partial z} = -\mu \frac{\partial H_y}{\partial t} \quad , \tag{64}$$

and

$$\frac{\partial H_y}{\partial z} = -\sigma E_x \quad , \tag{65}$$

where the subscripts x and y indicate the polarization. Substitution of equation (65) into equation (64) or equation (64) into (65) yield

$$\frac{\partial^2 H_y}{\partial z^2} = \sigma\mu \frac{\partial H_y}{\partial t} \quad , \tag{66}$$

and

$$\frac{\partial^2 E_x}{\partial z^2} = \sigma\mu \frac{\partial E_x}{\partial t} \quad . \tag{67}$$

Since the fields will be resolved in terms of harmonic components it is natural to select harmonic solutions of the form

$$E_x(z,\omega,t) = E_x(z,\omega)\ e^{j\omega t} \quad , \tag{68}$$

and

$$H_y(z,\omega,t) = H_y(z,\omega)\ e^{j\omega t} \quad . \tag{69}$$

Substituting equations (68) and (69) into (64) through (67) results in

$$\frac{\partial E_x(z,\omega)}{\partial z} = -j\omega\mu\ H_y(z,\omega) \quad , \tag{70}$$

$$\frac{\partial H_y(z,\omega)}{\partial z} = -\sigma\ E_x(z,\omega) \quad , \tag{71}$$

$$\frac{\partial^2 H_y(z,\omega)}{\partial z^2} = j\omega\sigma\mu\ H_y(z,\omega) \quad , \tag{72}$$

and

$$\frac{\partial^2 E_x(z,\omega)}{\partial z^2} = j\omega\sigma\mu\ E_x(z,\omega) \quad . \tag{73}$$

Solutions of equations (72) and (73) can be written in the form

$$H_y(z,\omega) = H_{oy}(\omega)\, e^{-jkz} \quad , \tag{74}$$

and

$$E_x(z,\omega) = E_{ox}(\omega)\, e^{jkz} \quad , \tag{75}$$

where

$$k^2 = -j\sigma\omega\mu \quad , \tag{76}$$

or

$$k = \left(\frac{\omega\sigma\mu}{2}\right)^{\frac{1}{2}} (1-j) \quad . \tag{77}$$

Introducing the solutions (74) and (75) into the component equation (65) results in

$$\frac{E_{ox}(\omega)}{H_{oy}(\omega)} = \frac{jk}{\sigma} \quad ,$$

or

$$\frac{E_{ox}(\omega)}{H_{oy}(\omega)} = \left(\frac{\omega\mu}{2\sigma}\right)^{\frac{1}{2}} (j+1) \quad . \tag{78}$$

Using the identity

$$1+j = e^{j\pi/4} \cdot \sqrt{2} \quad , \tag{79}$$

and solving for the resistivity, equation (78) becomes

$$\rho = \frac{1}{\sigma} = \frac{1}{2\pi\mu f}\, e^{-j\pi/2} \left[\frac{E_{ox}(f)}{H_{oy}(f)}\right]^2 \quad , \tag{80}$$

where $f = \omega/2\pi$.

Assuming that the magnetotelluric field is due to a linearly polarized plane electromagnetic wave propagating from the air into the earth (see Figure 34) it is easy to see how the resistivity of a homogeneous, isotropic earth could be computed from the magnetotelluric field components using equation (80), provided one could separate the frequency components in the experimental observations.

Cagniard's paper [24] on the magnetotelluric field produced a renewal of interest in the use of the magnetotelluric field components for the interpretation of the electrical structure of the earth. Cagniard assumes stratified earth models in which the earth consists of two or more horizontal layers of contrasting resistivity. Equation (80), which gives the resistivity for an unlayered earth, may also be used for a layered earth, in which case the computed quantity, ρ, is referred to as the apparent resistivity, ρ_a. Cagniard's proposal involves the plotting of an apparent resistivity versus the square root of the period of the wave, but he does not show how one should resolve the experimental observations which resemble a stochastic time series into frequency components.

Cantwell considered the magnetotelluric field components as samples of stationary stochastic processes and applied the numerical methods of Blackman and Tukey to the data. Cantwell showed that Cagniard's basic formula for the apparent resistivity may be expressed in terms of power spectra as

$$\rho_a = 0.2\, T \frac{P_E(f)}{P_H(f)} \quad , \tag{81}$$

where ρ_a = apparent resistivity, ohm meters,

T = period in seconds,

$P_E(f)$ = power spectral density of the telluric field component in (millivolts/kilometer)^2 per cycle per second,

$P_H(f)$ = power spectral density of the orthogonal component of the horizontal magnetic field in (gammas)^2 per cycle per second,

0.2 = dimensional constant chosen to make the equation correct.

Cagniard provides a template for interpreting the apparent resistivity in terms of electrically conducting layers when the data are plotted as a graph of ρ_a versus $T^{1/2}$ on log-log paper. However, the present data do not show evidence of an electrical interface so they are plotted versus frequency. The vertical scale is compressed to reduce the scatter of the points and to facilitate the drawing of a curve through the points. Figure 35 contains plots of apparent resistivity based on the East-West telluric field and the North-South magnetic field for 1 and 2 September. Figure 36 contains a similar plot based on the other pair of components of the magnetotelluric field. The computed values of apparent resistivity are given in Tables 19-22. The latter data are restricted to the outputs of the high-pass filter because of the uncertainties in the low-passed data.

The four curves plotted in Figures 35 and 36 are mutually consistent and they indicate a resistivity of 6 ohm meters over the frequency range 0.1 to 7 cpks. The apparent resistivity is essentially constant over this frequency range and there is no evidence of stratification of the earth's conductivity. The difference between the apparent resistivities obtained from the two components of the telluric field are not sufficiently different to suggest any horizontal anisotropy in the earth's resistivity at the relevant depths.

This determination of the apparent resistivity of the earth is not inconsistent with the results of previous theoretical and experimental studies. Cantwell interprets the resistivity profile in Massachusetts as a layer 70 kilometers thick with a resistivity of 8,000 ohm meters underlain by a zone of much lower resistivity. The frequency range covered by the present study is not so low that the layer determined by Cantwell has no effect on the measurements. However, the results of Figures 35 and 36 suggest that the resistivity of the material below the layer determined by Cantwell is 6 ohm meters. The present data do not establish a thickness for either of the layers nor of the resistivity contrast. However, since a change of frequency of a factor of 100 is equivalent to a change of depth of a factor of 10 for resistivity determinations [25], one feels safe in concluding that the layer

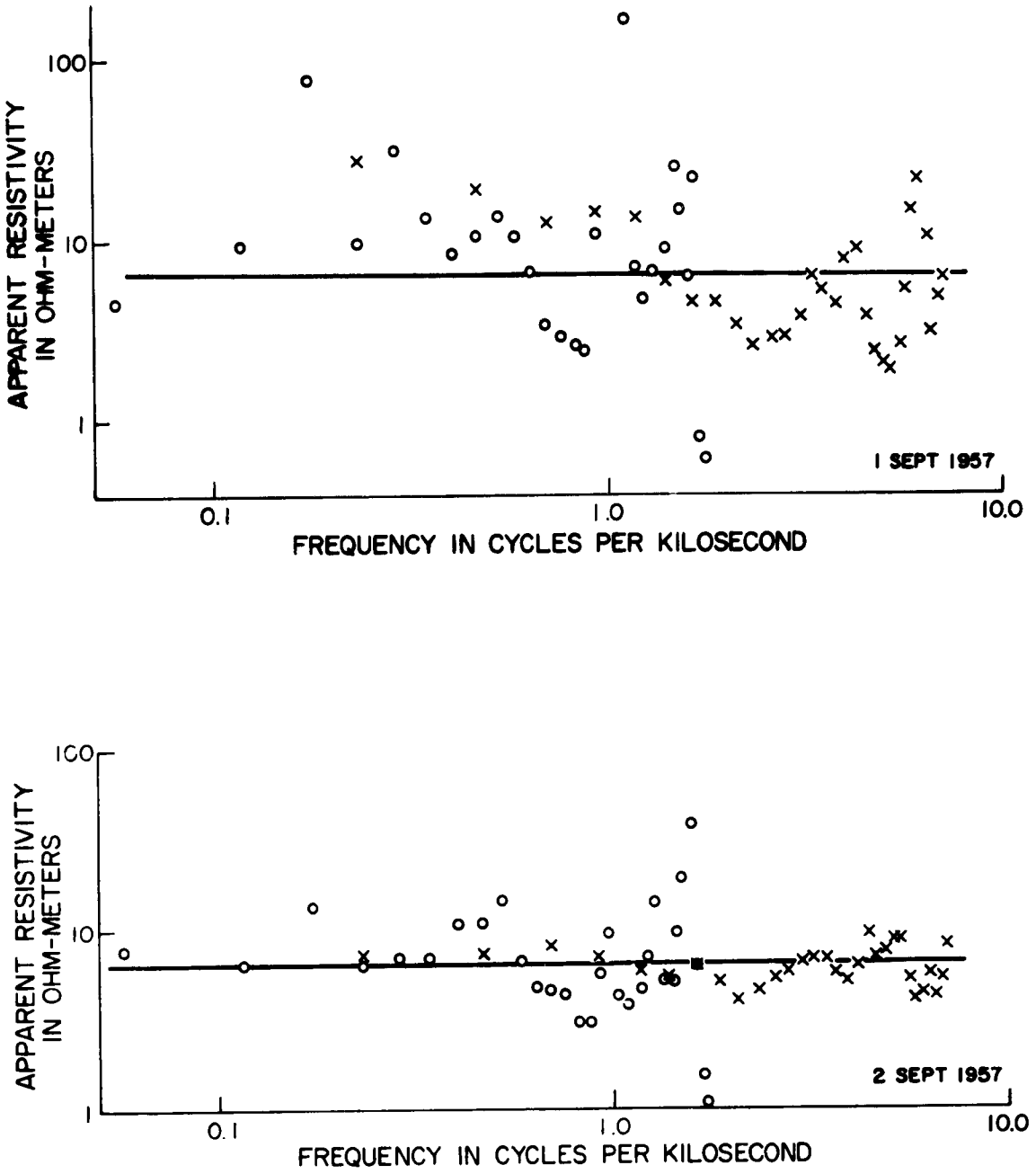

FIGURE 35

THE APPARENT RESISTIVITY VERSUS FREQUENCY DETERMINED FROM EAST-WEST COMPONENT OF TELLURIC FIELD AT TBILISI 1 AND 2 SEPTEMBER 1957

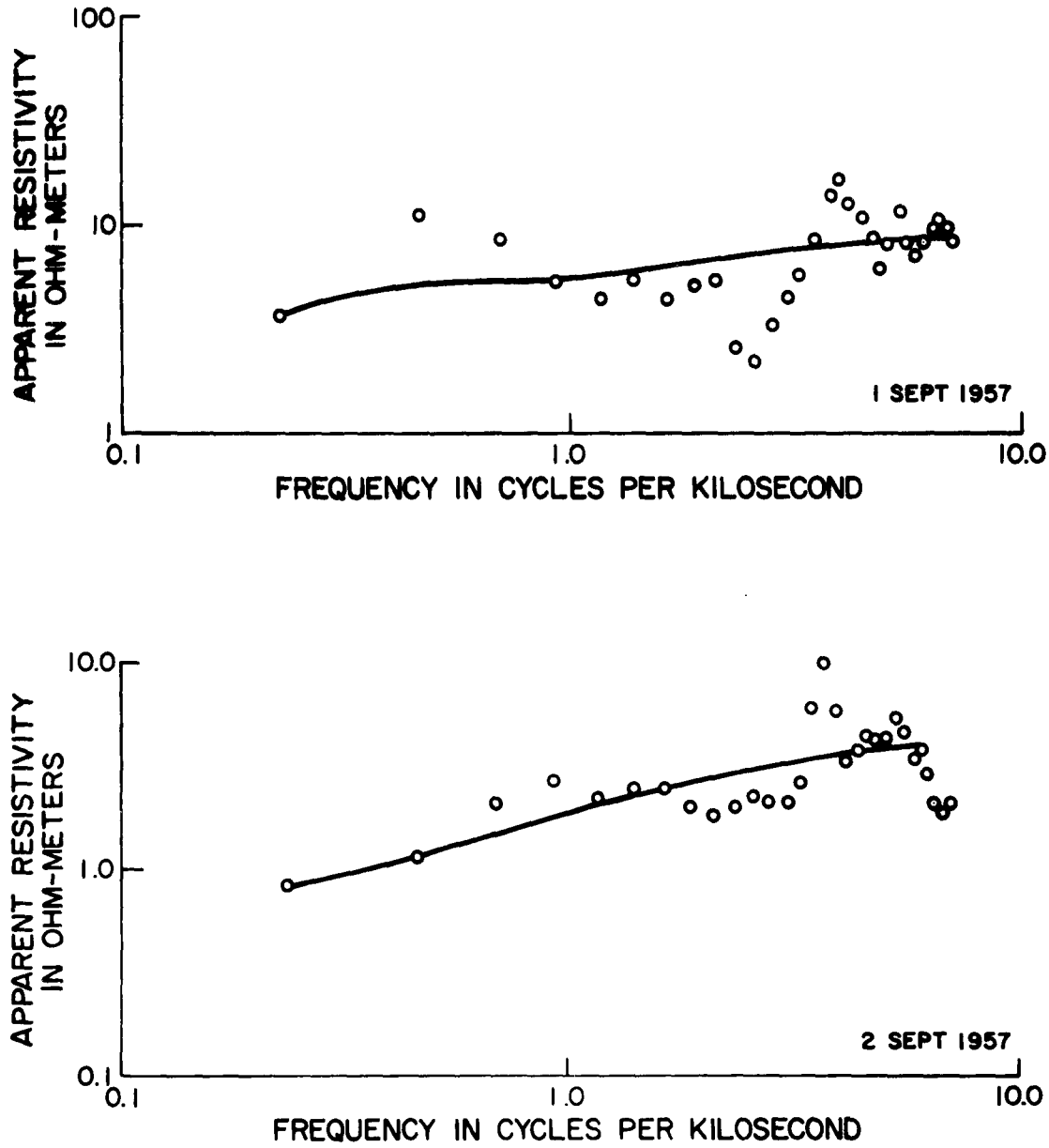

FIGURE 36

THE APPARENT RESISTIVITY VERSUS FREQUENCY DETERMINED FROM NORTH-SOUTH COMPONENT OF TELLURIC FIELD AT TBILISI 1 AND 2 SEPTEMBER 1957

APPARENT RESISTIVITY IN OHM METER

	FRQUENCY CPS	PERIOD SEC	EAST MAGNETIC NORTH TELLURIC	NORTH MAGNETIC EAST TELLURIC
1	.000E+00	.00	.000000E+00	.000000E+00
2	.231E-03	4320.00	.369279E+01	.281286E+02
3	.463E-03	2160.00	.113957E+02	.194253E+02
4	.694E-03	1440.00	.840330E+01	.129704E+02
5	.926E-03	1080.00	.521944E+01	.144856E+02
6	.116E-02	864.00	.436688E+01	.129919E+02
7	.139E-02	720.00	.531387E+01	.600730E+01
8	.162E-02	617.14	.427588E+01	.463612E+01
9	.185E-02	540.00	.519203E+01	.465192E+01
10	.208E-02	480.00	.523871E+01	.343634E+01
11	.231E-02	432.00	.252099E+01	.265340E+01
12	.255E-02	392.73	.220273E+01	.234180E+01
13	.278E-02	360.00	.319496E+01	.298110E+01
14	.301E-02	332.31	.448339E+01	.391637E+01
15	.324E-02	308.57	.575062E+01	.632859E+01
16	.347E-02	288.00	.829431E+01	.548903E+01
17	.370E-02	270.00	.135819E+02	.461995E+01
18	.394E-02	254.12	.163477E+02	.820012E+01
19	.417E-02	240.00	.129818E+02	.948598E+01
20	.440E-02	227.37	.108044E+02	.337316E+01
21	.463E-02	216.00	.829462E+01	.242292E+01
22	.486E-02	205.71	.608538E+01	.215063E+01
23	.509E-02	196.36	.834416E+01	.190608E+01
24	.532E-02	187.83	.110422E+02	.273064E+01
25	.556E-02	180.00	.802813E+01	.533159E+01
26	.579E-02	172.80	.717575E+01	.145645E+02
27	.602E-02	166.15	.811710E+01	.227996E+02
28	.625E-02	160.00	.927438E+01	.103059E+02
29	.648E-02	154.29	.101736E+02	.316596E+01
30	.671E-02	148.97	.961852E+01	.494256E+01
31	.694E-02	144.00	.821618E+01	.621548E+01

TABLE 19

APPARENT RESISTIVITY AT TBILISI 1 SEPTEMBER 1957 (HIGH-PASS FILTERED).

APPARENT RESISTIVITY IN OHM METER

	FRQUENCY CPS	PERIOD SEC	EAST MAGNETIC NORTH TELLURIC	NORTH MAGNETIC EAST TELLURIC
1	.000E+00	.00	.000000E+00	.000000E+00
2	.579E-04	17280.00	.500494E+00	.460016E+01
3	.116E-03	8640.00	-.123966E+02	.912174E+01
4	.174E-03	5760.00	-.327064E+02	.794878E+02
5	.231E-03	4320.00	-.185662E+02	.970748E+01
6	.289E-03	3456.00	.449952E+02	.318607E+02
7	.347E-03	2880.00	.822454E+02	.132243E+02
8	.405E-03	2468.57	.592236E+02	.859154E+01
9	.463E-03	2160.00	-.535531E+02	.109381E+02
10	.521E-03	1920.00	-.811736E+02	.135725E+02
11	.579E-03	1728.00	-.177620E+02	.103109E+02
12	.637E-03	1570.91	.129386E+02	.665483E+01
13	.694E-03	1440.00	-.386669E+02	.344252E+01
14	.752E-03	1329.23	-.501727E+02	.294153E+01
15	.810E-03	1234.29	-.701871E+01	.261474E+01
16	.868E-03	1152.00	.316108E+02	.241598E+01
17	.926E-03	1080.00	.937247E+02	.104742E+02
18	.984E-03	1016.47	.162591E+03	-.108015E+02
19	.104E-02	960.00	-.281032E+02	-.168648E+02
20	.110E-02	909.47	-.588788E+02	.164810E+03
21	.116E-02	864.00	.145700E+02	.710142E+01
22	.122E-02	822.86	.238263E+02	.471713E+01
23	.127E-02	785.45	-.234684E+02	.675195E+01
24	.133E-02	751.30	-.656952E+02	.650437E+01
25	.139E-02	720.00	-.466601E+02	.838515E+01
26	.145E-02	691.20	-.337360E+02	.250693E+02
27	.150E-02	664.62	-.582475E+02	.149382E+02
28	.156E-02	640.00	-.120231E+02	.608273E+01
29	.162E-02	617.14	.264310E+02	.222851E+01
30	.168E-02	595.86	.149784E+02	.810969E+00
31	.174E-02	576.00	.780885E+01	.602586E+00

TABLE 20

APPARENT RESISTIVITY AT TBILISI 1 SEPTEMBER 1957 (LOW-PASS FILTERED).

APPARENT RESISTIVITY IN OHM METER

	FROUENCY CPS	PERIOD SEC	EAST MAGNETIC NORTH TELLURIC	NORTH MAGNETIC EAST TELLURIC
1	.000E+00	.00	.000000E+00	.000000E+00
2	.231E-03	4320.00	.848561E+00	.705163E+01
3	.463E-03	2160.00	.112731E+01	.720980E+01
4	.694E-03	1440.00	.208879E+01	.805363E+01
5	.926E-03	1080.00	.256123E+01	.719720E+01
6	.116E-02	864.00	.222840E+01	.596853E+01
7	.139E-02	720.00	.240491E+01	.546525E+01
8	.162E-02	617.14	.243540E+01	.613543E+01
9	.185E-02	540.00	.201286E+01	.511269E+01
10	.208E-02	480.00	.186138E+01	.414423E+01
11	.231E-02	432.00	.200885E+01	.470676E+01
12	.255E-02	392.73	.222912E+01	.534337E+01
13	.278E-02	360.00	.219383E+01	.586071E+01
14	.301E-02	332.31	.219664E+01	.664984E+01
15	.324E-02	308.57	.260272E+01	.685374E+01
16	.347E-02	288.00	.581040E+01	.677598E+01
17	.370E-02	270.00	.996367E+01	.587172E+01
18	.394E-02	254.12	.583734E+01	.520250E+01
19	.417E-02	240.00	.335621E+01	.641130E+01
20	.440E-02	227.37	.399993E+01	.877473E+01
21	.463E-02	216.00	.443690E+01	.707639E+01
22	.486E-02	205.71	.446603E+01	.762637E+01
23	.509E-02	196.36	.444960E+01	.862782E+01
24	.532E-02	187.83	.539938E+01	.867567E+01
25	.556E-02	180.00	.477207E+01	.558615E+01
26	.579E-02	172.80	.349082E+01	.432838E+01
27	.602E-02	166.15	.374401E+01	.563683E+01
28	.625E-02	160.00	.292866E+01	.586957E+01
29	.648E-02	154.29	.209665E+01	.433147E+01
30	.671E-02	148.97	.198033E+01	.568006E+01
31	.694E-02	144.00	.202499E+01	.831898E+01

TABLE 21

APPARENT RESISTIVITY AT TBILISI 2 SEPTEMBER 1957 (HIGH-PASS FILTERED).

APPARENT RESISTIVITY IN OHM METER

	FRQUENCY CPS	PERIOD SEC	EAST MAGNETIC NORTH TELLURIC	NORTH MAGNETIC EAST TELLURIC
1	.000E+00	.00	.000000E+00	.000000E+00
2	.579E-04	17280.00	-.450131E+01	.753286E+01
3	.116E-03	8640.00	.515451E+02	.622565E+01
4	.174E-03	5760.00	.108739E+03	.134203E+02
5	.231E-03	4320.00	-.399511E+03	.631158E+01
6	.289E-03	3456.00	-.142292E+03	.683122E+01
7	.347E-03	2880.00	.290387E+03	.696730E+01
8	.405E-03	2468.57	.152132E+03	.102615E+02
9	.463E-03	2160.00	-.160802E+03	.105180E+02
10	.521E-03	1920.00	.115600E+01	.154988E+02
11	.579E-03	1728.00	.604839E+03	.652822E+01
12	.637E-03	1570.91	.503195E+03	.475916E+01
13	.694E-03	1440.00	.926298E+01	.468358E+01
14	.752E-03	1329.23	-.176087E+03	.422466E+01
15	.810E-03	1234.29	-.157443E+03	.318379E+01
16	.868E-03	1152.00	-.145195E+03	.300343E+01
17	.926E-03	1080.00	-.550225E+02	.569165E+01
18	.984E-03	1016.47	-.947606E+03	.951582E+01
19	.104E-02	960.00	-.334956E+04	.430453E+01
20	.110E-02	909.47	-.107317E+04	.393863E+01
21	.116E-02	864.00	.691856E+01	.440579E+01
22	.122E-02	822.86	-.752885E+02	.731142E+01
23	.127E-02	785.45	-.232905E+03	.131430E+02
24	.133E-02	751.30	-.482368E+03	.536235E+01
25	.139E-02	720.00	-.148510E+03	.529453E+01
26	.145E-02	691.20	.376149E+03	.967943E+01
27	.150E-02	664.62	.520689E+03	.197032E+02
28	.156E-02	640.00	-.591264E+02	.372136E+02
29	.162E-02	617.14	-.131727E+03	.634290E+01
30	.168E-02	595.86	-.270762E+01	.150332E+01
31	.174E-02	576.00	.124518E+02	.110285E+01

TABLE 22

APPARENT RESISTIVITY AT TBILISI 2 SEPTEMBER 1957 (LOW-PASS FILTERED).

whose resistivity is 6 ohm meters extends from about 70 to 700 kilometers below the surface.

The survey paper by Tozer [1] shows plots of resistivity versus depth computed theoretically by several authors. These plots indicate that a resistivity of 6 ohm meters is typical of a depth of 500 kilometers.

Frequency Response of the Earth

Use of Random Functions to Determine the Frequency Response of a Linear Filter

Consider a linear filter such as shown in Figure 37. Let the input, $u(t)$, be a member function of a stationary random process. The output, $v(t)$, will also be a stationary random process [9, 18]. Recalling equation (1), the output may be written in terms of the input through the relation

$$v(t) = \int_{0^-}^{\infty} u(t-\sigma)\, W(\sigma)\, d\sigma \quad , \tag{82}$$

where W is the impulsive response of the filter. Shifting the time scale by an amount τ results in

$$v(t+\tau) = \int_{0^-}^{\infty} u(t+\tau-\sigma)\, W(\sigma)\, d\sigma \quad . \tag{83}$$

Multiplying (83) by $u(t)$ and taking $u(t)$ inside the integral results in

$$u(t)\, v(t+\tau) = \int_{0^-}^{\infty} u(t)\, u(t+\tau-\sigma)\, W(\sigma)\, d\sigma \quad . \tag{84}$$

Integrating with respect to τ, multiplying by $1/\tau$, and taking the limit as τ increases without limit results in

$$\lim_{T\to\infty} \frac{1}{T} \int_{-T/2}^{T/2} u(t)\, v(t+\tau)\, d\tau = \lim_{T\to\infty} \frac{1}{T} \int_{-T/2}^{T/2} \int_{0^-}^{\infty} W(\sigma)\, u(t)\, u(t+\tau-\sigma)\, d\sigma d\tau. \tag{85}$$

The order of integration on the right hand side of equation (85) may be inverted so that

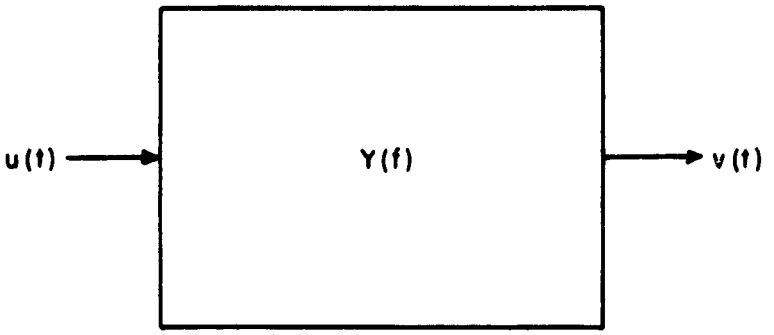

FIGURE 37
THE LINEAR FILTER

$$\lim_{T\to\infty} \frac{1}{T} \int_{-T/2}^{T/2} u(t)\, u(t+\tau)\, d\tau = \int_{0^-}^{\infty} W(\sigma) \lim_{T\to\infty} \int_{-T/2}^{T/2} u(t)\, u(t+\tau-\sigma)\, d\tau d\sigma. \qquad \ldots(86)$$

Using the definitions of auto- and cross-correlations (86) may be written as

$$C_{uv}(\tau) = \int_{0^-}^{\infty} W(\sigma)\, C_{uu}(\tau-\sigma)\, d\sigma \quad . \qquad (87)$$

Taking the Fourier transform of (87) and using the definition of Y(f) results in

$$P_{uv}(f) = Y(f)\, P_{uu}(f) \qquad (88)$$

or

$$Y(f) = \frac{P_{uv}(f)}{P_{uu}(f)} \quad . \qquad (89)$$

The phase delay is given by

$$\theta(f) = \arctan \left[\frac{P_{uv}^{odd}(f)}{P_{uv}^{even}(f)} \right] , \qquad (90)$$

in accordance with the previous discussion of cross-power. Equation (89) shows how the frequency response of a linear filter may be determined from the ratio of the cross-power (between the input and output) to the auto power of the input.

Frequency Response of the Earth as a Linear Filter

Assuming that the earth behaves as a linear filter with the variation of a horizontal component of the earth's magnetic field as the random input or driving function and the corresponding component of the telluric field as the output or resulting function, the frequency response of the earth can be computed using equation (89).

Specifically, the frequency response of the earth is computed from

$$Y_{earth}(f) = \frac{|P_{HE}(f)|}{P_{HH}(f)} \qquad (91)$$

where $|P_{HE}(f)|$ is the magnitude of the cross-power between the magnetic and electric field components,

$P_{HH}(f)$ is the (auto-) power spectrum of the magnetic field component.

Results using the above relation are tabulated in Tables 23, 24, 25, and 26, and plotted in Figures 38 and 39. These plots show that the frequency response is proportional to the square root of frequency, a characteristic of a uniform conductor.

It is felt that (91) is a more significant way of looking at the electrical properties of the earth since it includes the coherency between the components whereas Cagniard's formula as used by Cantwell (81) does not.

A Comparison Between Observed Free Earth Periods and Peaks in the Geomagnetic Power Spectrum

A recent paper by Ness, Harrison, and Slichter [25] reports values of the periods of the free oscillation of the earth as observed with a gravimeter during the Chilean earthquake of 22 May 1960. These reported values of the periods of the spherical modes are of interest here since the frequency range of the power spectra computed from low-pass filtered data recorded at Tbilisi is the same as the frequency range of the oscillations of the earth.

One would expect that the earth (a conductor) oscillating in its magnetic field would experience induced alternating currents with frequencies corresponding to the frequency of oscillation. With this in mind, the data for 1 and 2 September were subjected to power spectral analysis using 60 lags instead of 30 lags as were used to compute the results shown in Chapter IV. The results of this computation are plotted in Figures 40 and 41. To permit careful examination of all peaks in the power spectra, the graphs were plotted on semi-logarithmic paper with frequency on the linear scale. Table 27 shows a comparison between the observed free oscillation modes and the peaks in the

FREQUENCY RESPONSE OF THE EARTH

	FRQUENCY CPS	PERIOD SEC	EAST MAGNETIC NORTH TELLURIC	NORTH MAGNETIC EAST TELLURIC
1	.000E+00	.00	.000000E+00	.000000E+00
2	.231E-03	4320.00	.101969E-01	.853222E-01
3	.463E-03	2160.00	.493573E-01	.149597E+00
4	.694E-03	1440.00	.669767E-01	.123002E+00
5	.926E-03	1080.00	.302052E-01	.104105E+00
6	.116E-02	864.00	.631482E-01	.140551E+00
7	.139E-02	720.00	.346207E-01	.121555E+00
8	.162E-02	617.14	.920681E-01	.733017E-01
9	.185E-02	540.00	.127906E+00	.121134E-01
10	.208E-02	480.00	.111542E+00	.162631E-01
11	.231E-02	432.00	.346192E-01	.240620E-01
12	.255E-02	392.73	.325292E-01	.352688E-02
13	.278E-02	360.00	.600825E-01	.245335E-01
14	.301E-02	332.31	.119530E+00	.328242E-01
15	.324E-02	308.57	.120579E+00	.642141E-01
16	.347E-02	288.00	.492887E-01	.914414E-01
17	.370E-02	270.00	.187579E+00	.583060E-01
18	.394E-02	254.12	.229296E+00	.897950E-01
19	.417E-02	240.00	.185926E+00	.138230E+00
20	.440E-02	227.37	.100954E+00	.501925E-01
21	.463E-02	216.00	.114234E+00	.104349E+00
22	.486E-02	205.71	.153928E+00	.616915E-01
23	.509E-02	196.36	.177725E+00	.326258E-01
24	.532E-02	187.83	.174232E+00	.118238E-01
25	.556E-02	180.00	.695956E-01	.449745E-01
26	.579E-02	172.80	.668888E-01	.104086E+00
27	.602E-02	166.15	.142239E+00	.113472E+00
28	.625E-02	160.00	.120917E+00	.519344E-01
29	.648E-02	154.29	.126937E+00	.668369E-01
30	.671E-02	148.97	.110482E+00	.873261E-01
31	.694E-02	144.00	.126772E+00	.545266E-01

TABLE 23

FREQUENCY RESPONSE OF THE EARTH AT TBILISI 1 SEPTEMBER 1957
(HIGH-PASS FILTERED).

FREQUENCY RESPONSE OF THE EARTH

	FRQUENCY CPS	PERIOD SEC	EAST MAGNETIC NORTH TELLURIC	NORTH MAGNETIC EAST TELLURIC
1	.000E+00	.00	.000000E+00	.000000E+00
2	.579E-04	17280.00	.611877E-01	.199394E-01
3	.116E-03	8640.00	.146646E+00	.472394E-01
4	.174E-03	5760.00	.526207E+00	.174514E+00
5	.231E-03	4320.00	.284271E+00	.712551E-01
6	.289E-03	3456.00	.552774E+00	.113932E+00
7	.347E-03	2880.00	.692595E+00	.899333E-01
8	.405E-03	2468.57	.792441E+00	.953534E-01
9	.463E-03	2160.00	.984499E+00	.135264E+00
10	.521E-03	1920.00	.120130E+01	.133782E+00
11	.579E-03	1728.00	.680756E+00	.944733E-01
12	.637E-03	1570.91	.284679E+00	.816333E-01
13	.694E-03	1440.00	.236046E+00	.473494E-01
14	.752E-03	1329.23	.193189E+00	.307885E-01
15	.810E-03	1234.29	.236278E+00	.188990E-01
16	.868E-03	1152.00	.429752E+00	.227554E-01
17	.926E-03	1080.00	.108716E+01	.958468E-01
18	.984E-03	1016.47	.358401E+01	.294314E-01
19	.104E-02	960.00	.237755E+01	.676752E-01
20	.110E-02	909.47	.341329E+00	.143106E+01
21	.116E-02	864.00	.879013E+00	.696158E-01
22	.122E-02	822.86	.838526E+00	.163315E-01
23	.127E-02	785.45	.575955E+00	.172748E+00
24	.133E-02	751.30	.589212E-01	.176334E+00
25	.139E-02	720.00	.795706E+00	.596801E-01
26	.145E-02	691.20	.194933E+01	.181606E+00
27	.150E-02	664.62	.269913E+01	.942051E-01
28	.156E-02	640.00	.253902E+01	.151827E+00
29	.162E-02	617.14	.136929E+01	.120261E+00
30	.168E-02	595.86	.412416E+00	.520709E-01
31	.174E-02	576.00	.156070E+00	.207917E-01

TABLE 24

FREQUENCY RESPONSE OF THE EARTH AT TBILISI 1 SEPTEMBER 1957
(LOW-PASS FILTERED)

FREQUENCY RESPONSE OF THE EARTH

	FRQUENCY CPS	PERIOD SEC	EAST MAGNETIC NORTH TELLURIC	NORTH MAGNETIC EAST TELLURIC
1	.000E+00	.00	.000000E+00	.000000E+00
2	.231E-03	4320.00	.976764E-02	.650262E-01
3	.463E-03	2160.00	.910998E-02	.948715E-01
4	.694E-03	1440.00	.962849E-02	.928413E-01
5	.926E-03	1080.00	.155341E-01	.101237E+00
6	.116E-02	864.00	.257682E-01	.125262E+00
7	.139E-02	720.00	.505343E-01	.121177E+00
8	.162E-02	617.14	.636224E-01	.877263E-01
9	.185E-02	540.00	.508070E-01	.539094E-01
10	.208E-02	480.00	.697188E-01	.980794E-01
11	.231E-02	432.00	.812226E-01	.880815E-01
12	.255E-02	392.73	.552767E-01	.995669E-01
13	.278E-02	360.00	.638727E-01	.148124E+00
14	.301E-02	332.31	.530786E-01	.172489E+00
15	.324E-02	308.57	.467134E-01	.131634E+00
16	.347E-02	288.00	.559962E-01	.105226E+00
17	.370E-02	270.00	.141901E+00	.113286E+00
18	.394E-02	254.12	.105545E+00	.162493E+00
19	.417E-02	240.00	.416303E-01	.142467E+00
20	.440E-02	227.37	.162070E-01	.887039E-01
21	.463E-02	216.00	.461712E-01	.179781E+00
22	.486E-02	205.71	.981053E-01	.141287E+00
23	.509E-02	196.36	.225629E-01	.929740E-01
24	.532E-02	187.83	.828101E-01	.157651E+00
25	.556E-02	180.00	.739639E-01	.115606E+00
26	.579E-02	172.80	.787050E-01	.857313E-01
27	.602E-02	166.15	.934917E-01	.162163E+00
28	.625E-02	160.00	.782442E-01	.178053E+00
29	.648E-02	154.29	.640537E-01	.122874E+00
30	.671E-02	148.97	.572892E-01	.119543E+00
31	.694E-02	144.00	.550426E-01	.141179E+00

TABLE 25

FREQUENCY RESPONSE OF THE EARTH AT TBILISI 2 SEPTEMBER 1957
(HIGH-PASS FILTERED).

FREQUENCY RESPONSE OF THE EARTH

	FROUENCY CPS	PERIOD SEC	EAST MAGNETIC NORTH TELLURIC	NORTH MAGNETIC EAST TELLURIC
1	.000E+00	.00	.000000E+00	.000000E+00
2	.579E-04	17280.00	.755187E-01	.387248E-01
3	.116E-03	8640.00	.676029E+00	.605887E-01
4	.174E-03	5760.00	.547115E+01	.938761E-01
5	.231E-03	4320.00	.410514E+01	.812649E-01
6	.289E-03	3456.00	.329376E+01	.904950E-01
7	.347E-03	2880.00	.194887E+01	.104736E+00
8	.405E-03	2468.57	.866527E+01	.114458E+00
9	.463E-03	2160.00	.855671E+01	.104173E+00
10	.521E-03	1920.00	.115806E+02	.110836E+00
11	.579E-03	1728.00	.112466E+02	.980232E-01
12	.637E-03	1570.91	.877049E+01	.108320E+00
13	.694E-03	1440.00	.589231E+01	.925608E-01
14	.752E-03	1329.23	.233444E+01	.697059E-01
15	.810E-03	1234.29	.180260E+01	.708847E-01
16	.868E-03	1152.00	.241089E+01	.703739E-01
17	.926E-03	1080.00	.870650E+01	.932386E-01
18	.984E-03	1016.47	.161906E+02	.228691E+00
19	.104E-02	960.00	.422229E+02	.152142E+00
20	.110E-02	909.47	.270247E+02	.122393E+00
21	.116E-02	864.00	.181826E+02	.664645E-01
22	.122E-02	822.86	.674702E+01	.152660E+00
23	.127E-02	785.45	.640139E+01	.285730E+00
24	.133E-02	751.30	.105808E+02	.158877E+00
25	.139E-02	720.00	.112287E+02	.159786E+00
26	.145E-02	691.20	.907293E+01	.227359E+00
27	.150E-02	664.62	.106955E+02	.316741E+00
28	.156E-02	640.00	.827762E+01	.311763E+00
29	.162E-02	617.14	.370629E+01	.360359E-01
30	.168E-02	595.86	.571317E+00	.302870E-01
31	.174E-02	576.00	.898697E+00	.357218E-01

TABLE 26

FREQUENCY RESPONSE OF THE EARTH AT TBILISI 2 SEPTEMBER 1957
(LOW-PASS FILTERED).

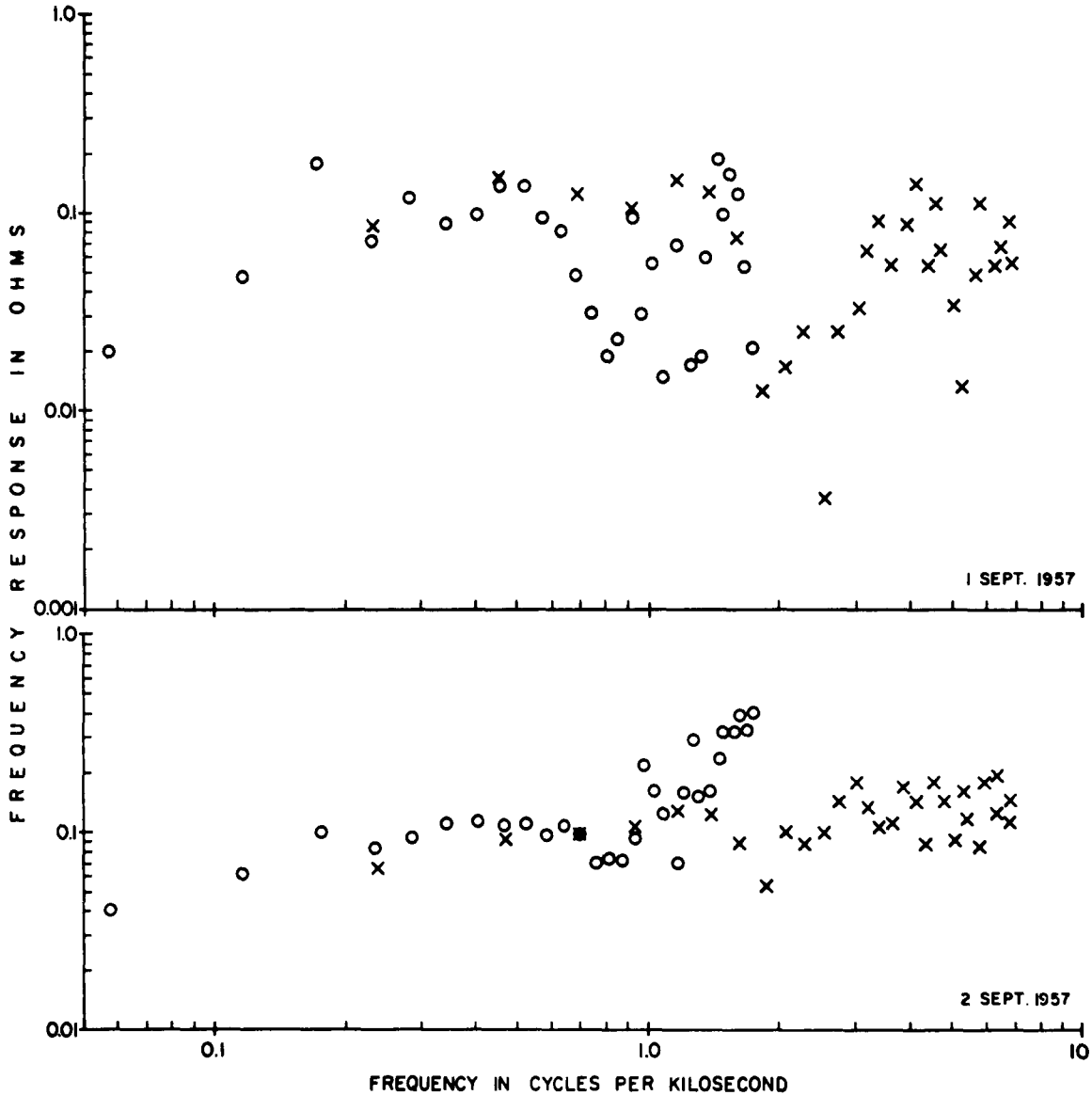

FIGURE 38

THE FREQUENCY RESPONSE OF THE EARTH VERSUS FREQUENCY DETERMINED FROM EAST-WEST COMPONENT OF TELLURIC FIELD AT TBILISI 1 AND 2 SEPTEMBER 1957

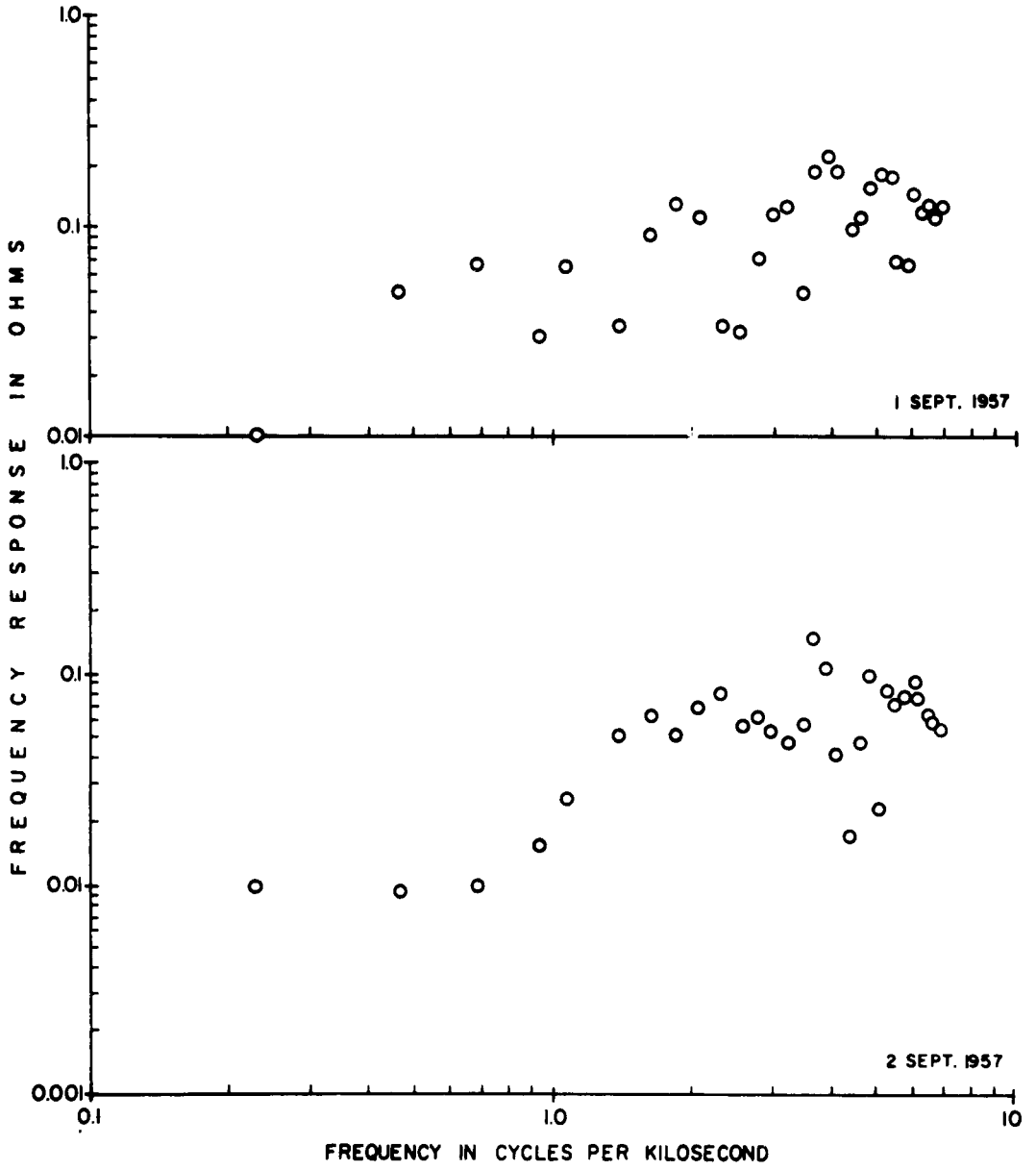

FIGURE 39

THE FREQUENCY RESPONSE OF THE EARTH VERSUS FREQUENCY DETERMINED FROM NORTH-SOUTH COMPONENT OF TELLURIC FIELD AT TBILISI 1 AND 2 SEPTEMBER 1957

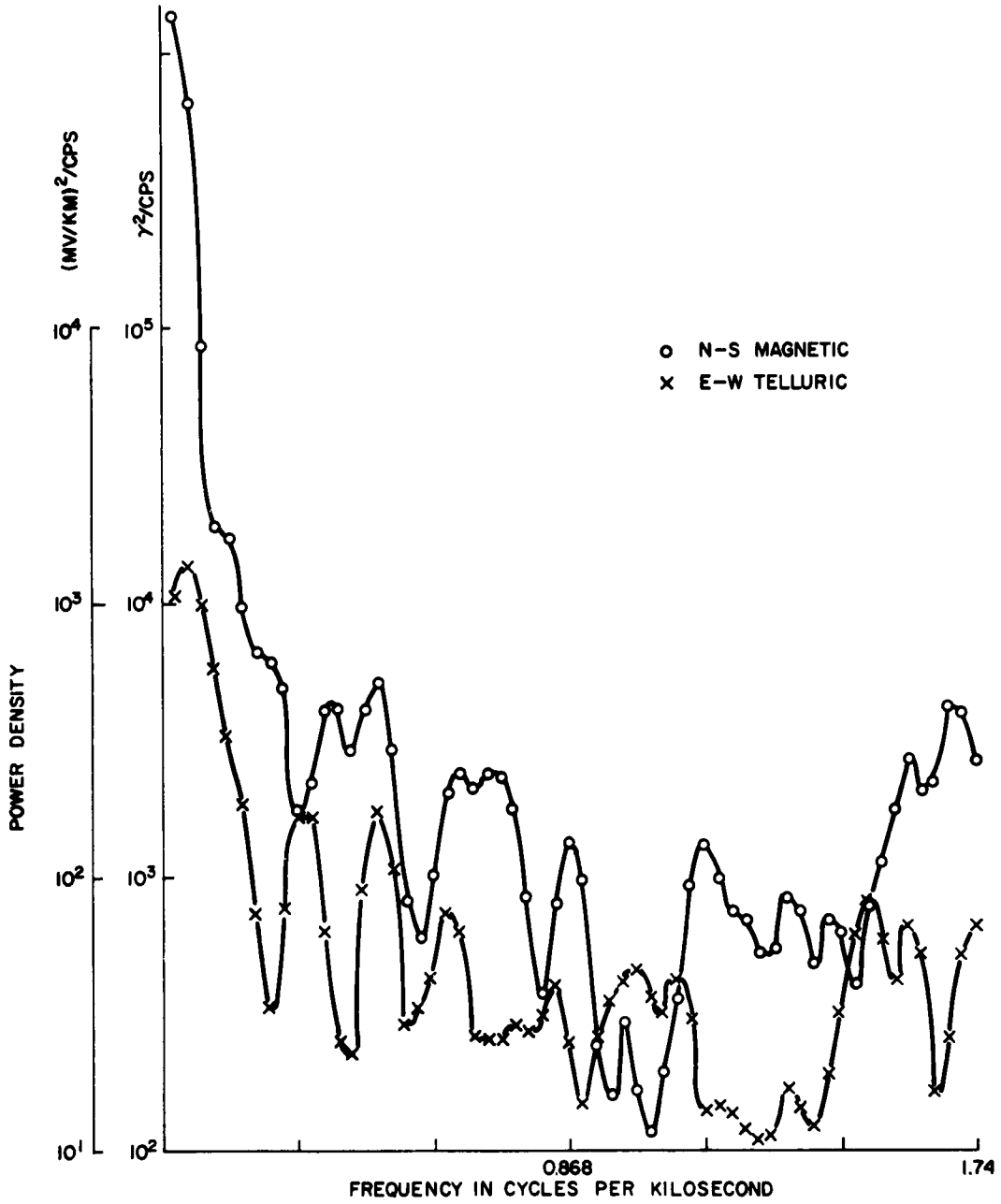

FIGURE 40
THE POWER SPECTRA OF THE NORTH-SOUTH MAGNETIC AND EAST-WEST TELLURIC FIELDS AT TBILISI 1 SEPTEMBER 1957

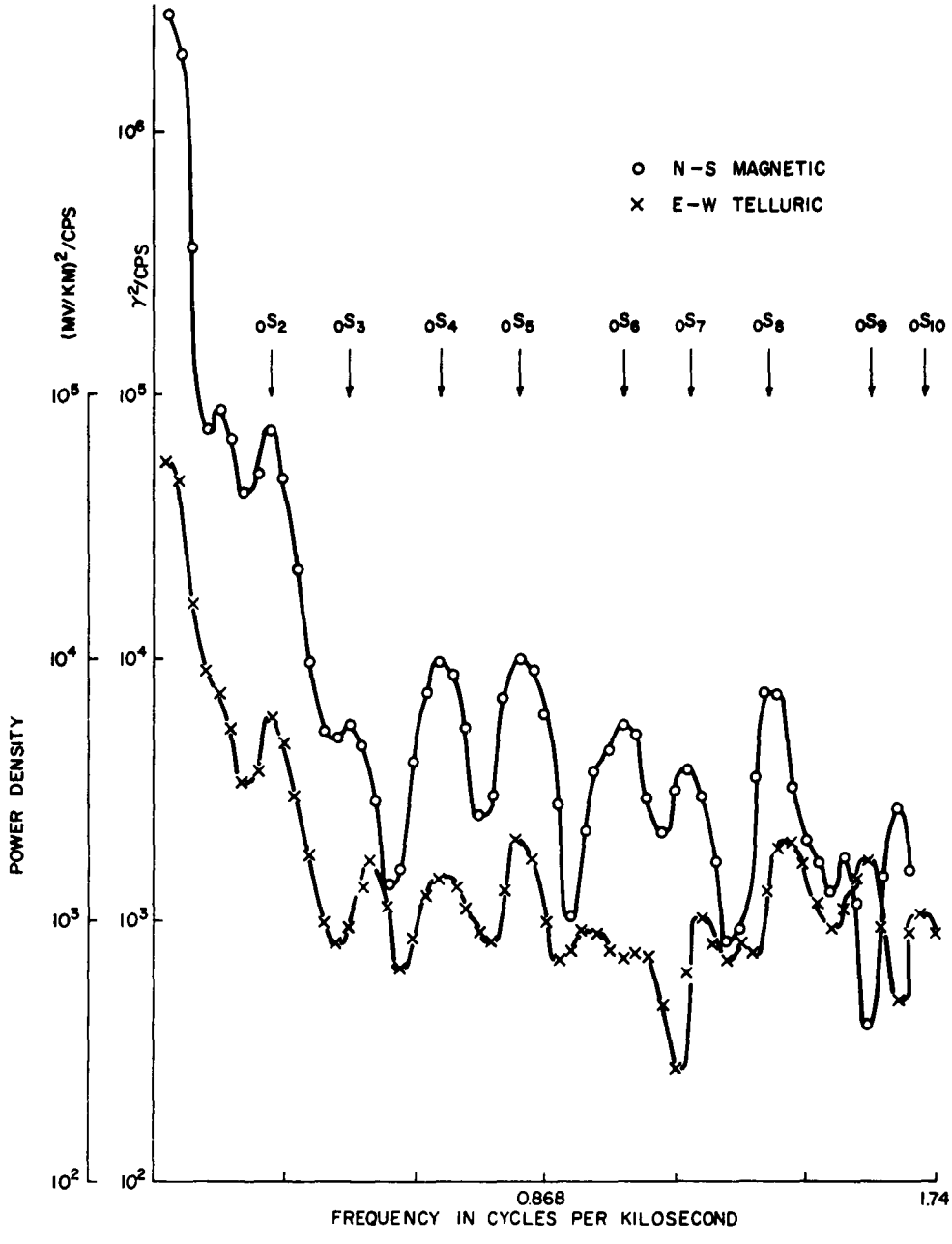

FIGURE 41
THE POWER SPECTRA OF THE NORTH-SOUTH MAGNETIC AND EAST-WEST TELLURIC FIELDS AT TBILISI 2 SEPTEMBER 1957

TABLE 27

COMPARISON BETWEEN FREE EARTH PERIODS OBSERVED WITH A GRAVIMETER AND PEAKS IN THE GEOMAGNETIC POWER SPECTRA

Periods are for the spheroidal mode ${}_0S_\ell$

Order, ℓ	Gravimeter Period Minutes	E-W Telluric Period		N-S Magnetic Period	
		Minutes	% Difference	Minutes	% Difference
2	54.98	60.4	-9.9	60.4	-9.9
3	35.87	33.88	+5.5	38.4	+7.05
4	25.85	26.18	-1.3	26.18	-1.3
5	19.83	20.56	-0.37	20.56	-0.37
6	16.07	15.57	+3.1	16.00	-0.4
7	13.42	13.72	-2.3	14.05	-4.7
8	11.78	12.00	-1.9	12.26	-4.1
9	10.57	10.57	+1.0	10.86	-2.7
10	9.685	9.76	-0.83	no value	

computed power spectra. The strong components (N-S magnetic and E-W telluric) on 2 September were chosen for comparison since these data are the most reliable (see Chapter VI).

The frequency resolution and confidence intervals of the spectra presented here do not permit positive statements about this interesting comparison. It is only suggested that physically the induced currents are possible and that their existence may be evidenced by peaks in the power spectrum of the magnetotelluric field.

BIBLIOGRAPHY

1. D. C. Tozer, The electrical properties of the earth's interior, Physics and Chemistry of the Earth, 3, 414 (1959). Pergamon Press, London.

2. George H. Hopkins, Jr., A survey of past and present investigations of the natural earth currents, Report No. 113, Electrical Engineering Research Laboratory of The University of Texas, 1 April 1960.

3. J. A. Fleming, Terrestrial magnetism and electricity, McGraw-Hill Book Company, Inc., New York (1939).

4. International association of geomagnetism and aeronomy, description of geomagnetic observatories, Part II (July, 1957); Part III (July, 1959).

5. V. Troitskaya, Earth-current installations at the stations of the USSR, Annals of the International Geophysical Year, IV, Part 5, 322-329, Pergamon Press, New York (1957).

6. M. Eschenhagen, Magnetic intensity variometers, Terrestrial Magnetism and Atmospheric Electricity, V, 59-62 (1900).

7. R. B. Blackman and J. W. Tukey, The measurement of power spectra, Dover Publications, Inc., New York (1959).

8. Claude E. Shannon, Communication in the presence of noise, Proceedings of the Institute of Radio Engineers, 37, 10-21, January, 1949.

9. Julius S. Bendat, Principles and applications of random noise theory, John Wiley and Sons, Inc., New York, 1958.

10. D. Ransom Whitney, Elements of mathematical statistics, Henry Holt and Company, New York, 1959.

11. H. M. James, N. B. Nichols and R. S. Phillips, Theory of Servomechanisms, MIT Radiation Laboratory, Series No. 25, McGraw-Hill Book Company, Inc.

12. G. P. Wadsworth, E. A. Robinson, J. G. Bryan, and P. M. Hurley, Detection of reflections on seismic records by linear operators, Geophysics, 18, 539-586 (1953).

13. C. W. Horton, On the design of a time-domain filter, An unpublished manuscript.

14. W. Munk, F. Snodgrass, and M. Tucker, Spectra of low frequency ocean waves, Bull., Scripps Inst. Oceanog. University California, 7, 299 (1959).

15. W. B. Davenport, Jr., R. A. Johnson, and D. Middleton, Statistical errors in measurements on random time functions, Journal of Applied Physics, 23, 377-388, 1952.

16. N. R. Goodman, On the joint estimation of the spectra, cospectrum, and quadrature spectrum of a two-dimensional stationary gaussian process, A Ph.D. Thesis submitted to Princeton University (March, 1957).

17. J. Halcombe Laning, Jr. and Richard H. Battin, Random processes in automatic control, McGraw-Hill Book Company, Inc., 1956.

18. N. Wiener, Extrapolation, interpolation, and smoothing of stationary time series, John Wiley and Sons, Inc., New York, 1949.

19. Stanford Goldman, Information theory, Prentice-Hall, Inc., New York 1953.

20. Thomas Cantwell, Detection and analysis of low frequency magnetotelluric signals, A Ph.D. Thesis submitted to Massachusetts Institute of Technology (January, 1960).

21. C. W. Horton and A. A. J. Hoffman, Magnetotelluric fields in the frequency range 0.03 to 7 cycles per kilosecond: Part I. Power spectra, a paper presented at the Conference on Telluric and Geomagnetic Field Variations, The University of Texas, Austin, Texas, October, 1961, and submitted to the Journal of Research of the National Bureau of Standards, Section D., Radio Propagation.

22. C. W. Horton and A. A. J. Hoffman, Magnetotelluric fields in the frequency range 0.03 to 7 cycles per kilosecond: Part II, Geophysical interpretation, a paper presented at the Conference on Telluric and Geomagnetic Field Variations, The University of Texas, Austin, Texas, October, 1961, and submitted to the Journal of Research of the National Bureau of Standards, Section D, Radio Propagation.

23. George Hopkins, Jr., P. F. Law, and R. R. Boothe, Jr., Initial observations of earth current and magnetic field micropulsations, Electrical Engineering Research Laboratory, The University of Texas, Report No. 112, 2 December, 1959.

24. R. R. Boothe, B. M. Fannin, and F. X. Bostick, Jr., A geomagnetic micropulsation measuring system utilizing air-core coils as detectors, Report 115, Electrical Engineering Research Laboratory, The University of Texas, 1 August 1960.

25. Louis Cagniard, Basic theory of the magneto-telluric method of geophysical prospecting, Geophysics, 18, 605 (1953).

26. J. A. Stratton, Electromagnetic theory, McGraw-Hill Book Company, Inc., New York, 1941.

27. N. F. Ness, J. C. Harrison and L. B. Slichter, Observations of the free oscillations of the earth, Journal of Geophysical Research, 66, No. 2, February 1961.

Initial distribution of this document has been made in accordance with a list on file in the Technical Reports Group of The Johns Hopkins University, Applied Physics Laboratory.